NASA TECHNICAL REPORT

NASA TR R-312

NASA TR R-312

USE OF TETRAFLUOROMETHANE TO SIMULATE REAL-GAS EFFECTS ON THE HYPERSONIC AERODYNAMICS OF BLUNT VEHICLES

by Robert A. Jones and James L. Hunt

Langley Research Center

Langley Station, Hampton, Va.

NATIONAL AERONAUTICS AND SPACE ADMINISTRATION • WASHINGTON, D. C. • JUNE 1969

NASA TR R-312

USE OF TETRAFLUOROMETHANE TO SIMULATE REAL-GAS EFFECTS ON THE HYPERSONIC AERODYNAMICS OF BLUNT VEHICLES

By Robert A. Jones and James L. Hunt

Langley Research Center
Langley Station, Hampton, Va.

NATIONAL AERONAUTICS AND SPACE ADMINISTRATION

For sale by the Clearinghouse for Federal Scientific and Technical Information
Springfield, Virginia 22151 – CFSTI price $3.00

USE OF TETRAFLUOROMETHANE TO SIMULATE REAL-GAS EFFECTS ON THE HYPERSONIC AERODYNAMICS OF BLUNT VEHICLES

By Robert A. Jones and James L. Hunt
Langley Research Center

SUMMARY

An experimental and theoretical study was made of the use of tetrafluoromethane (CF_4) in low hypersonic flows as a means of simulating the flow field over the forebody of blunt configurations in hypersonic flight where dissociation of the gas in the shock layer gives large density ratios across the shock wave. A pilot model hypersonic CF_4 blowdown tunnel at the Langley Research Center was built and studied. With this facility a normal-shock density ratio of 12.1 was obtained at a Mach number of 6 with stagnation conditions of 1650 N/cm^2 and 736° K. The results of the investigation indicate that flow fields over the forebody of blunt configurations for real-gas conditions resulting in normal-shock density ratios up to 17 can be simulated by this method. A computer program for isentropic flow of CF_4 as well as flow across normal and oblique shocks was set up. Plots of various flow parameters are presented as a function of free-stream Mach number for various stagnation temperatures. A method for computing axisymmetric nozzle contours which includes a correction for boundary-layer displacement thickness is described.

INTRODUCTION

At supersonic and hypersonic speeds the aerodynamic characteristics, including the pressure distribution, shock shape, drag, and stability, of very blunt, low-fineness-ratio bodies are determined almost exclusively by the flow field over the forebody. The inviscid forebody flow in turn is essentially independent of Mach number and depends mainly on the density ratio across the normal shock and the body geometry. (See, for example, the discussion of Mach number independence principle in ref. 1 and the discussion of real-gas effects on the flow field of several high-drag planetary entry bodies in ref. 2.) Therefore, the inviscid forebody flow can be simulated in a wind tunnel if the normal-shock density ratio of flight can be matched.

For hypersonic flight of large vehicles in planetary atmospheres with equilibrium gas conditions, density ratios as high as 20 are encountered. These large density ratios result from chemical dissociation of the molecules in the high-temperature gas behind

the shock. However, the maximum normal-shock density ratio that can be achieved in air wind tunnels, even in those with large specific-energy content, is usually less than 8 because the small size of the models precludes the attainment of chemical equilibrium in the forebody shock layer. Thus, a means of experimentally simulating high shock density ratios is needed.

It has been proposed (refs. 3 and 4) that flow-field calculations for blunt bodies where real-gas effects are significant can be greatly simplified by the use of ideal-gas relations but with a low value of the specific-heat ratio to obtain the correct shock density ratio. It also appears possible that the desired density ratios may be obtained experimentally with no dissociation by testing in a relatively low-temperature flow of a gas that has a low ratio of specific heats. If the Mach number is sufficiently high to apply the Mach number independence principle, then the desired inviscid forebody flow field can be simulated. If the Reynolds number is matched also, then the entire forebody flow field can be simulated.

The use of gases other than air in aerodynamic facilities has been considered by many previous investigators. For example, Chapman (ref. 5) considered several gases and gas mixtures including tetrafluoromethane (CF_4) for various applications. He showed that for a given subsonic Mach number, Reynolds number, and pressure, a gas-mixture wind tunnel having the same specific-heat ratio as air could be smaller and thus require much less power. Also it has been shown that by using gases other than air, it is possible to match free-stream Mach number at much lower stagnation temperatures. The helium tunnels now in operation are examples of this application. The use of CF_4 has also been considered to obtain high Mach numbers at lower stagnation temperatures (ref. 6) but was found to be somewhat impractical for that purpose. The only previous attempt known to the authors to simulate the real-gas effects on flows over very blunt bodies at high speeds by the use of a gas with a low ratio of specific heats is that of reference 7 in which a mixture of water vapor and oxygen is proposed.

The purpose of this paper is to (1) discuss the normal-shock density ratio as a simulation parameter for blunt-body flows, (2) propose the use of CF_4 as a test gas in order to obtain high shock density ratios, (3) present some results of an experimental investigation in both a wind tunnel and a ballistic range using CF_4 as the test gas, and (4) present equations and charts for the compressible flow characteristics of CF_4.

A small (7.6-cm-diameter test section) CF_4 tunnel with a conical nozzle was built and put into operation at the Langley Research Center in October 1965. Later, a ballistic-range investigation at the Naval Ordnance Laboratory (NOL) using CF_4 as the test gas was supported by NASA (Langley Research Center) to study effects of high density ratios on the aerodynamics of three very blunt low-fineness-ratio configurations. Some of the results from both these investigations are presented herein. Also, the

design characteristics of a facility which would be inexpensive to build and simple to operate but would enable the correct simulation of real-gas density-ratio conditions for blunt configurations are presented. A few of the results (obtained in the small CF_4 wind tunnel) that show the sensitivity of the flow field over a tension-shell configuration to high shock density ratios have been published in reference 8. Some of the results obtained in the NOL ballistic-range investigation are given in reference 9.

This report includes appendixes by James L. Hunt, Kathryn A. Smith, Robert B. Reynolds, and Lillian R. Boney, of the Langley Research Center, which present calculation procedures for evaluating isentropic expansions and flow across shocks in CF_4, a method for determining hypersonic nozzle contours for CF_4, and related computer programs.

SYMBOLS

A	inviscid test-section area
A^*	area at sonic throat
C_D	drag coefficient
H	enthalpy
M	Mach number
p	pressure
r	radius
R_1	free-stream Reynolds number (based on base diameter)
s	surface distance from stagnation point
T	temperature
u	velocity
x,y	coordinates
γ	ratio of specific heats

Δ	shock standoff distance
ϵ	inverse density ratio, ρ_1/ρ_2
θ	shock-wave inclination angle
μ	viscosity
ρ	density

Subscripts:

b	base
eff	effective
max	maximum
n	nose
0	free-stream stagnation conditions
1	free-stream static conditions
2	static condition behind normal shock
3	stagnation condition behind normal shock

BLUNT-BODY FLOW-FIELD SIMULATION

Ideal-Gas Flow Fields

For high-speed flight in an atmosphere the chemical dissociation of the gas in the shock layer can result in a marked increase in density ratio across the strong bow shock compared with a lower speed or lower temperature flow of the same gas where no dissociation takes place. Under conditions where dissociation is present, the aerodynamic characteristics of very blunt vehicles (shock-wave angles larger than 50°) depend primarily on this shock density ratio (ref. 1) and not on the Mach number if $M_1 > 4$. Three

blunt configurations which will be used to illustrate this strong dependence of aerodynamic characteristics on shock density ratio are shapes being studied by NASA as possible Mars probe/lander vehicles. These three configurations are shown in figure 1. In order to land a payload on the surface of Mars and make use of aerodynamic braking in the thin atmosphere, a large high-drag vehicle is required. Because of the large amount of CO_2 ir the Mars atmosphere and the large size of the vehicle, high shock density ratios will be encountered even at velocities as low as 3000 m/sec.

The changes in aerodynamic characteristics which are due to the large shock density ratios associated with high-speed flight are primarily the result of changes in surface pressures acting on the forebody. The surface pressures are affected by a change in shock density ratio in two ways: First, the level of pressure at the stagnation point is changed, and second, the nondimensional distribution of surface pressure relative to stagnation-point pressure is changed. This dependence on shock density ratio can be illustrated by considering the flow of a perfect gas about a blunt body. The density-ratio effect on the stagnation-point pressure level is easy to estimate. From conservation of mass and momentum across a normal shock, the following equation is obtained:

$$\frac{p_2 - p_1}{\rho_1 u_1^2} = 1 - \epsilon \tag{1}$$

which holds true for both ideal and real gases. For high Mach numbers p_1 can be neglected compared with p_2, and the flow from the shock to the stagnation point can be considered incompressible so that equation (1) reduces to

$$\frac{p_3}{\rho_1 u_1^2} = 1 - \frac{\epsilon}{2} \tag{2}$$

This effect on the vehicle drag coefficient of a given shape can be approximated as

$$\frac{(C_D)_{\text{large density ratio}}}{(C_D)_{\text{small density ratio}}} = \frac{(2 - \epsilon)_{\text{large density ratio}}}{(2 - \epsilon)_{\text{small density ratio}}} \tag{3}$$

For a blunt vehicle in flight with a shock density ratio $1/\epsilon$ of 15, the forebody drag would be increased about 5 percent over that measured in a conventional high Mach number air tunnel (where the maximum density ratio is 6) because of this increase in stagnation-point pressure level.

The surface pressure distributions for the spherical segment, the 120° cone, and the 140° cone have been computed for ideal-gas flow using a one-strip integral method (ref. 10) at various shock density ratios and free-stream Mach numbers. These results are shown in figures 2 and 3. The pressure distribution for the spherical segment

(fig. 2) is affected by density ratio mainly at large values of s/r_n where the effects on drag and moments are largest. Figure 2 shows that the effects of free-stream Mach number on pressure distribution are negligible for Mach numbers of 6 or larger. The results for the 120° cone (fig. 3(a)) also show a negligible effect of Mach number on surface pressure. For density ratios somewhat above 10 the sonic point moves forward from the base of the cone. Since the program requires the sonic-point location to be at the point of maximum radius, no solutions could be obtained for the 120° cone at a density ratio of 20. Solutions were obtained for the 140° cone (fig. 3(b)) at a density ratio of 20. For this case the flow over the conical portion is almost sonic; this gives the sharp decrease in pressure near the sphere-cone juncture $\left(s/r_b \approx 0.08\right)$. The results shown in figures 2 and 3 indicate that for bodies as blunt as these, the primary factor governing the aerodynamic characteristics is the shock density ratio. Therefore this shock density ratio must be simulated when such shapes are studied experimentally.

Other aerodynamic characteristics of blunt bodies which depend primarily on shock density ratio are the shock shape and shock standoff distance. The shock shapes of these blunt bodies calculated by the method of reference 10 are given in figures 4 and 5. Here again it is apparent that Mach number has very little effect. Both the shock shape and the standoff distance at the stagnation point are strongly dependent on the shock density ratio.

Real-Gas Flow Fields

The surface pressure distributions for real-gas equilibrium flow have been calculated for all three shapes of figure 1 in reference 2. The results of these calculations are presented in figures 6, 7, and 8. The value $\rho_2/\rho_1 = 5.6$ corresponds to an ideal gas at a Mach number of 9 with $\gamma = 1.4$; the value of $\rho_2/\rho_1 = 16.7$ corresponds to a condition near peak heating and peak dynamic pressure for entry into an assumed Mars atmosphere (model 2 of ref. 11). The blunt-cone pressure distribution of figure 7 was made for a 130° cone since that was the smallest cone angle for which the sonic point was located at the rearward corner for a shock density ratio of 16.7 and thus the smallest cone angle for which solutions could be obtained with the method used in reference 2. The trends shown by the data of figures 6 and 7 are in close agreement with the ideal-gas calculations shown in figures 2 and 3; this indicates that real-gas equilibrium flow and ideal-gas flow give about the same surface pressure distribution at high Mach numbers provided the value of the normal-shock density ratio is the same. Therefore, even when real-gas effects are present, the density ratio is still the dominant parameter as long as the bow shock is strong and the fineness ratio is low.

Predicted Simulation in CF_4

In order to duplicate high density ratios obtained in flight at high hypersonic speeds in a wind tunnel without dissociation, the test gas must have a low ratio of specific heats. Tetrafluoromethane (CF_4) was selected as the working fluid for this simulation because of its low ratio of specific heats, low boiling point, thermal stability, and low vibrational relaxation time, and also because it is a readily available, colorless, odorless, nontoxic gas that is easily reclaimed; however, no exhaustive search to find the best test gas for this particular type of simulation was made. Much of the physical and chemical property data for CF_4 used in this study was obtained from the manufacturer of CF_4. Some of the physical properties are given in table I.

TABLE I.- PHYSICAL PROPERTIES OF TETRAFLUOROMETHANE (CF_4)

Molecular weight	88.01
Boiling point at 1 atm*, ^{o}K	145
Freezing point, ^{o}K	89.4
Critical temperature, ^{o}K	227.33
Critical pressure, atm	36.96
Critical volume, cm^3/mole	141
Critical density, kg/m^3	0.626×10^3
Density, liquid at 193^{o} K, kg/m^3	1.317×10^3
Density, saturated vapors at boiling point, kg/m^3	7.62
Specific heat, liquid at 193^{o} K, J/kg-^{o}K	1.23×10^3
Specific heat, vapors at 1 atm and 298^{o} K, J/kg-^{o}K	0.707×10^3
Specific-heat ratio at 1 atm and 298^{o} K	1.159
Heat of vaporization at boiling point, J/kg	136.0×10^3

*1 atm = 101 kN/m^2.

The method of reference 12 was used to compute the equilibrium composition of CF_4 as a function of temperature for several pressures covering the range that would normally be used in a wind tunnel, and it was found that no dissociation occurred for temperatures lower than 1600^{o} K. A more complete description of the properties of CF_4, including the equations of state, and the computer programs used to calculate conditions for isentropic expansion and flow across normal and oblique shocks in CF_4 are given in appendixes A and C. Some of the flow variables of interest which were computed as described in appendix A have been plotted as functions of pertinent parameters for the ranges of stagnation chamber pressure and temperature studied. The stagnation enthalpy H_0, which is practically independent of stagnation pressure in the range from 1034 to 1724 N/cm^2, is given as a function of stagnation temperature T_0 in figure 9. Plots of $u_1/\sqrt{2H_0}$, γ_1, T_1/T_0, p_1/p_0, $\rho_1 u_1/\mu_1$, $\rho_1 u_1^2/2p_0$, ρ_2/ρ_1, p_3/p_0, p_3/p_1, γ_2/γ_1,

and $\rho_2 u_2/\mu_0$ against M_1 are presented in figures 10 to 20 for $T_0 = 478^\circ$, 588°, 700°, and 811° K. The specific-heat ratio, unit Reynolds number, and Reynolds number behind normal shock are given for stagnation pressures of 1034, 1378, and 1724 N/cm^2. The other flow variables are independent (within the accuracy of the plots) of stagnation pressure in the range from 1034 to 1724 N/cm^2). Figure 16 shows that for a temperature of 811° K, a shock density ratio of 13.6 is obtained at a Mach number of 7. The calculations of appendix A show that for 1400° K, a shock density ratio of 14.5 is obtained. At this same temperature a value of 15.6 can be obtained if the Mach number is increased to 8 rather than 7.

Similar calculations have been made by the method of appendix A for test conditions in a ballistic range. Plots of the density, temperature, and pressure ratios across a normal shock as a function of velocity in 100 percent CF_4 are shown in figures 21 to 23. The ambient temperature in the range is assumed to be room temperature (294° K) and the plots are accurate within 4 percent for range pressures from 30 to 1000 N/m^2. Calculations are not shown for launch velocities greater than 1500 m/sec because dissociation of CF_4 in the shock layer could occur at these higher velocities. Figure 21 indicates that shock density ratios up to 17 can be obtained by using CF_4 as the test gas in a ballistic range.

The shock density ratio and Reynolds number simulation capability of the CF_4 facility (assuming a 2.5-cm-diameter model and a realistic pressure range) is shown in figure 24, and that of several other facilities at the Langley Research Center, which are thought to be typical of most facility capabilities, is shown in figure 25. Also shown in both figures are two entry trajectories typical of very blunt high-drag vehicles. Both these trajectories are based on the assumption of chemical equilibrium in the shock layer. The Earth entry trajectory is for an entry angle of 90°, an entry velocity of 5600 m/sec, a ballistic coefficient of 146 kg/m^2, and a diameter of 0.67 m. The Mars trajectory is for an assumed atmosphere of 2000 N/m^2 (model 2, ref. 11), an entry angle of 90°, an entry velocity of 8700 m/sec, a ballistic coefficient of 23.5 kg/m^2, and a diameter of 5 m. The "knee" of the trajectories corresponds roughly to conditions of peak heating and peak dynamic pressure. Figure 24 shows the simulation capability of a CF_4 wind tunnel operating in the Mach number range from 3 to 8 and that of a CF_4 ballistic range at velocities from 450 to 1500 m/sec. A comparison of figures 24 and 25 shows that with CF_4 the ability to simulate shock density ratios which occur with high-speed atmospheric entry is increased. Therefore the use of a relatively low velocity flow of CF_4 should greatly facilitate the study of real-gas effects on the aerodynamics of blunt entry configurations (those having shock-wave angles larger than 50°).

The variation of shock density ratio with shock-wave inclination angle θ for a CF_4 flow at a Mach number of 6 and a stagnation temperature of 811° K is shown in

figure 26. Also shown is the shock-density-ratio variation of an ideal gas at a Mach number of 6 with a value of γ which results in the same normal-shock density ratio as CF_4. These two curves are compared with one for equilibrium air at an altitude of 70 km and a velocity of 5240 m/sec; for these conditions the free-stream Mach number is 16.5 and the normal-shock density ratio is 12.7 (same value as for the other two curves). This plot shows that for shock waves with θ greater than about 60°, the CF_4 simulation gives very nearly the same shock-density-ratio variation as would occur in flight in the earth's atmosphere for equilibrium conditions at a Mach number of 16.5 and an altitude of 70 km. It also demonstrates that for shock-wave angles greater than about 60°, the CF_4 simulation gives approximately the same result as an ideal gas at the same Mach number and with the value of specific-heat ratio adjusted to give the same value of the normal-shock density ratio ρ_2/ρ_1. The CF_4 simulation method should therefore be very accurate for bodies blunt enough to have bow shock-wave angles of 60° or greater. At a shock-wave angle of 50°, the density ratio in CF_4 is 87.5 percent of that which occurs in equilibrium air at the stated conditions. This difference is believed to be within acceptable limits for engineering calculations; thus, blunt bodies have been heretofore defined in this report as bodies blunt enough to have bow shock waves of 50° or greater.

PILOT CF_4 TUNNEL

Apparatus

A schematic diagram of the 7.6-cm CF_4 tunnel is given in figure 27. The CF_4 supply consisted of bottles each containing about 32 kg at a pressure of 1440 N/cm^2. The small bag-type pneumatic accumulator was used together with a check-valve arrangement to pump the CF_4 into the large accumulator at the pressure desired for a test. When the desired pressure was reached in the large accumulator, the high-pressure air regulator was set at this value and the valve between the large air bag and air supply was opened. As CF_4 was used during a test, the large air bag inflated and thus maintained a constant tunnel stagnation pressure for times as long as 3 minutes and eliminated any chance of contamination of the CF_4.

The heat exchanger consisted of several long coiled stainless-steel tubes immersed in a bath of molten lead. Energy was supplied by electrical strip heaters which were also immersed in the lead. The heat exchanger, the line from the heat exchanger to the stagnation chamber, and the stagnation chamber itself were all heated by electrical strip heaters and wrapped with insulation. The lead bath could be maintained at any temperature up to 812° K but the line and stagnation chamber metal temperatures were limited to a maximum of 534° K. This system could supply CF_4 at stagnation conditions up to 2000 N/cm^2 and 750° K.

The nozzle was conical with a 5° half-angle, a 1.32-mm-diameter throat, and a 7.6-cm-diameter test section. The tunnel exhausted into a 1200-m^3 vacuum sphere which could be pumped to pressures as low as 25 N/m^2. No attempts were made to reclaim the CF_4, although it should be possible to do so easily since it is a heavy gas with a relatively high critical temperature (227.33° K) and a relatively low critical pressure (36.96 atm).

Experimental Results and Discussion

Several different measurements have been made in this pilot facility. The primary purpose of these measurements was to demonstrate that high normal-shock density ratios could be obtained with this facility and to verify the theoretical test conditions calculated by the method discussed in the appendixes. A secondary purpose was to study the operating characteristics so that a more nearly optimum facility could be designed. Measurements of the stream pitot pressure, test-section wall static pressure, stagnation chamber pressure and temperature, shock standoff distances, and shock shapes for several different configurations were made for a range of total temperatures and pressures.

Nominal test-section conditions.- Although tests were made for a wide range of stagnation temperatures and pressures, a preponderance of data were obtained at stagnation conditions of 736° K and 1650 N/cm^2. These conditions are referred to subsequently as the nominal test conditions. The corresponding test-section conditions as determined from the measured stagnation pressure ratio across the normal shock and the measured ratio of free-stream static to free-stream stagnation pressure in conjunction with the real-gas calculation procedure of appendix A (figs. 11 to 19) are presented in table II.

TABLE II.- NOMINAL TEST-SECTION CONDITIONS

Condition	Value calculated by method of appendix A for –	
	$p_3/p_0 = 1.13 \times 10^{-3}$ *	$p_1/p_0 = 2.25 \times 10^{-5}$ *
M_1	6.06	6.20
ρ_2/ρ_1	12.2	12.3
γ_1	1.190	1.205
γ_2/γ_1	0.925	0.900

*Measured value at $p_0 = 1650\ N/cm^2$ and $T_0 = 736°$ K.

Density ratio measurement.- Since the primary concern of this report is the simulation of forebody flow fields of blunt configurations by matching the normal-shock density ratio without dissociating the test gas, a more direct method for verifying this ratio was desired.

Normal-shock density ratios in the test section were determined from the shock standoff distance measured for a sphere by using the following relation:

$$\frac{\Delta}{r} = 0.76\epsilon \tag{4}$$

This relation is an empirical fit to the theories of references 13, 14, and 15 and has been shown to predict very accurately the shock standoff distance for spheres. A test-section normal-shock density ratio of 12.1 was determined with this method for the nominal stagnation test conditions $\left(p_0 = 1650\ N/cm^2 \text{ and } T_0 = 736^\circ\ K\right)$. This value compares favorably with those from the real-gas calculations (12.2 and 12.3) given in table II. These values are more than twice the normal-shock density ratio which can be obtained in an air wind tunnel operating as an ideal-gas facility.

Effective test-section conditions.- As discussed previously in the section "Blunt-Body Flow-Field Simulation," it should be possible to calculate approximately the flow field about very blunt bodies using ideal-gas relations for some effective Mach number and specific-heat ratio provided that the correct normal-shock density ratio is obtained. One method for determining the values of effective Mach number and effective specific-heat ratio is to solve the following two ideal-gas equations simultaneously using the value of the normal-shock density ratio determined from the measured shock standoff distance of a sphere and the measured ratio of stagnation pressure behind the normal shock to the total pressure in the stagnation chamber.

$$\epsilon = \frac{\left(\gamma_{eff} - 1\right)M_{eff}^2 + 2}{\left(\gamma_{eff} + 1\right)M_{eff}^2} \tag{5}$$

$$\frac{p_3}{p_0} = \left[\frac{\left(\gamma_{eff} + 1\right)M_{eff}^2}{\left(\gamma_{eff} - 1\right)M_{eff}^2 + 2}\right]^{\frac{\gamma_{eff}}{\gamma_{eff}-1}} \left[\frac{\gamma_{eff} + 1}{2\gamma_{eff}M_{eff}^2 - \left(\gamma_{eff} - 1\right)}\right]^{\frac{1}{\gamma_{eff}-1}} \tag{6}$$

The solution of these equations for the nominal test conditions $\left(\epsilon = 0.0826,\ p_3/p_0 = 1.13 \times 10^{-3}\right)$ gives an effective Mach number of 5.78 and an effective specific-heat ratio of 1.12. A comparison of calculated pressure distributions and shock shapes

based on ideal-gas theory at these effective conditions with experimental data is needed for verification of this method.

Operational characteristics.- The nominal stagnation temperature and pressure ($T_0 = 736^\circ$ K and $p_0 = 1650$ N/cm^2) resulted in approximately the largest value for the normal-shock density ratio that was obtained in the pilot facility. (See table II.) Since the specific-heat ratio of CF_4 decreases with an increase in temperature (fig. 11), a few attempts to obtain higher shock density ratios by testing at higher temperatures were made. However, the ratio of test-section area to throat area of the pilot CF_4 tunnel was fixed at a value of 3300 and the decrease in γ associated with higher temperatures also caused a reduction in test-section Mach number. (See fig. 28.) The decrease in Mach number with a decrease in γ offset the desired increase in shock density ratio so that a value of 12.1 was the highest realized in this pilot facility. The variation of area ratio with Mach number is shown in figure 28 for CF_4 at two different stagnation temperatures. This figure shows that if the Mach number is 6 at 589° K, an increase in stagnation temperature to 811° K while the area ratio is kept constant will result in a decrease in Mach number to 5.3.

Some tests were made at stagnation temperatures as low as 275° K and stagnation pressures of about 1650 N/cm^2. At these conditions the Mach number was about 8 and the normal-shock density ratio was about 10. Even at this low stagnation temperature, no condensation of CF_4 in the test-section flow was evident. Other tests were made to determine the vacuum required to operate the tunnel since CF_4 gives a very low test-section static pressure (fig. 13). At the nominal test conditions the pilot facility required a sphere pressure of 30 N/m^2.

Comparison of shock shapes in air and CF_4.- A comparison of shock shapes for the 120° blunt cone configuration obtained in the pilot CF_4 tunnel and the Langley Mach 8 variable-density hypersonic tunnel is shown in figure 29. The CF_4 shadowgraph was taken at the nominal test conditions where the normal-shock density ratio was approximately 12.1. The schlieren in the Mach 8 tunnel was taken in air at a Mach number of 8, a specific-heat ratio of 1.4, and a normal-shock density ratio of 5.56. There are two notable differences in these shock shapes. At the higher shock density ratio in CF_4, the standoff distance is considerably less. Also in CF_4 the shock over the conical portion of the body is almost linear and thus indicates a supersonic or near-supersonic flow in the shock layer downstream of the spherical nose as compared with the highly curved shock and corresponding subsonic flow in air. Although no force or pressure-distribution data have been obtained in this pilot facility (the small size of the model, 15-mm diameter, makes such measurements difficult), it is believed that the results discussed herein

demonstrate the feasibility and desirability of this type of facility for simulating real-gas effects on the aerodynamic characteristics of blunt high-drag entry vehicles.

Design calculations for contoured nozzle.- As a result of these exploratory tests a Mach 6 nozzle with a 16.4-cm-diameter test section has been designed for CF_4 at stagnation conditions of 811° K and 1724 N/cm^2. A real-gas program was used to calculate the contoured axisymmetric nozzle, and a correction for boundary-layer displacement thickness was included. The details of this calculation procedure are discussed in appendix B.

BALLISTIC-RANGE TESTS

Ballistic ranges have the capability of obtaining high normal-shock density ratios in the actual gas of a planetary atmosphere, but to do this, they must operate with high free-stream pressures in order to achieve equilibrium composition of the gas in the shock layer because of the very small size of the models. These high pressures result in very rapid damping of the model motions and limit the stability data that can be obtained. If CF_4 is used as the test gas and the models are flown at much lower speeds so that no dissociation occurs, the desired high shock density ratio can be obtained at any test-section pressure and data can be obtained at conditions giving optimum motion of the model for data reduction.

With these considerations in mind, an exploratory investigation in a ballistic range using CF_4 as the test gas was undertaken by the Naval Ordnance Laboratory with NASA support. This was done as part of an extensive investigation of the three shapes shown in figure 1. Most of the data were obtained in air; however, several launches were made in CF_4 to study the aerodynamics of these shapes at high shock density ratios. For these CF_4 experiments small amounts of air (5 to 10 percent) were present and the concentration along the length of the range varied from almost pure CF_4 to mixtures of about 90 percent CF_4 and 10 percent air. Since the properties of these mixtures may be somewhat different from pure CF_4, the present results should be used with some reservation.

Launches were made at or near 460 and 1500 m/sec in CF_4. Spheres as well as the three high-drag configurations were tested, and measurements of the shock standoff distance for the spheres were used to verify the actual shock density ratio. The highest shock density ratios obtained in air at launch velocities of 5000 m/sec were about 9, whereas ratios as high as 17 were obtained in the CF_4 tests at launch velocities of about 1500 m/sec.

Drag is one of the most accurately measured quantities in a ballistic range test. When the drag force is nondimensionalized by the dynamic pressure $\frac{1}{2}\rho_1 u_1^2$ to obtain

a drag coefficient, an error due to uncertainty in gas composition is introduced. This error is due to the uncertainty in the density of the gas in the test section. Since the pressure is kept constant by pumping and since air leaks into the test section between the time of measurement of the gas density and the time of launching, the density is actually somewhat less than the value used for data reduction. Therefore the drag-coefficient values computed from the measured data are somewhat less than the actual values at the time of launch.

The measured drag coefficients of the three shapes in air and CF_4 are shown in figures 30 to 32. The drag coefficient is always higher for the high density ratios obtained in CF_4. This increase is particularly large for the tension shell (fig. 32). The difference in shock shape for the tension shell in air and CF_4 is also more pronounced. Shadowgraphs of the flow field of the tension shell in air and in CF_4 at approximately the same Mach number are shown in figure 33. The flow over the tension shell is sensitive to boundary-layer separation which can alter the shock shape as well as the forces. A discussion of the Reynolds number and wall-temperature effect on separation and on the shock shape for this configuration is given in reference 8. The results of reference 8 and tests made in the ballistic range at different Reynolds numbers indicate that the boundary-layer flow is attached for both shadowgraphs shown in figure 33. Shadowgraphs of the flow over the 120° cone in both air and CF_4 are shown in figure 34.

The increases in drag at the higher shock density ratios in CF_4 shown in figures 30 to 32 are in agreement with the trends based upon the theoretical considerations discussed previously in the section entitled "Blunt-Body Flow-Field Simulation." It is apparent that useful studies of real-gas effects (high shock density ratios) on the aerodynamics of blunt configurations in ballistic ranges can be made by using CF_4 as the test gas.

CONCLUDING REMARKS

An exploratory experimental and theoretical investigation of the use of tetrafluoromethane (CF_4) as a test gas in wind-tunnel and ballistic-range facilities to simulate certain flow-field characteristics of very blunt vehicles in high-speed flight where dissociation takes place in the shock layer indicated the following:

1. The effects of dissociation in the shock layer of very blunt vehicles on the aerodynamic characteristics, such as shock shape, shock standoff distance, stagnation-point pressure level, surface pressure distribution, and forces and moments, can be simulated by matching the density ratio across the normal shock.

2. Comparison of shock shapes of a 120° blunt cone configuration obtained in the pilot CF_4 tunnel at a shock density ratio of 12.1 with the shock shape obtained in a Mach 8

air tunnel at a shock density ratio of 5.6 and with shock shapes calculated by a one-strip integral method for ideal gases at a range of shock density ratios from 5 to 20 demonstrates the strong dependence of the flow field on shock density ratio and the validity of simulating high-shock-density-ratio flows by using CF_4.

3. The use of CF_4 as the test gas in both wind tunnels and ballistic ranges is a practical and relatively simple method of obtaining test conditions with large normal-shock density ratios.

4. Tests made in a small pilot model CF_4 wind tunnel confirmed real-gas calculations for test conditions in CF_4. Measurements of pitot pressure and free-stream static pressure were in good agreement with calculations of isentropic expansion and flow across shock waves in CF_4. Experimentally determined normal-shock density ratios obtained by measuring the shock standoff distance for a sphere were in agreement with calculated values.

5. Values of normal-shock density ratio as high as 12.1 were obtained in this pilot CF_4 wind tunnel at a stagnation pressure of 1650 N/cm^2, a stagnation temperature of 736° K, and a free-stream Mach number of 6.1.

6. Exploratory tests using CF_4 in a ballistic range demonstrated that shock density ratios as high as 17 can be obtained at launch velocities of only 1500 m/sec, whereas the highest shock density ratios obtained on models of the same size in air was about 9 at launch velocities of 5000 m/sec.

7. Measurements of drag for three different blunt configurations in the ballistic range indicated a definite increase at the high shock density ratios obtained in CF_4. These results were in agreement with the trends of theoretical predictions.

Langley Research Center,
National Aeronautics and Space Administration,
Langley Station, Hampton, Va., March 12, 1969,
129-01-03-07-23.

APPENDIX A

CALCULATION PROCEDURE FOR EVALUATING ISENTROPIC EXPANSIONS AND FLOW ACROSS NORMAL AND OBLIQUE SHOCKS IN TETRAFLUOROMETHANE

By James L. Hunt, Kathryn A. Smith,
and Robert B. Reynolds

Tetrafluoromethane (CF_4) is a nonlinear polyatomic molecule (ref. 16). Its nine vibrational energy modes display anharmonic oscillator characteristics having four fundamental frequencies, two of which are threefold degenerate and one of which is twofold degenerate. The acute temperature dependence of the vibrational energy of this molecule reveals itself in the specific heats at constant pressure and volume and their ratio γ. Thus, an isentropic expansion in CF_4 is a variable γ expansion, being neither calorically nor thermally perfect. The dependence of γ on temperature along with its small (compared with temperature) dependence on density is vividly displayed in the discontinuity in γ that occurs across strong shocks.

A calculation procedure for evaluating isentropic expansions and flow behind normal and oblique shocks in CF_4 is presented herein in the order in which it was programed for the digital computer. In this analysis the CF_4 was at all times assumed to be in thermodynamic equilibrium. At 298° K and 10.1325 N/cm^2 the overall vibrational relaxation time of CF_4 is approximately 8.2×10^{-7} sec (ref. 17). The general theory for the relaxation of a system of harmonic oscillators predicts that the relaxation time varies inversely with pressure to the first power and decreases monotonically with temperature (ref. 18). For polyatomic gases this temperature dependence is given, according to the present consensus, as $e^{T^{-1/3}}$ (refs. 19 and 20). For the temperature regime of interest in this report only a small fraction of the vibrational energy is stored in the anharmonic modes (0.025 percent at 100° K and 2.9 percent at 1000° K (ref. 16)).

In each case for all the flow models studied, the use of the thermodynamic-equilibrium assumption was justified by a comparison of the vibrational relaxation distances (velocity of flow multiplied by a local relaxation time calculated from the harmonic relation for the dominant vibrational mode) with flow lengths (radius of model forebody, nozzle Mach cone length, etc.). For example,

(1) The relaxation times and distances for isentropic expansion in the Mach 6, CF_4 nozzle (design method, design conditions, and nozzle coordinates are presented in appendix B) at various axial stations are as follows:

Axial station, cm	Mach number	Relaxation time, sec	Relaxation distance, cm
	0	3.2×10^{-9}	
0	1.0	6.6×10^{-9}	2.2×10^{-4}
.04	1.3	8.3×10^{-9}	3.1×10^{-4}
2.9	3.1	2.5×10^{-7}	1.9×10^{-2}
7.6	4.5	7.0×10^{-6}	6.3×10^{-1}
65.9	6.0	2.2×10^{-4}	2.2×10^{1}

The fact that the axial length of the Mach cone in this nozzle (50.4 cm) is more than twice the relaxation distance at a Mach number of 6 (22.5 cm) indicates that equilibrium exists in the free stream at the test-section location.

(2) Behind a normal shock at a Mach number of 6 (for the table III nozzle) the relaxation time is 3.3×10^{-6} sec and the relaxation distance is 0.026 cm. According to equation (4), the shock standoff distance on a 3.2-cm-diameter sphere (average model base diameter tested) for the nominal test-section design conditions is 0.0958 cm, approximately 3.7 times the relaxation distance.

(3) Behind a normal shock in a ballistic range with an ambient pressure of 2666 N/m^2 and temperature of 294° K for a projectile velocity of 1524 m/sec, the relaxation time is 2.2×10^{-7} sec and the relaxation distance is 1.7×10^{-3} cm. The smallest model fired at this velocity for the ballistic-range test discussed in this report had a base radius of 1.58 cm. A sphere with this radius would have a shock standoff distance (eq. (4)) of 0.0709 cm, more than 40 times the relaxation distance.

SYMBOLS

The following symbols are used in this appendix in addition to some of those defined in the body of the paper:

A_2, A_3, A_4, A_5, A_6 constants in equation of state (eq. (A1))

a speed of sound

a_4 constant in equation for specific heat at zero pressure (eq. (A4))

B_2, B_3, B_4, B_5, B_6 constants in equation of state (eq. (A1))

b constant in equation of state (eq. (A1))

b_4 constant in equation for specific heat at zero pressure (eq. (A4))

C_2, C_3, C_5 constants in equation of state (eq. (A1))

c_4 constant in equation for specific heat at zero pressure (eq. (A4))

c_p specific heat at constant pressure

c_v specific heat at constant volume

c_v^* specific heat at zero pressure

d_4 constant in equation for specific heat at zero pressure

g acceleration due to gravity

J unit conversion factor

j mechanical equivalent of heat

K constant in equation of state (eq. (A1))

R gas constant

S entropy

T_c critical temperature

V specific volume

α constant in equation of state (eq. (A1))

δ flow deflection angle

Ξ_N functional representation of conservation of mass (eq. (A11))

Ψ_N functional representation of conservation of momentum (eq. (A12))

Ω_N functional representation of conservation of energy (eq. (A13))

Subscripts:

i	point in isentropic expansion
r	reference
N	normal
t	tangential

GENERAL EQUATIONS

The equation of state of CF_4 and an expression for its viscosity were obtained from E. I. du Pont de Nemours & Company. The equation of state is

$$p = \frac{RT}{V - b} + \frac{A_2 + B_2T + C_2e^{-KT}}{(V - b)^2} + \frac{A_3 + B_3T + C_3e^{-KT}}{(V - b)^3} + \frac{A_4 + B_4T}{(V - b)^4}$$

$$+ \frac{A_5 + B_5T + C_5e^{-KT}}{(V - b)^5} + (A_6 + B_6T)e^{\alpha V} \qquad \text{(A1)}$$

where p is given in lb/in^2, V in ft^3/lb, and T in ^oR and where

$$R = 1.219336 \times 10^{-1}$$
$$A_2 = -2.162959$$
$$B_2 = 2.135114 \times 10^{-3}$$
$$C_2 = -1.8941131 \times 10^{1}$$
$$A_3 = 4.404057 \times 10^{-3}$$
$$B_3 = 1.282818 \times 10^{-5}$$
$$C_3 = 5.39776 \times 10^{-1}$$
$$A_4 = 1.921072 \times 10^{-4}$$
$$B_4 = -3.918263 \times 10^{-7}$$
$$A_5 = -4.481049 \times 10^{-6}$$
$$B_5 = 9.062318 \times 10^{-9}$$
$$C_5 = -4.836678 \times 10^{-5}$$
$$A_6 = 5.83882 \times 10^{7}$$
$$B_6 = -9.26392 \times 10^{4}$$
$$b = 1.5000 \times 10^{-3}$$
$$K = 9.76798 \times 10^{-3}$$
$$\alpha = -6.61199 \times 10^{2}$$

The following expression was used for the viscosity of CF_4:

$$\mu = 149.5\left(\frac{T}{T_c}\right)^{3/2} \frac{1.22}{\left(\frac{T}{T_c}\right) + 0.22} \tag{A2}$$

where μ is in micropoise and T_c is the critical temperature (409.5° R).

The specific heat at constant volume is

$$c_v = c_v^* + J \int_{\infty}^{V} T\left(\frac{\partial^2 p}{\partial T^2}\right)_V dV \tag{A3}$$

A third-degree expression in temperature was obtained for c_v^* from a curve fit of points calculated from two overlapping fourth-degree expressions for c_v^* presented in reference 16 for a temperature range of 540° to 9000° R and a third-degree expression (obtained from E. I. du Pont de Nemours & Co.) for a temperature range of 180° to 1170° R. Each of these three expressions for c_v^* were curve fits of points calculated from partition functions. The equation for specific heat at zero pressure c_v^* used herein was fitted over a temperature interval of 180° to 2500° R and is

$$c_v^* = a_4 + b_4 T + c_4 T^2 + d_4 T^3 \tag{A4}$$

where c_v^* is in Btu/lb-°R and

$$a_4 = 1.90458084 \times 10^{-2}$$
$$b_4 = 3.00892783 \times 10^{-4}$$
$$c_4 = -1.30237441 \times 10^{-7}$$
$$d_4 = 1.96802894 \times 10^{-11}$$

Evaluating the integral term of equation (A3) by the equation of state (A1) gives

$$c_v = c_v^* - JTK^2 e^{-KT} \frac{C_2}{V - b} + \frac{C_3}{2(V - b)^2} + \frac{C_5}{4(V - b)^4} \tag{A5}$$

where $J = 1.850505 \times 10^{-1}$ Btu-in^2/(ft^3-lb).

The specific heat at constant pressure is

$$c_p = c_v - TJ \frac{\left[(\partial p/\partial T)_V\right]^2}{(\partial p/\partial V)_T} \tag{A6}$$

ISENTROPIC EXPANSION

Consider the isentropic expansion of CF_4 in a nozzle where the stagnation chamber pressure p_0 and temperature T_0 are specified. (The equation of state specifies V_0.)

The governing statement in the expansion is that the entropy remains constant:

$$S_0 - S_r = \int_{T_r}^{T_0} \frac{c_v\, dT}{T} + J \int_{V_r}^{V_0} \left(\frac{\partial p}{\partial T}\right)_V dV = S_i - S_r = \int_{T_r}^{T_i} \frac{c_v\, dT}{T} + J \int_{V_r}^{V_i} \left(\frac{\partial p}{\partial T}\right)_V dV \qquad (A7)$$

where the subscript r represents reference conditions taken herein as

$$S_r = 0.848 \quad \text{for} \quad \begin{cases} T_r = 820^{\circ}\ \text{R} \\ p_r = 1\ \text{psia} \\ V_r = 100\ \text{ft}^3/\text{lb} \end{cases}$$

This point was obtained from reference 21 where the datum enthalpy-entropy point was taken as zero at absolute zero for CF_4 in the solid state.

The subscript i represents the ith point in the expansion. Here, the temperature to which the flow is to be expanded isentropically is designated T_i. Thus, the two thermodynamic variables T_i and $S_0 = S_i$ completely specify a point in the expansion from which all other thermodynamic variables at this point, and hence flow quantities, may be calculated.

For simplicity of form, it is advantageous to express the thermodynamic variables at a point in the expansion as a function of T_i and V_i rather than T_i and S_i. The value of V_i is calculated from the following integrated form of equation (A7):

$$\begin{aligned} S_i - S_r = {} & a_4 \log_e \frac{T_i}{T_r} + b_4(T_i - T_r) + \frac{c_4}{2}(T_i^2 - T_r^2) + \frac{d_4}{3}(T_i^3 - T_r^3) \\ & + JK\left(e^{-KT_i} - e^{-KT_r}\right)\left[\frac{C_2}{V_r - b} + \frac{C_3}{2(V_r - b)^2} + \frac{C_5}{4(V_r - b)^4}\right] + JR \log_e\left(\frac{V_i - b}{V_r - b}\right) \\ & - J\left(B_2 - KC_2e^{-KT_i}\right)\left(\frac{1}{V_i - b} - \frac{1}{V_r - b}\right) - \frac{J\left(B_3 - KC_3e^{-KT_i}\right)}{2}\left[\frac{1}{(V_i - b)^2} - \frac{1}{(V_r - b)^2}\right] \\ & - \frac{J\left(B_5 - KC_5e^{-KT_i}\right)}{4}\left[\frac{1}{(V_i - b)^4} - \frac{1}{(V_r - b)^4}\right] - JB_4\left[\frac{1}{3(V_i - b)^3} - \frac{1}{3(V_r - b)^3}\right] \\ & + JB_6\left(\frac{e^{\alpha V_i}}{\alpha} - \frac{e^{\alpha V_r}}{\alpha}\right) \end{aligned} \qquad (A8)$$

The enthalpy H_i expressed as a function of T_i and V_i is

$$H_i - H_r = \int_{T_r}^{T_i}\left[c_v + V\left(\frac{\partial p}{\partial T}\right)_V\right]dT + \int_{V_r}^{V_i}\left[V\left(\frac{\partial p}{\partial V}\right)_T + T\left(\frac{\partial p}{\partial T}\right)_V\right]dV \tag{A9}$$

and becomes in integrated form

$$\begin{aligned}
H_i - H_r = {} & a_4(T_i - T_r) + b_4\frac{T_i^2 - T_r^2}{2} + c_4\frac{T_i^3 - T_r^3}{3} + d_4\frac{T_i^4 - T_r^4}{4} + J\left[e^{-KT_i}(KT_i + 1) - e^{-KT_r}(KT_r + 1)\right]\left[\frac{C_2}{V_r - b} + \frac{C_3}{2(V_r - b)^2} + \frac{C_5}{4(V_r - b)^4}\right] \\
& + JV_r\left[\frac{R}{V_r - b}(T_i - T_r) + \frac{B_2(T_i - T_r) + C_2\left(e^{-KT_i} - e^{-KT_r}\right)}{(V_r - b)^2} + \frac{B_3(T_i - T_r) + C_3\left(e^{-KT_i} - e^{-KT_r}\right)}{(V_r - b)^3} + \frac{B_4(T_i - T_r)}{(V_r - b)^4}\right. \\
& \left. + \frac{B_5(T_i - T_r) + C_5\left(e^{-KT_i} - e^{-KT_r}\right)}{(V_r - b)^5} + B_6e^{\alpha V_r}(T_i - T_r)\right] - J\left\{RT_i\left[\log_e\left(\frac{V_i - b}{V_r - b}\right) + \frac{b}{V_r - b} - \frac{b}{V_i - b}\right]\right. \\
& + 2\left(A_2 + B_2T_i + C_2e^{-KT_i}\right)\left[\frac{1}{V_r - b} + \frac{b}{2(V_r - b)^2} - \frac{1}{V_i - b} - \frac{b}{2(V_i - b)^2}\right] + 3\left(A_3 + B_3T_i + C_3e^{-KT_i}\right)\left[\frac{1}{2(V_r - b)^2} + \frac{b}{3(V_r - b)^3} - \frac{1}{2(V_i - b)^2} - \frac{b}{2(V_i - b)^3}\right] \\
& + 4A_4\left[\frac{1}{3(V_r - b)^3} + \frac{b}{4(V_r - b)^4} - \frac{1}{3(V_i - b)^3} - \frac{b}{4(V_i - b)^4}\right] + 5\left(A_5 + B_5T_i + C_5e^{-KT_i}\right)\left[\frac{1}{4(V_r - b)^4} + \frac{b}{5(V_r - b)^5} - \frac{1}{4(V_i - b)^4} - \frac{b}{5(V_i - b)^5}\right] \\
& + \left\{\frac{JV_i^2}{2}\left[\frac{-4B_4T_i}{(V_i - b)^5} + A_6\alpha e^{\alpha V_i} + B_6T_i\alpha e^{\alpha V_i}\right] + JV_i\left[\frac{B_4T_i}{(V_i - b)^4} + A_6e^{\alpha V_i} + B_6T_ie^{\alpha V_i}\right] - \frac{JV_r^2}{2}\left[\frac{-4B_4T_i}{(V_r - b)^5} + A_6\alpha e^{\alpha V_r} + B_6T_i\alpha e^{\alpha V_r}\right]\right. \\
& \left. - JV_r\left[\frac{B_4T_i}{(V_r - b)^4} + A_6e^{\alpha V_r} + B_6T_ie^{\alpha V_r}\right]\right\} + JT_i\left\{R\log_e\left(\frac{V_i - b}{V_r - b}\right) - \left(B_2 - KC_2e^{-KT_i}\right)\left(\frac{1}{V_i - b} - \frac{1}{V_r - b}\right)\right. \\
& \left. - \frac{B_3 - KC_3e^{-KT_i}}{2}\left[\frac{1}{(V_i - b)^2} - \frac{1}{(V_r - b)^2}\right] - B_4\left[\frac{1}{3(V_i - b)^3} - \frac{1}{3(V_r - b)^3}\right] - \frac{B_5 - KC_5e^{-KT_i}}{4}\left[\frac{1}{(V_i - b)^4} - \frac{1}{(V_r - b)^4}\right] + \frac{B_6}{\alpha}\left(e^{\alpha V_i} - e^{\alpha V_r}\right)\right\}
\end{aligned} \tag{A10}$$

where $H_r = 200$ Btu/lb at reference conditions (ref. 21). The total enthalpy H_0 can be computed from equation (A10) by substituting the stagnation temperature and volume in place of the values at a given point in the expansion.

For a given point in the expansion (assuming T_i and V_i have been calculated for this point), the pressure p_i can be obtained by using equation (A1) and the viscosity μ_i, by using equation (A2). Other flow quantities of interest to this investigation at points in the expansion are given in the following equations:

Limiting velocity:

$$u_l = \sqrt{2gj(H_0 - H_{sv})}$$

where H_{sv} is the enthalpy of saturated vapor extrapolated (from points presented in ref. 21) to zero pressure and is approximately 2.27×10^5 joules/kg; g is the acceleration of gravity; and j is the mechanical equivalent of heat.

Local velocity:

$$u_i = \sqrt{2gj(H_0 - H_i)}$$

Local specific heat ratio:

$$\gamma_i = (c_p)_i / (c_v)_i$$

where $(c_p)_i$ and $(c_v)_i$ are given by equations (A6) and (A5), respectively.

Local speed of sound:

$$a_i = \left[\gamma\left(\frac{\partial p}{\partial \rho}\right)_T\right]_i^{1/2}$$

Local Mach number:

$$M_i = u_i / a_i$$

The other flow parameters used in this report are easily obtained from the foregoing relations.

FLOW BEHIND NORMAL AND OBLIQUE SHOCK WAVES IN CF_4

In the previous section, CF_4 was expanded isentropically from specified stagnation conditions to a given Mach number. In this section, the flow behind two-dimensional, infinitesimally thin, normal and oblique shock waves when the process is always in a state of equilibrium will be considered.

Static Conditions Behind Shock

The following diagram illustrates the problem being considered and the notation that will be used throughout this analysis:

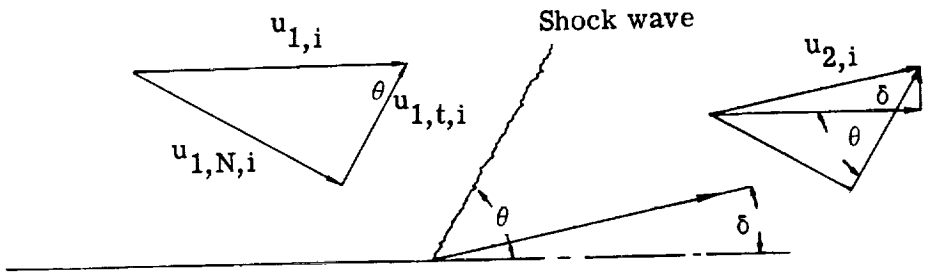

where

$$\left(u_{1,i}\right)\sin\,\theta = u_{1,N,i}$$

$$\left(u_{1,i}\right)\cos\,\theta = u_{1,t,i} = u_{2,t,i}$$

The governing conservation equations are as follows:

For mass,

$$\frac{u_{1,N,i}}{V_{1,i}} = \frac{u_{2,N,i}}{V_{2,i}} = \Xi_{N,i} \tag{A11}$$

For momentum,

$$p_{1,i} + \frac{1}{g}\frac{\left(u_{1,N,i}\right)^2}{V_{1,i}} = p_{2,i} + \frac{1}{g}\frac{\left(u_{2,N,i}\right)^2}{V_{2,i}} = \Psi_{N,i} \tag{A12}$$

For energy,

$$H_{1,i} + \frac{\left(u_{1,N,i}\right)^2}{2gj} = H_{2,i} + \frac{\left(u_{2,N,i}\right)^2}{2gj} = \Omega_{N,i} \tag{A13}$$

Substituting $u_{2,N,i} = \Xi_{N,i}V_{2,i}$ from the conservation equation for mass into the conservation equations for momentum and energy and noting that all thermodynamic variables have been previously expressed as functions of temperature and specific volume give

$$p\left(T_{2,i},V_{2,i}\right) + \frac{1}{g}\left[\Xi_N\left(T_{1,i},V_{1,i},\theta_i\right)\right]^2 V_{2,i} = \psi_N\left(T_{1,i},V_{1,i},\theta_i\right) \tag{A14}$$

and

$$H\left(T_{2,i},V_{2,i}\right) + \frac{\left[\Xi_N\left(T_{1,i},V_{1,i},\theta_i\right)\right]^2\left(V_{2,i}\right)^2}{2gj} = \Omega_N\left(T_{1,i},V_{1,i},\theta_i\right) \tag{A15}$$

where $H\left(T_{2,i},V_{2,i}\right)$ is the functional representation of the static enthalpy behind the shock (eq. (A10)) and $p\left(T_{2,i},V_{2,i}\right)$ is the functional representation of the static pressure

behind the shock (equation of state, eq. (A1)). Thus for given stream conditions designated by expansion points in the previous section, equations (A14) and (A15) for a given shock-wave inclination angle (either normal or oblique shocks) are expressed in terms of two unknowns $T_{2,i}$ and $V_{2,i}$. These two equations were solved simultaneously for the two unknowns with a digital computer program.

The thermodynamic and flow quantities behind a particular shock wave are stipulated herein (once the independent variables $T_{2,i}$ and $V_{2,i}$ are known) by the following equations:

Velocity:

$$u_{2,i} = \left[\left(u_{2,N,i}\right)^2 + \left(u_{2,t,i}\right)^2\right]^{1/2}$$

where

$$u_{2,N,i} = \Xi_N\left(T_{1,i}, V_{1,i}, \theta_i\right) V_{2,i}$$

and

$$u_{2,t,i} = u_{1,t,i}$$

Ratio of specific heats:

$$\gamma_{2,i} = \frac{c_p\left(T_{2,i}, V_{2,i}\right)}{c_v\left(T_{2,i}, V_{2,i}\right)}$$

Speed of sound:

$$a_{2,i} = \left[\gamma\left(\frac{\partial p}{\partial \rho}\right)_T\right]_{2,i}^{1/2}$$

Mach number:

$$M_{2,i} = \frac{u_{2,i}}{a_{2,i}}$$

The functional relations expressed in these equations are given in the section of this appendix entitled "General Equations."

Total Conditions Behind Shock

With the static conditions behind a given shock wave determined as outlined in the previous section, the total conditions behind this shock can be obtained by bringing the flow to rest isentropically. The governing statement in this compression process is that the entropy (stipulated by the static condition behind the shock) remains constant; that is,

$$S_{2,i} = S(T_{2,i}, V_{2,i}) = \text{Constant} = S(T_3, V_3)_i \tag{A16}$$

where $T_{3,i}$ and $V_{3,i}$ are the respective stagnation temperature and specific volume behind the ith shock.

A second equation in terms of $T_{3,i}$ and $V_{3,i}$ which stipulates the final point in this compression process (the point at which the velocity is zero) is obtained from the fact that the total enthalpy is constant on either side of the shock. Thus,

$$H_0 = H(T_0, V_0) = H(T_3, V_3)_i \tag{A17}$$

Equations (A16) and (A17) were solved simultaneously for the two unknowns with a digital computer program. Once $T_{3,i}$ and $V_{3,i}$ were determined, $p_{3,i}$ was calculated from the equation of state:

$$p_{3,i} = p(T_3, V_3)_i$$

COMPUTER PROGRAMS FOR EVALUATING ISENTROPIC EXPANSIONS AND FLOWS ACROSS NORMAL AND OBLIQUE SHOCKS IN CF_4

FORTRAN IV Control Data series 6000 computer programs were developed for evaluating isentropic expansions and flows across normal and oblique shocks in CF_4 in the format presented in the previous sections of this appendix. The abstracts and listings for these programs are given in appendix C. Inputs common (need to be input with first case only) to these programs are

Symbol	Machine name	Comments
R	R	Gas constant, 1.219336×10^{-1} $(ft^3)(psia)/lb\text{-}^oR$
A_2	A2	Constants in equation of state
A_3	A3	
A_4	A4	
A_5	A5	
A_6	A6	
B_2	B2	
B_3	B3	
B_4	BIGB4	
B_5	B5	
B_6	B6	

Symbol	Machine name	Comments
C_2	C2	Constants in equation of state
C_3	C3	
C_5	C5	
b	BLIT	
α	AL	
-K	XKK	
a_4	Z4	Constants in curve fit of c_v*
b_4	B4	
c_4	C4	
d_4	D4	
J	XJ	1.850505×10^{-1} Btu-in^2/(ft^3-lb)
g	GEE	32.3 ft/sec^2
j	AJA	778 ft-lb/Btu
T_c	TZ	409.5° R
T_r	TREF	820° R
p_r	PREF	1.0 psia
S_r	SREF	0.848 Btu/lb-°R
H_r	HREF	200 Btu/lb

Program A: Isentropic Expansion and Static Conditions Behind Normal and Oblique Shock Waves in Tetrafluoromethane

The primary inputs to this program are the stagnation conditions for a particular isentropic expansion p_0 and T_0 and a tabulation of values of T_i $(T_i < T_0)$ in a decreasing sequence which stipulates the stations to which the flow is to be expanded. For each of these T_i stations the flow quantities and thermodynamic properties are calculated and tabulated.

For the shock-wave calculations, a minimum Mach number and a shock-wave angle θ are specified. At all T_i stations for which the local Mach number exceeds the specified value, static properties behind a shock at the input θ are calculated and tabulated. The program is set up so that the shock portion is activated when the stream Mach number exceeds 3.

Input

Symbol	Machine name	Comments
p_0	PEE	Total conditions from which the flow is expanded
T_0	TEE	
T_i	TEI	Table listed in descending order

Input

Symbol	Machine name	Comments
	IEND	Number of entries in TEI table
$T_{2,i}$	TC	"Estimates tables" correspond to values of T_i for $M_1 \geq 3$
$V_{2,i}$	VC	
	A	Initial estimate
	B	Upper limit
	DELTX	Iteration increment
	E1	Relative error criterion
	E2	Absolute error criterion
	MAXI	Maximum number of iterations
θ	THETA	Shock angle

Used to find V_0 and V_1

Output

Symbol	Machine name	Comments
V_0	V0	Total conditions
p_0 (Input)	P0	
H_0	H0	
S_0	S0	
γ_0	GAMMA	
T_r (Input)	TREF	Reference conditions
p_r (Input)	PREF	
T_i (Input table)	TEMPERATURE	Stream static properties listed in corresponding sequence
V_i	VOLUME	
p_i	PRESSURE	
H_i	ENTHALPY	
M_i	MACH NO	
u_i	VELOCITY	
$(c_p)_i$	CP	
$(c_v)_i$	CV	
γ_i	GAMMA	
a_i	ACCELERATION [speed of sound]	
μ_i	VISCOSITY	
$(R_1/ft)_i$	REYNOLDS NO/FT	
$(p_1/p_0)_i$	P1/P0	
$(T_1/T_0)_i$	T1/T0	

Output Symbol	Machine name	Comments
$V_{2,i}$	VOLUME2	Static conditions behind shock at specified θ
$T_{2,i}$	TEMPERATURE2	
$p_{2,i}$	PRESSURE2	
$u_{2,i}$	VELOCITY2	
$M_{2,i}$	MACH NO2	
$H_{2,i}$	ENTHALPY2	
$\rho_{2,i}$	RHO2	
$(c_v)_{2,i}$	CV2	
$(c_p)_{2,i}$	CP2	
$\gamma_{2,i}$	GAMM2	
$a_{2,i}$	SPEED OF SOUND	
$(T_2/T_0)_i$	T2/T0	Static condition ratios across shock
$(V_1/V_2)_i$	V1/V2	
$(T_2/T_1)_i$	T2/T1	
$(p_2/p_1)_i$	P2/P1	
$u_{1,N,i}$	U1N	Velocity components parallel and normal to shock
$u_{1,t,i}$	U1T	
$u_{2,t,i}$		
$u_{2,N,i}$	U2N	

Program B: Ballistic-Range Normal Shock

The normal-shock portion of the preceding program was used with input modifications in evaluation of the normal-shock static-density, static-temperature, and static-pressure ratios given in figures 21 to 23 as functions of velocity in conjunction with ballistic-range tests conducted in CF_4. The inputs to this program are range static temperature and pressure along with projectile velocity.

Input Symbol	Machine name	Comments	
T_i	TEI	Ballistic-range static conditions	Corresponding sequence
p_i	PEI		
u_i	UI	Projectile velocity	
	IEND	Number of sequential entries	

Input

Symbol	Machine name	Comments
$T_{2,i}$	TC	"Estimates table" entries correspond to T_i, p_i, and u_i
$V_{2,i}$	VC	
	A	Initial estimate
	B	Upper limit
	DELTX	Iteration increment
	E1	Relative error criterion
	E2	Absolute error criterion
	MAXI	Maximum number of iterations

used to find values of V_i

Output

Symbol	Machine name	Comments
T_i (Input)	TEMPERATURE	Ballistic-range static conditions
p_i (Input)	PRESSURE	
V_i	VOLUME	
u_i (Input)	VELOCITY	
M_i	MACH NO	
H_i	ENTHALPY	
$(c_p)_i$	CP	
$(c_v)_i$	CV	
γ_i	GAMMA	
a_i	ACCELERATION [speed of sound]	
μ_i	VISCOSITY	
$T_{2,i}$	TEMPERATURE2	Static conditions behind normal shock
$p_{2,i}$	PRESSURE2	
$V_{2,i}$	VOLUME2	
$u_{2,i}$	VELOCITY2	
$M_{2,i}$	MACH NO2	
$H_{2,i}$	ENTHALPY2	
$\rho_{2,i}$	RHO2	
$(c_v)_{2,i}$	CV2	
$(c_p)_{2,i}$	CP2	
$\gamma_{2,i}$	GAMMA2	
$a_{2,i}$	SPEED OF SOUND	
ρ_2/ρ_1	V2/V1	Ratio of static conditions across shock
T_2/T_1	T2/T1	
p_2/p_1	P2/P1	

Program C: Total Conditions Behind Shock

For a given shock, the static temperature $T_{2,i}$ and static specific volume $V_{2,i}$ behind the shock determined from either of the preceding programs are used as inputs along with the stagnation temperature and pressure, in the case of the expansion problem, and the static temperature, static pressure, and projectile velocity, in the case of the ballistic-range problem, for a third computer program. This program was set up in the format presented in this appendix in the section entitled "Total Conditions Behind Shock" to determine these conditions.

Input

Symbol	Machine name	Comments
$p_0, p_{1,i}$	PEE	Total conditions for expansion case; static conditions for ballistic-range case
$T_0, T_{1,i}$	TEE	
$V_0, V_{1,i}$	VEE	
	IEND	Number of entries in following tables
M_1	XMACH	
u_1	U2I	Input zero for expansion case Input velocity for ballistic-range case
$T_{2,i}$	TEI	
$V_{2,i}$	VEI	
$(p_1/p_0)_i$	PRAT	Input 1 for ballistic-range case
$V_{3,i}$	VC	Estimates
$T_{3,i}$	TC	Estimates

Output

Symbol	Machine name	Comments
T_3	T2T	
V_3	V2T	
p_3	P2T	
S_2	S2	Entropy behind shock
p_3/p_0	P2T/P0	For ballistic-range case these ratios have the same value because of "ad hoc" substitution
p_3/p_1	P2T/P1	
T_3/T_0	T2T/T0	Becomes T_3/T_1 for ballistic-range case
V_3/V_0	V2T/V0	Becomes V_3/V_1 for ballistic-range case
H_0	H0	
S_0	S0	

APPENDIX B

HYPERSONIC NOZZLE CONTOURS FOR TETRAFLUOROMETHANE

By James L. Hunt and Lillian R. Boney

Inviscid axisymmetric contours for a Mach 6 nozzle for tetrafluoromethane (CF_4) at various stagnation conditions and maximum turning angles of the flow were calculated with the use of the computer program presented in reference 22. These calculations involved an application of the method of characteristics in which the real-gas variations of the thermodynamic properties of CF_4 in an isentropic expansion were required inputs.

As presented in reference 22, the viscous part of the program (Part III) that calculates the boundary-layer displacement thickness along the nozzle which must be added to the inviscid contour to obtain the physical-wall contour is restricted to a gas composed of diatomic or linear polyatomic molecules. The vibrational energy modes of these molecules display harmonic oscillator characteristics having only one fundamental frequency.

These "gas type" restrictions are imposed on the viscous part of the program through the expression for the local static enthalpy, which is written in reference 22 as

$$H = \frac{7}{2} T + \frac{\Theta}{e^{\Theta/T} - 1} \tag{B1}$$

where Θ is the characteristic molecular vibrational temperature and T is the static temperature. This equation includes real-gas effects due to vibration but no real-gas effects due to pressure; however, provisions are made in the program to account for real-gas effects due to pressure on enthalpy by multiplying equation (B1) by a correction factor expressed as a polynomial in pressure.

Tetrafluoromethane is a nonlinear polyatomic molecule, the vibrational energy modes of which display anharmonic oscillator characteristics having four fundamental frequencies. Thus, in order to make the boundary-layer displacement-thickness part of the program applicable to tetrafluoromethane, the expression for the static enthalpy in the program must be made to comply with this molecular description.

Since provisions are already made in the program to account for real-gas effects due to pressure through a correction factor rather than an equation of state, the enthalpy H must be expressed as a function of temperature only and may be stated as

$$H = E + RT \tag{B2}$$

where R is the gas constant and the internal energy E is

$$E = E_{tran} + E_{rot} + E_{vib}$$

From considerations of kinetic theory, the translation-energy contribution is

$$E_{tran} = \frac{3}{2} RT \tag{B3}$$

The rotational contribution for nonlinear polyatomic molecules is

$$E_{rot} = \frac{3}{2} RT \tag{B4}$$

In evaluating the vibrational contribution to the internal energy of CF_4, anharmonics may be neglected safely for lower vibrational levels, that is, at lower temperatures for which the neglect of the interaction of vibration and rotation is also permissible. Calculations based on expressions presented in reference 16 for both the harmonic and anharmonic energy terms show that the harmonic assumption (neglecting anharmonics) induces an error in the total vibrational energy of only 2.56×10^{-2} percent at 100° K and 2.88 percent at 1000° K. Since the stagnation temperature in the nozzle being designed was only 811° K, and in order to simplify the programing procedure, all vibrational contributions were assumed to be of a harmonic nature. The harmonic oscillator partition function Q_{vib} for CF_4 is (ref. 16)

$$Q_{vib} = \prod_{i=1}^{4} \left(1 - e^{-\Theta_i/T}\right)^{-g_i} \tag{B5}$$

where the degeneracies g for $i = 1, 2, 3$, and 4 are

$g_1 = 1$ $\quad \Theta_1 = 2341^{\circ}$ R $\quad (1300^{\circ}$ K)

$g_2 = 2$ $\quad \Theta_2 = 1127^{\circ}$ R $\quad (626^{\circ}$ K)

$g_3 = 3$ $\quad \Theta_3 = 3322^{\circ}$ R $\quad (1845^{\circ}$ K)

$g_4 = 3$ $\quad \Theta_4 = 1653^{\circ}$ R $\quad (918^{\circ}$ K)

Now

$$E_{vib} = RT^2 \frac{d\left(\log_e Q_{vib}\right)}{dT} \tag{B6}$$

The vibrational contribution to the internal energy is

$$E_{vib} = R \sum_{i=1}^{4} \frac{g_i \Theta_i}{e^{\Theta_i/T} - 1} \tag{B7}$$

Thus, the expression for the enthalpy of tetrafluoromethane, neglecting anharmonics and Van der Waal effects, becomes

$$\frac{H}{R} = 4T + \sum_{i=1}^{4} \frac{g_i \Theta_i}{e^{\Theta_i/T} - 1} \tag{B8}$$

All the changes (approximately 21 equations and "if" statements) made to the viscous part (Part III) of the nozzle design program of reference 22 to adapt it for use herein with CF_4 stem from the enthalpy expression in equation (B8). The form of the turbulent skin-friction law as used in reference 22 was left unchanged.

Part III of the FORTRAN IV IBM 7090 computer program presented in reference 22 which computes the displacement thickness along a nozzle and applies it to the inviscid results to yield a physical contour, as modified to comply with the molecular description of CF_4, is given in program D of appendix C. The flow properties at the edge of the inviscid region are supplied by Parts I and II of the parent program, the inputs and outputs having the same form as Part III. (For additional information, see ref. 22.)

Table III gives the coordinates of a Mach 6 nozzle with a test-section diameter of 16.4 cm designed with this program for CF_4 at a stagnation temperature of 811° K, a stagnation pressure of 1724 N/cm^2, and a turning angle of 18°. A sketch of this nozzle is shown in figure 35.

TABLE III.- CF_4 NOZZLE COORDINATES

[Mach number, 6; stagnation pressure, 1724 N/cm^2; stagnation temperature, 811° K; turning angle, 18°]

x		y		y (inviscid)		Mach number
in.	cm	in.	cm	in.	cm	
0.0000	0.0000	0.0637	0.1618	0.0625	0.1588	1.00
.1000	.2540	.0656	.1666	-----	-----	----
.2000	.5080	.0680	.1727	-----	-----	----
.3000	.7620	.0718	.1824	-----	-----	----
.4000	1.0160	.0771	.1958	-----	-----	----
.5000	1.2700	.0840	.2134	-----	-----	----
.6000	1.5240	.0930	.2362	-----	-----	----
.7000	1.7780	.1045	.2654	.1027	.2609	2.295
.8000	2.0320	.1196	.3038	-----	-----	----
.9000	2.2860	.1397	.3548	-----	-----	----
1.0000	2.5400	.1640	.4166	.1616	.4105	2.920
1.1000	2.7940	.1913	.4859	-----	-----	----
1.2000	3.0480	.2205	.5601	-----	-----	----
1.3000	3.3020	.2511	.6378	.2458	.6243	3.361
1.4000	3.5560	.2827	.7181	-----	-----	----
1.5000	3.8100	.3148	.7998	-----	-----	----
1.6000	4.0640	.3475	.8827	-----	-----	----
1.7000	4.3180	.3805	.9665	-----	-----	----
1.8000	4.5720	.4137	1.0508	.4046	1.0277	3.859
1.9000	4.8260	.4471	1.1356	-----	-----	----
2.0000	5.0800	.4806	1.2207	-----	-----	----
2.1000	5.3340	.5142	1.3061	-----	-----	----
2.2000	5.5880	.5480	1.3919	.566	1.4376	4.202
2.3000	5.8420	.5817	1.4775	-----	-----	----
2.4000	6.0960	.6154	1.5631	-----	-----	----
2.5000	6.3500	.6491	1.6487	-----	-----	----
2.6000	6.6040	.6822	1.7328	-----	-----	----
2.7000	6.8580	.7148	1.8158	-----	-----	----
2.8000	7.1120	.7470	1.8974	.724	3.2766	4.430
2.9000	7.3660	.7788	1.9782	-----	-----	----
3.0000	7.6200	.8101	2.0577	.786	1.9964	4.500

TABLE III.- CF_4 NOZZLE COORDINATES – Continued

x		y		y (inviscid)		Mach number
in.	cm	in.	cm	in.	cm	
3.1000	7.8740	0.8410	2.1361	----	-----	----
3.2000	8.1280	.8715	2.2136	----	-----	----
3.3000	8.3820	.9017	2.2903	----	-----	----
3.4000	8.6360	.9314	2.3658	0.903	2.2936	4.621
3.5000	8.8900	.9606	2.4399	----	-----	----
3.6000	9.1440	.9895	2.5133	----	-----	----
3.7000	9.3980	1.0180	2.5857	----	-----	----
3.9500	10.0330	1.0876	2.7625	----	-----	----
4.2000	10.6680	1.1548	2.9332	1.114	2.8296	4.811
4.4500	11.3030	1.2198	3.0983	----	-----	----
4.7000	11.9380	1.2829	3.2586	----	-----	----
4.9500	12.5730	1.3440	3.4138	----	-----	----
5.2000	13.2080	1.4032	3.5641	----	-----	----
5.4500	13.8430	1.4605	3.7097	----	-----	----
5.7000	14.4780	1.5160	3.8506	----	-----	----
5.9500	15.1130	1.5699	3.9875	----	-----	----
6.2000	15.7480	1.6220	4.1199	----	-----	----
6.4500	16.3830	1.6728	4.2489	----	-----	----
6.7000	17.0180	1.7223	4.3746	----	-----	----
6.9500	17.6530	1.7703	4.4966	----	-----	----
7.2000	18.2880	1.8170	4.6152	----	-----	----
7.4500	18.9230	1.8623	4.7302	1.775	4.5085	5.271
7.7000	19.5580	1.9063	4.8420	----	-----	----
7.9500	20.1930	1.9491	4.9507	----	-----	----
8.2000	20.8280	1.9906	5.0561	----	-----	----
8.4500	21.4630	2.0310	5.1587	----	-----	----
8.7000	22.0980	2.0703	5.2586	----	-----	----
8.9500	22.7330	2.1085	5.3556	----	-----	----
9.2000	23.3680	2.1458	5.4503	----	-----	----
9.4500	24.0030	2.1822	5.5428	----	-----	----
9.7000	24.6380	2.2176	5.6327	----	-----	----
9.9500	25.2730	2.2520	5.7201	----	-----	----
10.2000	25.9080	2.2855	5.8052	----	-----	----
10.4500	26.5430	2.3181	5.8880	----	-----	----

TABLE III.- CF_4 NOZZLE COORDINATES – Continued

x		y		y (inviscid)		Mach number
in.	cm	in.	cm	in.	cm	
10.7000	27.1780	2.3498	5.9685	----	-----	----
10.9500	27.8130	2.3806	6.0467	----	-----	----
11.2000	28.4480	2.4106	6.1229	----	-----	----
11.4500	29.0830	2.4397	6.1968	----	-----	----
11.7000	29.7180	2.4680	6.2687	----	-----	----
11.9500	30.3530	2.4956	6.3388	2.330	5.9182	5.605
12.2000	30.9880	2.5223	6.4066	----	-----	----
12.4500	31.6230	2.5484	6.4729	----	-----	----
12.7000	32.2580	2.5737	6.5372	----	-----	----
12.9500	32.8930	2.5982	6.5994	----	-----	----
13.2000	33.5280	2.6222	6.6604	----	-----	----
13.4500	34.1630	2.6456	6.7198	----	-----	----
13.7000	34.7980	2.6684	6.7777	----	-----	----
13.9500	35.4330	2.6907	6.8344	----	-----	----
14.2000	36.0680	2.7123	6.8892	----	-----	----
14.4500	36.7030	2.7334	6.9428	----	-----	----
14.7000	37.3380	2.7539	6.9949	----	-----	----
14.9500	37.9730	2.7738	7.0455	----	-----	----
15.2000	38.6080	2.7932	7.0947	----	-----	----
15.4500	39.2430	2.8120	7.1425	----	-----	----
15.7000	39.8780	2.8303	7.1890	----	-----	----
15.9500	40.5130	2.8481	7.2342	----	-----	----
16.2000	41.1480	2.8653	7.2779	----	-----	----
16.4500	41.7830	2.8820	7.3203	----	-----	----
16.7000	42.4180	2.8982	7.3614	----	-----	----
16.9500	43.0530	2.9139	7.4013	----	-----	----
17.2000	43.6880	2.9292	7.4402	2.679	6.805	5.839
17.4500	44.3230	2.9440	7.4778	----	-----	----
17.7000	44.9580	2.9583	7.5141	----	-----	----
17.9500	45.5930	2.9721	7.5491	----	-----	----
18.2000	46.2280	2.9855	7.5832	----	-----	----
18.4500	46.8630	2.9985	7.6162	----	-----	----
18.7000	47.4980	3.0111	7.6482	----	-----	----

TABLE III.- CF_4 NOZZLE COORDINATES – Concluded

x		y		y (inviscid)		Mach number
in.	cm	in.	cm	in.	cm	
18.9500	48.1330	3.0232	7.6789	----	----	----
19.2000	48.7680	3.0350	7.7089	----	----	----
19.4500	49.4030	3.0463	7.7376	----	----	----
19.7000	50.0380	3.0571	7.7650	----	----	----
19.9500	50.6730	3.0677	7.7920	----	----	----
20.2000	51.3080	3.0779	7.8179	----	----	----
20.4500	51.9430	3.0878	7.8430	----	----	----
20.7000	52.5780	3.0973	7.8671	----	----	----
20.9500	53.2130	3.1064	7.8903	----	----	----
21.2000	53.8480	3.1152	7.9126	----	----	----
21.4500	54.4830	3.1237	7.9342	----	----	----
21.7000	55.1180	3.1319	7.9550	2.777	7.054	5.944
21.9500	55.7530	3.1397	7.9748	----	----	----
22.2000	56.3880	3.1473	7.9941	----	----	----
22.4500	57.0230	3.1545	8.0124	----	----	----
22.7000	57.6580	3.1615	8.0302	----	----	----
22.9500	58.2930	3.1682	8.0472	----	----	----
23.2000	58.9280	3.1746	8.0635	----	----	----
23.4500	59.5630	3.1807	8.0790	----	----	----
23.7000	60.1980	3.1868	8.0945	----	----	----
23.9500	60.8330	3.1926	8.1092	----	----	----
24.2000	61.4680	3.1956	8.1168	----	----	----
24.4500	62.1030	3.2010	8.1305	----	----	----
24.7000	62.7380	3.2062	8.1437	----	----	----
24.9500	63.3730	3.2112	8.1564	----	----	----
25.2000	64.0080	3.2160	8.1686	----	----	----
25.4500	64.6430	3.2206	8.1803	----	----	----
25.7000	65.2780	3.2250	8.1915	----	----	----
25.9500	65.9130	3.2291	8.2019	2.801	7.115	5.999

APPENDIX C

DIGITAL COMPUTER PROGRAM LISTINGS

APPENDIX C – Continued

Program A

NASA-LANGLEY RESEARCH CENTER

01 5	01 7 PROGRAM NO	COMPUTER PROGRAM ABSTRACT	01 14 DATE
LAR	E 1263		10/68

01 20 TITLE OF PROGRAM (61 CHARACTERS MAXIMUM)
Isentropic Expansion and Static Conditions Behind Normal and Oblique Shock Waves in Tetrafluoromethane

PARENT PROGRAM: 02 14 CATEGORY | 02 15 SITE | 02 16 PROGRAM NO

02 26 CATEGORY	02 27 LANGUAGE NO 1	02 32 LANGUAGE NO 2	02 37 KEY WORDS (8 MAXIMUM SEPARATED BY COMMAS)
R	FØR6M		Isentropic, Expansion, Static, Shock, Tetrafluoromethane

WHO TO CONTACT ABOUT THE PROGRAM

05 14 CONTACT	05 28 SITE	05 31 ORGN CODE	05 39 PROJECT NO	05 45 NASA CENTER
K. A. Smith	LAR	11.170	RGL-168	

05 48 STATUS: ☐ A UNDER DEVELOPMENT ☐ B OPERATIONAL ☒ C COMPLETED

05 49 ☐ A THIS PROGRAM IS NOT FOR SHARING

DATES		05 58 REVISION CODE	TIME AND COST FOR DEVELOPMENT			
05 50 INITIATED	05 54 COMPLETED	☐ A REVISION ☐ B CANCELLATION	05 59 MANMONTHS (59 60 61 62 63)	05 64 MACHINE HOURS (64 65 66 67 68)	05 69 COMPUTER TYPE	05 74 TOTAL COST (DOLLARS) (74 75 76 77 78 79 80)
10/66	10/68				6000	

ELITE MARGIN | PICA MARGIN

CARD NUMBER | COLUMN 14

ABSTRACT

The relations for isentropic expansions and static conditions behind normal and oblique shock waves in equilibrium tetrafluoromethane are programed to yield the static thermodynamic properties of CF_4 in high-speed, one-dimensional flow. The primary inputs to this program are the stagnation conditions for a given expansion and a tabulation of temperatures to which the flow is to be expanded and processed through a specified shock.

APPENDIX C – Continued

Program A – Continued

```
      PROGRAM E1263(INPUT,OUTPUT,TAPE5=INPUT,TAPE6=OUTPUT,TAPE8)
$IBFTC ISEFRN  DECK,LIST
      COMMON A2,A3,A4,A5,B2,B3,B4,B5,C2,C3,C4,C5,XKK,R,TREF,VREF,BLIT,XJ
      COMMON D4,Z4,ESS,TUFF,CLOD,GEE,AJA,KX,P2I(30),U2I(30),H2I(30)
      COMMON PT2(30),RHO(30),TE2I(30),VE2I(30),CV2(30),CP2(30),GAM2(30)
      COMMON ACC2(30),XMACH2(30),RORAT(30),TRAT(30),PRAT(30),PTRAT(30)
      COMMON TH
      COMMON V1N(30),V2N(30),V1T(30)
      COMMON BIGB4,B6,A6,AL,TZ
      COMMON/CLUX/TC ,VC
      COMMON/DESP/VOODOO,ZULU
      EXTERNAL FOP
      DIMENSION TC(30),VC(30)
      DIMENSION P1ORAT(30),T1ORAT(30),REN(30)
      COMMON /RATS/PEE,TEE,VIS2(30),PT2ORT(30),P1T2RT(30),T2ORT(30)
      EQUIVALENCE (C3,G3),(C5,XJ3),(C2,D3)
      PO (XL,AT)=1./EXP(XL*AT)
      DIMENSION TEI(30),VEI(30),PEI(30),VI(30),GAM(30),SPEED(30)
      DIMENSIONXMACH(30),CP(30),CV(30),H(30),VIS(30)
      NAMELIST /DATA/A2,A3,A4,A5,A6,B2,B3,BIGB4,B5,B6,B4,AL,
     1C2,C3,C4,C5,XKK,XJ,R,BLIT,D4,PEE,TEE,GEE,AJA,NUMB,INT,Z4,A,B,
     2DELTX,IEND,TEI,E1,E2,MAXI,TREF,PREF,TZ,TC,VC,THETA
   99 READ(5,DATA)
      WRITE(6,DATA)
      WRITE(6,88)A2,A3,A4,A5,B2,B3,B4,B5
   88 FORMAT(10H0A2 5 B2 5//8E13.5)
      WRITE(6,89)C2,C3,C4,C5,XKK,XJ,R,BLIT
   89 FORMAT(20H0C2 5  K   J   R   B/8E13.5)
      WRITE(6,90)D4,PEE,TEE,GEE,AJA,NUMB,INT,Z4
   90 FORMAT(23H0D4  PO  TO  G  J  N  I/5E13.5,2I13,E14.5)
      KX=1
      TH=THETA*0.0174532925
      VOODOO=TEE
      ZULU=PEE
      CALL ITR2(SP,A,B,DELTX,FOP,E1,E2,MAXI,ICODE)
    1 VEE=SP
```

```
      VOODOO=TREF
      ZULU=PREF
      CALL  ITR2(SP,A,B,DELTX,FOP,E1,E2,MAXI,ICODE)
    2 VREF=SP
      WRITE(6,91)VREF
   91 FORMAT(5HOVREF/E14.5)
      CVO=CEV(VEE,TEE)
      CPO=CEP(VEE,TEE)+CVO
    3 GAMO=CPO/CVO
    4 ESS=ENT(VEE,TEE)
      CALL  EQU3(TEE,VEE,ANS3)
    5 HO=ANS3+200.
      UZ=SQRT(2.0*GEE*AJA*HO)
      VISO=149.5*(TEE/TZ)*SQRT(TEE/TZ)*1.22/(TEE/TZ+.22)
      VISO=0.672E-7*VISO
      VE=SQRT(2.*GEE*AJA*HO)
      WRITE(6,55)VE
   55 FORMAT(3HOVL///E15.5)
      DO  111  N=1,IEND
      TUFF=TEI(N)
      CALL  EQUA2(A,B,DELTX,E1,E2,MAXI,ANS)
    6 VEI(N)=ANS
      PEI(N)=PRES(VEI(N),TEI(N))
      CALL  EQU3(TEI(N),VEI(N),ANS3)
    7 H(N)=ANS3+200.
      VI(N)=SQRT(2.*GEE*AJA*ABS(HO-H(N)))
      CV(N)=CEV(VEI(N),TEI(N))
      CP(N)=CEP(VEI(N),TEI(N))+CV(N)
    8 GAM(N)=CP(N)/CV(N)
      SPEED(N)=SQRT(GAM(N)*PART(VEI(N),TEI(N))*4633.056)
      XMACH(N)=VI(N)/SPEED(N)
      VIS(N)=149.5*(TEI(N)/TZ)*SQRT(TEI(N)/TZ)* 1.22/(TEI(N)/TZ+.22)
    9 VIS(N)=0.672E-7*VIS(N)
      PICRAT(N)=PEI(N)/PEE
      TIORAT(N)=TEI(N)/TEE
   10 REN(N)=VI(N)/(VEI(N)*VIS(N))
      IF(XMACH(N).GT.3..AND.IEND.LT.31) CALL SHOCK(H(N),VI(N),PEI(N),VEI
     2(N),TEI(N))
  111 CONTINUE
      KQ=KX-1
      WRITE(6,52)VEE,PEE,HO,ESS,GAMO,TREF,PREF,VISO
   52 FORMAT(3H1VO,15X,2HPO,15X,2HHO,15X,2HSO,15X,5HGAMMA,15X,4HTREF,15X
     2,4HPREF,15X,4HMU-O//8E16.6)
      WRITE(6,56)(TEI(N),VEI(N),PEI(N),H(N),XMACH(N),N=1,IEND)
   56 FORMAT(12HOTEMPERATURE,15X,6HVOLUME,15X,8HPRESSURE,15X,8HENTHALPY,
```

```
     215X,7HMACH NO///(5E20.6))
      WRITE(6,54)(VI(J),CP(J),CV(J),GAM(J),SPEED(J),VIS(J),J=1,IEND)
   54 FORMAT(9H1VELOCITY,20X,2HCP,20X,2HCV,20X,5HGAMMA,15X,12HACCELERATI
     20N,15X,9HVISCOSITY///(6E21.6))
      WRITE(6,60) (P1ORAT(N),T1ORAT(N),REN(N),N=1,IEND)
   60 FORMAT(1H1,7X,5HP1/P0,15X,5HT1/T0,10X,14HREYNOLDS NO/FT/
     1(3E20.6))
      IF(IEND.LT.31)WRITE(6,57)(VE2I(K),TE2I(K),P2I(K),U2I(K),XMACH2(K),
     2H2I(K),K=1,KQ)
      IF(IEND.LT.31) WRITE(6,58)(RHO(K),CV2(K),CP2(K),GAM2(K),ACC2(K),
     1K=1,KQ)
      IF(IEND.LT.31)WRITE(6,59)(T2ORT(K),RORAT(K),TRAT(K),PRAT(K),K=1,
     1KQ)
   57 FORMAT(8H1VOLUME2,20X,12HTEMPERATURE2,12X,9HPRESSURE2,12X,9HVELOCI
     2TY2,12X,8HMACH NO2,12X,9HENTHALPY2///(6E21.5))
   58 FORMAT(1H1,8X,4HRHO2,20X,3HCV2,16X,3HCP2,16X,6HGAMM2,16X,
     114HSPEED OF SOUND//(5E21.5))
   59 FORMAT(1H1,7X,5HT2/T0,21X,5HV1/V2,20X,5HT2/T1,16X,5HP2/T1///
     1(4E21.5))
      IF(IEND.LT.31) WRITE(6,62)(V1N(K),V1T(K),V2N(K), VIS2(K),K=1,KQ)
   62 FORMAT(1H1,9X,3HU1N,18X,3HU1T,18X,3HU2N,18X,3HMU2///(4E21.5))
      WRITE(8) H0,VEE,GEE,KQ,IEND,UZ,VISO
      WRITE(8) ((GAM(I),P1ORAT(I),VI(I),T1ORAT(I),REN(I),VEI(I),
     1XMACH(I)),I=1,IEND)
      WRITE(8) ((GAM2(I),RORAT(I),VE2I(I),U2I(I),VIS2(I)),I=1,KQ)
      ENDFILE 8
      GO TO 99
      END
      FUNCTION FOP(V)
C     EQN OF STATE-USED TO FIND V AS A FUNCTION OF P+T                    FOP
      COMMON A2,A3,A4,A5,B2,B3,B4,B5,C2,C3,C4,C5,XKK,R,TREF,VREF,BLIT,XJ
      COMMON D4,Z4,ESS,TUFF,CLOD,GEE,AJA,KX,P2I(30),U2I(30),H2I(30)
      COMMON PT2(30),RHO(30),TE2I(30),VE2I(30),CV2(30),CP2(30),GAM2(30)
      COMMON ACC2(30),XMACH2(30),RORAT(30),TRAT(30),PRAT(30),PTRAT(30)
      COMMON TH
      COMMON V1N(30),V2N(30),V1T(30)
      COMMON BIGB4,B6,A6,AL,TZ
      P0 (XL,AT)=1./EXP(XL*AT)
      COMMON/DESP/VOODOO,ZULU
      T=VOODOO
      P=ZULU
      POT=P0(XKK,T)                                                       FOP
    1 FOP=P-(R*T)/(V-BLIT)-(A2+B2*T+C2*POT)/(V-BLIT)**2-(A3+B3*T+         FOP
     1C3*POT)/(V-BLIT)**3-(A4+BIGB4*T)/(V-BLIT)**4-(A5+B5*T+C5*POT)/     FOP
     2(V-BLIT)**5-(A6-B6*T)*EXP(AL*V)                                     FOP
```

```
      RETURN
      END
      SUBROUTINE EQU3(TE,VE,ANS3)
C     ENTHALPY                                                          EQU3
      COMMON A2,A3,A4,A5,B2,B3,B4,B5,C2,C3,C4,C5,XKK,R,TREF,VREF,BLIT,XJ
      COMMON D4,Z4,ESS,TUFF,CLOD,GEE,AJA,KX,P2I(30),U2I(30),H2I(30)
      COMMON PT2(30),RHO(30),TE2I(30),VE2I(30),CV2(30),CP2(30),GAM2(30)
      COMMON ACC2(30),XMACH2(30),RORAT(30),TRAT(30),PRAT(30),PTRAT(30)
      COMMON TH
      COMMON V1N(30),V2N(30),V1T(30)
      COMMON BIGB4,B6,A6,AL,TZ
      EQUIVALENCE (C3,G3),(C5,XJ3),(C2,D3)
      PO(XL,AT)=1./EXP(XL*AT)
    3 ANS3=Z4*(TE-TREF)+B4*(TE**2-TREF**2)/2.+C4*(TE**3-TREF**3)/3.+D4*
     2(TE**4-TREF**4)/4.+(PO(XKK,TE)*(XKK*TE+1.)-PO(XKK,TREF)*(XKK*TREF
     3+1.))*(XJ*D3/(VE-BLIT)+XJ*G3/(2.*(VE-BLIT)**2)+XJ*XJ3/(4.*(VE-
     4BLIT)**4))+XJ*(VE*R*(TE-TREF)/(VE-BLIT)+VE*(B2*(TE-TREF)+C2*(PO
     5(XKK,TE)-PO(XKK,TREF)))/(VE-BLIT)**2)+XJ*(VE*(B3*(TE-TREF)+C3*(PO
     6(XKK,TE)-PO(XKK,TREF)))/(VE-BLIT)**3)+XJ*(VE*(B5*(TE-TREF)+C5*(PO
     7(XKK,TE)-PO(XKK,TREF)))/(VE-BLIT)**5)-(R*TREF*(ALOG((VE-BLIT)/(VR
     8EF-BLIT))+BLIT/(VREF-BLIT)-BLIT/(VE-BLIT)))*XJ-(2.*(A2+B2*TREF+C2
     9*PO(XKK,TREF))*(1./(VREF-BLIT)+BLIT/(2.*(VREF-BLIT)**2)-1./(VE-
     ABLIT)-BLIT/(2.*(VE-BLIT)**2)))*XJ-(3.*(A3+B3*TREF+C3*PO(XKK,TREF
     B))*(1./(2.*(VREF-BLIT)**2)+BLIT/(3.*(VREF-BLIT)**3)-1./(2.*(VE-
     CBLIT)**2)-BLIT/(3.*(VE-BLIT)**3)))*XJ-(4.*A4*(1./(3.*(VREF-BLIT)
     D**3)+BLIT/(4.*(VREF-BLIT)**4)-1./(3.*(VE-BLIT)**3)-BLIT/(4.*(VE-
     EBLIT)**4)))*XJ
      ANS3=ANS3-((5.*(A5+B5*TREF+C5*PO(XKK,TREF)))*(1./(4.*(VREF-BLIT)
     2**4)+BLIT/(5.*(VREF-BLIT)**5)-1./(4.*(VE-BLIT)**4)-BLIT/(5.*(VE-
     3BLIT)**5)))*XJ+TREF*R*ALOG((VE-BLIT)/(VREF-BLIT))*XJ-TREF*(B2-XKK
     4*C2*PO(XKK,TREF))*(1./(VE-BLIT)-1./(VREF-BLIT))*XJ-TREF*(B3-XKK*
     5C3*PO(XKK,TREF))/2.*(1./(VE-BLIT)**2-1./(VREF-BLIT)**2)*XJ-TREF*
     6(B5-XKK*C5*PO(XKK,TREF))/4.*(1./(VE-BLIT)**4-1./(VREF-BLIT)**4)
     7*XJ
      EXAL=EXP(AL*VE)                                                   EQU3
      ALVR=AL*VREF
      EXAR=EXP(ALVR)
 3001 CONTINUE
    1 TEMP=XJ*VREF*((BIGB4*(TE-TREF)/(VREF-BLIT)**4) +B6*EXAR*(TE-TREF))EQU3
      DUM=BIGB4*TE/(VE-BLIT)**4                                         EQU3
      DUM1=A6*EXAL+B6*TE*EXAL                                           EQU3
      TEMP=TEMP+XJ*VE*(0.5*VE*(-4.*DUM/(VE-BLIT)+AL*DUM1)+ DUM+DUM1)    EQU3
      DUM=BIGB4*TE/(VREF-BLIT)**4                                       EQU3
      DUM1=A6*EXAR+B6*TE*EXAR                                           EQU3
    4 TEMP=TEMP-XJ*VREF*(0.5*VREF*(-4.*DUM/(VREF-BLIT)+AL*DUM1)+        EQU3
```

APPENDIX C – Continued

Program A – Continued

```
     1DUM+DUM1 )                                                                EQU3
      TEMP=TEMP+XJ*(BIGB4*TE*(1./(3.*(VREF-BLIT)**3)-1./(3.*(VE-BLIT)    EQU3
     1**3))+B6*TE*(EXAL-EXAR)/AL)                                               EQU3
    5 ANS3=ANS3+TEMP                                                            EQU3
      RETURN
      END
$IBFTC ENTROP  DECK,LIST
      FUNCTION ENT(VEE,TEE)
C     ENTROPY                                                                   ENT
      COMMON A2,A3,A4,A5,B2,B3,B4,B5,C2,C3,C4,C5,XKK,R,TREF,VREF,BLIT,XJ
      COMMON D4,Z4,ESS,TUFF,CLOD,GEE,AJA,KX,P2I(30),U2I(30),H2I(30)
      COMMON PT2(30),RHO(30),TE2I(30),VE2I(30),CV2(30),CP2(30),GAM2(30)
      COMMON ACC2(30),XMACH2(30),RORAT(30),TRAT(30),PRAT(30),PTRAT(30)
      COMMON TH
      COMMON V1N(30),V2N(30),V1T(30)
      COMMON BIGB4,B6,A6,AL,TZ
      EQUIVALENCE (C3,G3),(C5,XJ3),(C2,D3)
      PO (XL,AT)=1./EXP(XL*AT)
    1 ESS1=Z4*ALOG(TEE/TREF)+B4*(TEE-TREF)+C4*(TEE**2-TREF**2)/2.
      ESS2=ESS1+D4*(TEE**3-TREF**3)/3.+XJ*D3*XKK/(VREF-BLIT)*(PO(XKK,TEE
     2)-PO(XKK,TREF))
      ESS3=ESS2+XJ*G3*XKK/(2.*(VREF-BLIT)**2)*(PO(XKK,TEE)-PO(XKK,TREF))
      ESS4=ESS3+XJ*XJ3*XKK/(4.*(VREF-BLIT)**4)*(PO(XKK,TEE)-PO(XKK,TREF)
     2)
      ESS5=ESS4+(R*ALOG((VEE-BLIT)/(VREF-BLIT)))*XJ
      ESS6=ESS5-(B2-XKK*C2*PO(XKK,TEE))*(1./(VEE-BLIT)-1./(VREF-BLIT))*X
     2J
      ESS7=ESS6-(B3-XKK*C3*PO(XKK,TEE))/2.*(1./(VEE-BLIT)**2-1./(VREF-BL
     2IT)**2)*XJ
      ENT=ESS7-(B5-XKK*C5*PO(XKK,TEE))/4.*(1./(VEE-BLIT)**4-1./(VREF-BLI
     2T)**4)*XJ
      EXAL=EXP(AL*VEE)                                                          ENT
      ALVR=AL*VREF
      EXAR=EXP(ALVR)
 3001 CONTINUE
    2 ENT=ENT+XJ*(BIGB4*(1./(3.*(VREF-BLIT)**3)-1./(3.*(VEE-BLIT)**3))  ENT
     1+B6*(EXAL-EXAR)/AL)                                                       ENT
      RETURN
      END
$IBFTC PARTIL  DECK,LIST
      FUNCTION PART(V,T)
C     PARTIAL P W.R.T. RHO                                                      PART
      COMMON A2,A3,A4,A5,B2,B3,B4,B5,C2,C3,C4,C5,XKK,R,TREF,VREF,BLIT,XJ
      COMMON D4,Z4,ESS,TUFF,CLOD,GEE,AJA,KX,P2I(30),U2I(30),H2I(30)
      COMMON PT2(30),RHO(30),TE2I(30),VE2I(30),CV2(30),CP2(30),GAM2(30)
```

```
      COMMON ACC2(30),XMACH2(30),RORAT(30),TRAT(30),PRAT(30),PTRAT(30)
      COMMON TH
      COMMON V1N(30),V2N(30),V1T(30)
      COMMON BIGB4,B6,A6,AL,TZ
      EQUIVALENCE (C3,G3),(C5,XJ3),(C2,D3)
      PO (XL,AT)=1./EXP(XL*AT)
     1 PART=R*T*V**2/(V-BLIT)**2+4.*A4*V**2/(V-BLIT)**5+2.*V**2*(A2+B2*
     2T+C2*PO(XKK,T))/(V-BLIT)**3+3.*V**2*(A3+B3*T+C3*PO(XKK,T))/(V-BL
     3IT)**4+5.*V**2*(A5+B5*T+C5*PO(XKK,T))/(V-BLIT)**6
      EXAL=EXP(AL*V)                                                    PART
     2 PART=PART-(V**2)*(-4.*BIGB4*T/(V-BLIT)**5+A6*AL*EXAL+B6*T*AL*EXAL)PART
      RETURN
      END
$IBFTC CEEV    DECK,LIST
      FUNCTION CEV(VE,TE)
      COMMON A2,A3,A4,A5,B2,B3,B4,B5,C2,C3,C4,C5,XKK,R,TREF,VREF,BLIT,XJ
      COMMON D4,Z4,ESS,TUFF,CLOD,GEE,AJA,KX,P2I(30),U2I(30),H2I(30)
      COMMON PT2(30),RHO(30),TE2I(30),VE2I(30),CV2(30),CP2(30),GAM2(30)
      COMMON ACC2(30),XMACH2(30),RORAT(30),TRAT(30),PRAT(30),PTRAT(30)
      COMMON TH
      COMMON V1N(30),V2N(30),V1T(30)
      COMMON BIGB4,B6,A6,AL,TZ
      EQUIVALENCE (C3,G3),(C5,XJ3),(C2,D3)
      PO (XL,AT)=1./EXP(XL*AT)
     1 CEV=Z4+B4*TE+C4*TE**2+D4*TE**3-XJ*(D3*TE*XKK**2*PO(XKK,TE))/(VE-
     2BLIT)-XJ*(G3*TE*XKK**2*PO(XKK,TE))/(2.*(VE-BLIT)**2)-XJ*(XJ3*TE*
     3XKK**2*PO(XKK,TE))/(4.*(VE-BLIT)**4)
      RETURN
      END
      FUNCTION PRES(VE,TE)
C     EQUATION OF STATE                                                 PRES
      COMMON A2,A3,A4,A5,B2,B3,B4,B5,C2,C3,C4,C5,XKK,R,TREF,VREF,BLIT,XJ
      COMMON D4,Z4,ESS,TUFF,CLOD,GEE,AJA,KX,P2I(30),U2I(30),H2I(30)
      COMMON PT2(30),RHO(30),TE2I(30),VE2I(30),CV2(30),CP2(30),GAM2(30)
      COMMON ACC2(30),XMACH2(30),RORAT(30),TRAT(30),PRAT(30),PTRAT(30)
      COMMON TH
      COMMON V1N(30),V2N(30),V1T(30)
      COMMON BIGB4,B6,A6,AL,TZ
      PO (XL,AT)=1./EXP(XL*AT)
      POT=PO(XKK,TE)                                                    PRES
     1 PRES=R*TE/(VE-BLIT)+(A2+B2*TE+C2*POT)/(VE-BLIT)**2+(A3+B3*TE     PRES
     1+C3*POT)/(VE-BLIT)**3+(A4+BIGB4*TE)/(VE-BLIT)**4+(A5+B5*TE+C5*POT)PRES
     2/(VE-BLIT)**5+(A6+B6*TE)*EXP(AL*VE)                               PRES
      RETURN
      END
```

```
      FUNCTION CEP(VE,TE)
C     CP                                                                    CEP
      COMMON A2,A3,A4,A5,B2,B3,B4,B5,C2,C3,C4,C5,XKK,R,TREF,VREF,BLIT,XJ
      COMMON D4,Z4,ESS,TUFF,CLOD,GEE,AJA,KX,P2I(30),U2I(30),H2I(30)
      COMMON PT2(30),RHO(30),TE2I(30),VE2I(30),CV2(30),CP2(30),GAM2(30)
      COMMON ACC2(30),XMACH2(30),RORAT(30),TRAT(30),PRAT(30),PTRAT(30)
      COMMON TH
      COMMON V1N(30),V2N(30),V1T(30)
      COMMON BIGB4,B6,A6,AL,TZ
      EQUIVALENCE (C3,G3),(C5,XJ3),(C2,D3)
      PO (XL,AT)=1./EXP(XL*AT)
      EXAL=EXP(AL*VE)                                                       CEP
    1 DEN=R*TE/(VE-BLIT)**2+2.*(A2+B2*TE+C2*PO(XKK,TE))/(VE-BLIT)**3+3.
     2*(A3+B3*TE+C3*PO(XKK,TE))/(VE-BLIT)**4+4.*A4/(VE-BLIT)**5+5.*
     3(A5+B5*TE+C5*PO(XKK,TE))/(VE-BLIT)**6
      DEN=DEN-4.*BIGB4*TE/(VE-BLIT)**5+A6*AL*EXAL+B6*AL*TE*EXAL             CEP
      XNU=R/(VE-BLIT)+(B2-XKK*C2*PO(XKK,TE))/(VE-BLIT)**2+(B3-XKK*C3*
     2PO(XKK,TE))/(VE-BLIT)**3+(B5-XKK*C5*PO(XKK,TE))/(VE-BLIT)**5
      XNU =XNU+BIGB4/(VE-BLIT)**4+B6*EXAL                                   CEP
      XNUM=TE*XJ*XNU**2
    2 CEP =XNUM/DEN
      RETURN
      END
$IBFTC EQUA2
      SUBROUTINE EQUA2(A,B,DELTX,E1,E2,MAXI,ANS)
      EXTERNAL FOFX
      CALL ITR2(ANS,A,B,DELTX,FOFX,E1,E2,MAXI,ICODE)
      IF(ICODE.EQ.0)GO TO 100
      IF(ICODE.EQ.1)WRITE(6,10)
      IF(ICODE.EQ.2)WRITE(6,11)
      IF(ICODE.EQ.3)WRITE(6,12)
      IF(ICODE.EQ.4)WRITE(6,13)
   10 FORMAT(25H0MAX NUMBER OF ITERATIONS)
   11 FORMAT(12H0DELX=0 OR -)
   12 FORMAT(8H0NO ROOT)
   13 FORMAT(7H0A GT B)
  100 RETURN
      END
      FUNCTION FOFX(VX)
C     ENTROPY T6 GET V                                                      FOFX
      COMMON A2,A3,A4,A5,B2,B3,B4,B5,C2,C3,C4,C5,XKK,R,TREF,VREF,BLIT,XJ
      COMMON D4,Z4,ESS,TUFF,CLOD,GEE,AJA,KX,P2I(30),U2I(30),H2I(30)
      COMMON PT2(30),RHO(30),TE2I(30),VE2I(30),CV2(30),CP2(30),GAM2(30)
      COMMON ACC2(30),XMACH2(30),RORAT(30),TRAT(30),PRAT(30),PTRAT(30)
      COMMON TH
```

```
      COMMON V1N(30),V2N(30),V1T(30)
      COMMON BIGB4,B6,A6,AL,TZ
      EQUIVALENCE (C3,G3),(C5,XJ3),(C2,D3)
      PO (XL,AT)=1./EXP(XL*AT)
    1 TX=TUFF
      AND=ESS- Z4*ALOG(TX/TREF)-B4*(TX-TREF)-C4*(TX**2-TREF**2)/2.
      ANE=AND-D4*(TX**3-TREF**3)/3.-XJ*D3*XKK*(PO(XKK,TX)-PO(XKK,TREF))/
     2(VREF-BLIT)
      ANF=ANE- XJ*G3*XKK*(PO(XKK,TX)-PO(XKK,TREF))/(2.*(VREF-BLIT)**2)
      ANG=ANF- XJ*XJ3*XKK*(PO(XKK,TX)-PO(XKK,TREF))/(4.*(VREF-BLIT)**4)
      ANH=ANG-XJ*R*ALOG((VX-BLIT)/(VREF-BLIT))+(B2-XKK*C2*PO(XKK,TX))*(1
     2./(VX-BLIT)-1./(VREF-BLIT))*XJ
      ANI=ANH+(B3-XKK*C3*PO(XKK,TX))*(1./(VX-BLIT)**2-1./(VREF-BLIT)**2)
     2/2.*XJ
      FOFX=ANI+(B5-XKK*C5*PO(XKK,TX))*(1./(VX-BLIT)**4-1./(VREF-BLIT)**4
     2)/4.*XJ
    2 FOFX=FOFX-XJ*(BIGB4*(1./(3.*(VREF-BLIT)**3)-1./(3.*(VX-BLIT)**3)) FOFX
     1+B6*(EXP(AL*VX)-EXP(AL*VREF))/AL)                                  FOFX
      RETURN
      END
$IBFTC SHOC    DECK,LIST
      SUBROUTINE SHOCK(H,VEL,P,V,T)
      COMMON A2,A3,A4,A5,B2,B3,B4,B5,C2,C3,C4,C5,XKK,R,TREF,VREF,BLIT,XJ
      COMMON D4,Z4,ESS,TUFF,CLOD,GEE,AJA,KX,P2I(30),U2I(30),H2I(30)
      COMMON PT2(30),RHO(30),TE2I(30),VE2I(30),CV2(30),CP2(30),GAM2(30)
      COMMON ACC2(30),XMACH2(30),RORAT(30),TRAT(30),PRAT(30),PTRAT(30)
      COMMON TH
      COMMON V1N(30),V2N(30),V1T(30)
      COMMON BIGB4,B6,A6,AL,TZ
      COMMON/CLUX/TC,VC
      COMMON/DOPE/A,B,C,PRAY
      COMMON/PRTS/ PXTV,PVTV
      COMMON /RATS/PEE,TEE,VIS2(30),PT2ORT(30),P1T2RT(30),T2ORT(30)
      DIMENSION IPIVOT(2),INDEX(2,2)
      DIMENSION TC(30),VC(30)
      DIMENSION HOPE(25),BEG(25),TEMP(25)
      DIMENSION AMAT(2,2),BMAT(2)
      EQUIVALENCE (C3,G3),(C5,XJ3),(C2,D3)
      EXTERNAL FONC,FOND
    3 ICHEK=0
      EL=1./144.
      K=KX
      VLN=VEL*SIN(TH)
      A=H+VLN**2/50082.
      B=P+(EL/32.174)*VLN**2/V
```

```
      C=VLN/V
      UT=VEL*COS(TH)
      V1N(K)=VLN
      V1T(K)=UT
 8000 FORMAT(5H1SHOC,5X,2HA=E15.8,5X,2HB=E15.8,5X,2HC=E15.8,
     12HV=E15.8,5X,4HVEL=E15.8)
      WRITE(6,8000) A,B,C,V,VEL
      MAXI=30
      E1=.0001
      E2=0.0001
      PRAY=TC(K)
      HOPE(1)=VC(K)
   77 DO 59 IND=1,30
C     H(T,V)
      HTV=FOND(HOPE(1))
C     P(T,V)
      PTV=FONC(HOPE(1))
      WRITE(6,9000) HTV,PTV
 9000 FORMAT(6E17.8)
C     PX(T,V)
      PXTV=FONCX(HOPE(1))
C     PV(T,V)
      PVTV=FONCV(HOPE(1))
      WRITE(6,9000) PXTV,PVTV
C     HX(T,V)
      HXTV=FONDX(HOPE(1))
C     HV(T,V)
      HVTV=FONDV(HOPE(1))
      WRITE(6,9000) HXTV,HVTV
      AMAT(2,1)=HXTV
      AMAT(2,2)=HVTV
      AMAT(1,1)=PXTV
      AMAT(1,2)=PVTV
      BMAT(2)=(-HTV)
      BMAT(1)=(-PTV)
      WRITE(6,2000) BMAT,AMAT
      CALL MATINV(AMAT,2,BMAT,1,DETERM,IPIVOT,INDEX,2,ISCALE)
      WRITE(6,2000) BMAT
      WRITE(6,2000) HOPE(1),PRAY,PTV,HTV
 2000 FORMAT(6E20.8)
      DEL1=ABS(BMAT(1)/PRAY )
      DEL2=ABS(BMAT(2)/HOPE(1))
      IF((  DEL1 .LE.E1).AND.(DEL2    .LE.E2))  GO TO 60
      PRAY=PRAY+BMAT(1)
      HOPE(1)=HOPE(1)+BMAT(2)
```

```
   59 CONTINUE
C      TOO MANY ITERATIONS HERE
       WRITE(6,2001)
 2001  FORMAT(15HOMAX ITERATIONS)
       RETURN
   60  CONTINUE
       WRITE(6,1000) PRAY,HOPE(1)
 1000  FORMAT( 7H ROOTS=E15.8,E20.8)
    1  FORMAT(5H HOPE,20X,3HBEG,20X,4HTEMP/3E22.6)
       VE2I(K)=HOPE(1)
       TE2I(K)=PRAY
       P2I(K)=PRES(VE2I(K),TE2I(K))
       UN=C*VE2I(K)
       V2N(K)=UN
       U2I(K)=SQRT((UN**2)+(UT**2))
       CALL EQU3(TE2I(K),VE2I(K),ENTH)
       H2I(K)=ENTH + 200.0
       RHO(K)=1./VE2I(K)
       CV2(K)=CEV(VE2I(K),TE2I(K))
       CP2(K)=CEP(VE2I(K),TE2I(K))+CV2(K)
       GAM2(K)=CP2(K)/CV2(K)
       ACC2(K)=SQRT(ABS(GAM2(K))*ABS(PART(VE2I(K),TE2I(K)))*4633.056)
       XMACH2(K)=U2I(K)/ACC2(K)
       RORAT(K)=VE2I(K)/V
       TRAT(K)=TE2I(K)/T
       PRAT(K)=P2I(K)/P
       RORAT(K)=V/VE2I(K)
       T2ORT(K)=TE2I(K)/TEE
       VIS2(K)=       (149.5*(TE2I(K)/TZ)*SQRT(TE2I(K)/TZ)*1.22/(TE2I(K)/
      1TZ+.22))
       VIS2(K)=VIS2(K)*0.672E-7
    5  KX=KX+1
       RETURN
       END
$IBFTC FOND     DECK
       FUNCTION FOND(VE)
C      ENTHALPY FOR NEWTON-RAPHSON                                          FOND
       COMMON A2,A3,A4,A5,B2,B3,B4,B5,C2,C3,C4,C5,XKK,R,TREF,VREF,BLIT,XJ
       COMMON D4,Z4,ESS,TUFF,CLOD,GEE,AJA,KX,P2I(30),U2I(30),H2I(30)
       COMMON PT2(30),RHO(30),TE2I(30),VE2I(30),CV2(30),CP2(30),GAM2(30)
       COMMON ACC2(30),XMACH2(30),RORAT(30),TRAT(30),PRAT(30),PTRAT(30)
       COMMON TH
       COMMON V1N(30),V2N(30),V1T(30)
       COMMON BIGB4,B6,A6,AL,TZ
       COMMON/DOPE/A,B,C,PRAY
```

```
      EQUIVALENCE (C3,G3),(C5,XJ3),(C2,D3)
      PO (XL,AT)=1./EXP(XL*AT)
      TE=PRAY
    1 H6 =Z4*(TE-TREF)+B4*(TE**2-TREF**2)/2.+C4*(TE**3-TREF**3)/3.+D4*
     2(TE**4-TREF**4)/4.+(PO(XKK,TE)*(XKK*TE+1.)-PO(XKK,TREF)*(XKK*TREF
     3+1.))*(XJ*D3/(VREF-BLIT)+XJ*G3/(2.*(VREF-BLIT)**2)+XJ*XJ3/(4.*
     4(VREF-BLIT)**4))+XJ*(VREF*R*(TE-TREF)/(VREF-BLIT)+VREF*(B2*(TE-
     5TREF)+C2*(PO(XKK,TE)-PO(XKK,TREF)))/(VREF-BLIT)**2)+XJ*(VREF*(B3*
     6(TE-TREF)+C3*(PO(XKK,TE)-PO(XKK,TREF)))/(VREF-BLIT)**3)+XJ*(VREF*
     7(B5*(TE-TREF)+C5*(PO(XKK,TE)-PO(XKK,TREF)))/(VREF-BLIT)**5)-(R*TE*
     8(ALOG((VE-BLIT)/(VREF-BLIT))+BLIT/(VREF-BLIT)-BLIT/(VE-BLIT)))*XJ
      H7=H6-(2.*(A2+B2*TE+C2*PO(XKK,TE))*(1./(VREF-BLIT)+BLIT/(2.*(VREF-
     2BLIT)**2)-1./(VE-BLIT)-BLIT/(2.*(VE-BLIT)**2)))*XJ
      H8=H7-(3.*(A3+B3*TE+C3*PO(XKK,TE))*(1./(2.*(VREF-BLIT)**2)+BLIT/(3
     2.*(VREF-BLIT)**3)-1./(2.*(VE-BLIT)**2)-BLIT/(3.*(VE-BLIT)**3)))*XJ
      H9=H8-(4.*A4*(1./(3.*(VREF-BLIT)**3)+BLIT/(4.*(VREF-BLIT)**4)-1./(
     23.*(VE-BLIT)**3)-BLIT/(4.*(VE-BLIT)**4)))*XJ
      H10=H9-((5.*(A5+B5*TE+C5*PO(XKK,TE)))*(1./(4.*(VREF-BLIT)**4)+BLIT
     2/(5.*(VREF-BLIT)**5)-1./(4.*(VE-BLIT)**4)-BLIT/(5.*(VE-BLIT)**5)))
     3*XJ
      H11=H10+TE*R*ALOG((VE-BLIT)/(VREF-BLIT))*XJ
      H12=H11-TE*(B2-XKK*C2*PO(XKK,TE))*(1./(VE-BLIT)-1./(VREF-BLIT))*XJ
      H13=H12-TE*(B3-XKK*C3*PO(XKK,TE))/2.*(1./(VE-BLIT)**2-1./(VREF-BLI
     2T)**2)*XJ
      H14=H13-TE*(B5-XKK*C5*PO(XKK,TE))/4.*(1./(VE-BLIT)**4-1./(VREF-BLI
     2T)**4)*XJ
      FOND=H14+C**2*VE**2/(2.*GEE*AJA)-A  +200.
      EXAL=EXP(AL*VE)                                                    EQU3
      ALVR=AL*VREF
      EXAR=EXP(ALVR)
 3001 CONTINUE
      TEMP=XJ*VREF*((BIGB4*(TE-TREF)/(VREF-BLIT)**4) +B6*EXAR*(TE-TREF))EQU3
      DUM=BIGB4*TE/(VE-BLIT)**4                                          EQU3
      DUM1=A6*EXAL+B6*TE*EXAL                                            EQU3
      TEMP=TEMP+XJ*VE*(0.5*VE*(-4.*DUM/(VE-BLIT)+AL*DUM1)+ DUM+DUM1)     EQU3
      DUM=BIGB4*TE/(VREF-BLIT)**4                                        EQU3
      DUM1=A6*EXAR+B6*TE*EXAR                                            EQU3
      TEMP=TEMP-XJ*VREF*(0.5*VREF*(-4.*DUM/(VREF-BLIT)+AL*DUM1)+         EQU3
     1DUM+DUM1)                                                          EQU3
      TEMP=TEMP+XJ*(BIGB4*TE*(1./(3.*(VREF-BLIT)**3)-1./(3.*(VE-BLIT)    EQU3
     1**3))+B6*TE*(EXAL-EXAR)/AL)                                        EQU3
      ANS3=ANS3+TEMP                                                     EQU3
    2 FOND=FOND+TEMP                                                     FOND
      RETURN
      END
```

```
$IBFTC FONC    DECK
       FUNCTION FONC(VE)
C      EQ. OF STATE FOR NEWTON-RAPHSON                                          FONC
       COMMON A2,A3,A4,A5,B2,B3,B4,B5,C2,C3,C4,C5,XKK,R,TREF,VREF,BLIT,XJ
       COMMON D4,Z4,ESS,TUFF,CLOD,GEE,AJA,KX,P2I(30),U2I(30),H2I(30)
       COMMON PT2(30),RHO(30),TE2I(30),VE2I(30),CV2(30),CP2(30),GAM2(30)
       COMMON ACC2(30),XMACH2(30),RORAT(30),TRAT(30),PRAT(30),PTRAT(30)
       COMMON TH
       COMMON V1N(30),V2N(30),V1T(30)
       COMMON BIGB4,B6,A6,AL,TZ
       EQUIVALENCE (C3,G3),(C5,XJ3),(C2,D3)
       COMMON/DOPE/A,B,C,PRAY
       PO (XL,AT)=1./EXP(XL*AT)
       EL=1./144.
       TE=PRAY
       POT=PO(XKK,TE)                                                           PRES
     1 FONC=R*TE/(VE-BLIT)+(A2+B2*TE+C2*POT)/(VE-BLIT)**2+(A3+B3*TE+            FONC
      1C3*POT)/(VE-BLIT)**3+(A4+BIGB4*TE)/(VE-BLIT)**4+(A5+B5*TE+C5*POT)       FONC
      2/(VE-BLIT)**5+(A6+B6*TE)*EXP(AL*VE)+(EL/GEE)*C**2*VE-B                   FONC
       RETURN
       END
       FUNCTION FONDX(VE)
C      PARTIAL H W.R.T. T                                                       FONDX
       COMMON/PRTS/ PXTV,PVTV
       COMMON A2,A3,A4,A5,B2,B3,B4,B5,C2,C3,C4,C5,XKK,R,TREF,VREF,BLIT,XJ
       COMMON D4,Z4,ESS,TUFF,CLOD,GEE,AJA,KX,P2I(30),U2I(30),H2I(30)
       COMMON PT2(30),RHO(30),TE2I(30),VE2I(30),CV2(30),CP2(30),GAM2(30)
       COMMON ACC2(30),XMACH2(30),RORAT(30),TRAT(30),PRAT(30),PTRAT(30)
       COMMON TH
       COMMON V1N(30),V2N(30),V1T(30)
       COMMON BIGB4,B6,A6,AL,TZ
       COMMON/DOPE/A,B,C,PRAY
       EQUIVALENCE (C3,G3),(C5,XJ3),(C2,D3)
       PO (XL,AT)=1./EXP(XL*AT)
     1 TE=PRAY
       FONDX=Z4+B4*TE+C4*TE**2-XJ*((D3*TE*(XKK**2)*PO(XKK,TE))/(VE-BLIT))
      1-XJ*((G3*TE*(XKK**2)*PO(XKK,TE))/(2.0*(VE-BLIT)**2))
      2-XJ*((XJ3*TE*(XKK**2)*PO(XKK,TE))/(4.0*(VE-BLIT)**4))
      3+VE*PXTV+D4*TE**3
       ALVR=AL*VREF
       EXAR=EXP(ALVR)
 3001  CONTINUE
       EXAL=EXP(AL*VE)                                                          FONDX
       DUM=BIGB4/(VE  -BLIT)**4                                                 FONDX
       DUM1=B6*EXAL                                                             FONDX
```

```
      TEMP=XJ* VE *(DUM+DUM1+VE*(-4.*DUM/(VE-BLIT)+AL*DUM1))                FONDX
      TEMP=TEMP-0.5*XJ*VREF*VREF*(-4.*BIGB4/(VREF-BLIT)**5+B6*AL*EXAR)      FONDX
    2 FONDX=TEMP+FONDX+XJ*(BIGB4*(1./(3.*(VREF-BLIT)**3)-1./(3.*(VE-        FONDX
     1BLIT)**3))+(B6/AL)*(EXAL-EXAR))                                        FONDX
      RETURN
      END
      FUNCTION FONCX(VE)                                                    FONCX
C     PARTIAL OF P(V,T) W.R.T. T
      COMMON/PRTS/ PXTV,PVTV
      COMMON A2,A3,A4,A5,B2,B3,B4,B5,C2,C3,C4,C5,XKK,R,TREF,VREF,BLIT,XJ
      COMMON D4,Z4,ESS,TUFF,CLOD,GEE,AJA,KX,P2I(30),U2I(30),H2I(30)
      COMMON PT2(30),RHO(30),TE2I(30),VE2I(30),CV2(30),CP2(30),GAM2(30)
      COMMON ACC2(30),XMACH2(30),RORAT(30),TRAT(30),PRAT(30),PTRAT(30)
      COMMON TH
      COMMON V1N(30),V2N(30),V1T(30)
      COMMON BIGB4,B6,A6,AL,TZ
      EQUIVALENCE (C3,G3),(C5,XJ3),(C2,D3)
      COMMON/DOPE/A,B,C,PRAY
      PO (XL,AT)=1./EXP(XL*AT)
      EL=1./144.
    1 TE=PRAY
      FONCX=R /(VE-BLIT)+(B2-C2*XKK*PO(XKK,TE))/(VE-BLIT)**2
     1+(B3-C3*XKK*PO(XKK,TE))/(VE-BLIT)**3 +(B5-C5*XKK*PO(XKK,TE))
     2/(VE-BLIT)**5
    2 FONCX=FONCX+BIGB4/(VE-BLIT)**4+B6*EXP(AL*VE)                          FONCX
      RETURN
      END
      FUNCTION FONDV(VE)                                                    FONDV
C     PARTIAL  H W.R.T. V
      COMMON/PRTS/ PXTV,PVTV
      COMMON A2,A3,A4,A5,B2,B3,B4,B5,C2,C3,C4,C5,XKK,R,TREF,VREF,BLIT,XJ
      COMMON D4,Z4,ESS,TUFF,CLOD,GEE,AJA,KX,P2I(30),U2I(30),H2I(30)
      COMMON PT2(30),RHO(30),TE2I(30),VE2I(30),CV2(30),CP2(30),GAM2(30)
      COMMON ACC2(30),XMACH2(30),RORAT(30),TRAT(30),PRAT(30),PTRAT(30)
      COMMON TH
      COMMON V1N(30),V2N(30),V1T(30)
      COMMON BIGB4,B6,A6,AL,TZ
      COMMON/DOPE/A,B,C,PRAY
      EQUIVALENCE (C3,G3),(C5,XJ3),(C2,D3)
      PO (XL,AT)=1./EXP(XL*AT)
    1 TE=PRAY
      FONDV=VE*PVTV +TE*PXTV +(C**2)*VE/( GEE*AJA)
      EXAL=EXP(AL*VE)                                                       FONDV
      DUM=BIGB4*TE/(VE-BLIT)**4                                             FONDV
      DUM1=A6*EXAL                                                          FONDV
```

```
      DUM2=B6*TE*EXAL                                                    FONDV
      TEMP=2.0*XJ*VE*(-4.*DUM/(VE-BLIT)+AL*(DUM1+DUM2))+XJ*(2.0*(DUM+    FONDV
     1DUM2)+DUM1)                                                        FONDV
     2 FONDV=FONDV+TEMP+0.5*XJ*VE*VE*(20.*DUM/(VE-BLIT)**2+(AL**2)*      FONDV
     1(DUM1+DUM2))                                                       FONDV
      RETURN
      END
$IBFTC FONCV   LIST
      FUNCTION FONCV(VE)
C     PARTIAL OF  P(V,T) W.R.T. V                                        FONCV
      COMMON/PRTS/ PXTV,PVTV
      COMMON A2,A3,A4,A5,B2,B3,B4,B5,C2,C3,C4,C5,XKK,R,TREF,VREF,BLIT,XJ
      COMMON D4,Z4,ESS,TUFF,CLOD,GEE,AJA,KX,P2I(30),U2I(30),H2I(30)
      COMMON PT2(30),RHO(30),TE2I(30),VE2I(30),CV2(30),CP2(30),GAM2(30)
      COMMON ACC2(30),XMACH2(30),RORAT(30),TRAT(30),PRAT(30),PTRAT(30)
      COMMON TH
      COMMON V1N(30),V2N(30),V1T(30)
      COMMON BIGB4,B6,A6,AL,TZ
      EQUIVALENCE (C3,G3),(C5,XJ3),(C2,D3)
      COMMON/DOPE/A,B,C,PRAY
      PO (XL,AT)=1./EXP(XL*AT)
      EL=1./144.
      TE=PRAY
      POT=PO(XKK,TE)                                                     FONCV
     1 FONCV=(-R*TE)/(VE-BLIT)**2-2.0*(A2+B2*TE+C2*POT)/(VE-BLIT)**3     FONCV
     1-3.0*(A3+B3*TE+C3*POT)/(VE-BLIT)**4-4.0*(A4+BIGB4*TE)/(VE-BLIT)**5FONCV
     2-5.0*(A5+B5*TE+C5*POT)/(VE-BLIT)**6+AL*(A6+B6*TE)*EXP(AL*VE)      FONCV
     3+(EL/GEE)*C**2                                                    FONCV
      RETURN
      END

$DATA A2=-2.162959,A3=4.04057E-3,A4=1.921072E-4,A5=-4.481049E-6,
A6=5.83882E7, BIGB4=-3.918263E-7, AL=-6.61199E2, B6=-9.26392E4,
XKK=.976E-2,B2=2.135114E-3,B3=1.282818E-5,B4=3.00892783E-4,
B5=9.062318E-9,XJ=.185053,
C2=-18.941131,C3=0.539776,C4=-1.30237441E-7,C5=-4.836678E-5,
R=0.1219336,BLIT=0.15E-2,D4=1.96802894E-11,PEE=0.1026,
TEE=260,GEE=32.174,AJA=778.3,A=.008,B=12000,DELTX=2,
TREF=820,PREF=1,TZ=409.5,Z4=1.90458084E-2,
TEI=5*532,E1=.00001,E2=.00001,MAXI=30,NUMB=5,INT=0,
IEND=30,
THETA=90,
 PEE=2000,
 TEE=1460,
 MAXI=30,
```

```
 TEI=1440,1420,1380,1340,1310,1280,1240,1190,1140,1090,1040,985,940,900,860,
      820, 780, 740, 700, 660, 620, 580, 540, 500, 470, 440,410,380,360,340,
 VC(1)=0.8,1.02,1.5,2.0,2.5,3.0,3.75,8.0,14.0,20.0,25.0,31.0,50.0,80.0,100.0,
       150.0,200.0,250.0,325.0,
 TC(1)=19*1447$
$DATA
 PEE=2000,
 TEE=1260,
 MAXI=30,
 TEI=1245,1230,1200,1160,1120,1080,1020,1000,960,920,880,840,800,750,700,650,
      600, 575, 550, 525, 500, 475, 450, 425,400,375,350,325,300,275,
 VC(1)=0.4,0.58,0.89,1.39,2.2,3.6,4.5,6.2,8.0,10.0,14.0,19.0,25.0,34.0,47.0,
       65.0,91.0,128.0,190.0,
 TC(1)=19*1240$
$DATA
 PEE=2000,
 TEE=1060,
 MAXI=30,
 TEI=1030,1035,1020,1000,965,930,880,830,785,745,700,675,640,600,575,550,
      525, 500, 475, 450,425,400,375,350,325,300,275,250,225,200,
 VC(1)=0.3,0.44,0.689,0.875,1.12,1.44,1.88,2.46,3.26,4.34,5.84,7.91,10.83,
       15.0,20.9,30.0,42.0,70.0,91.0,
 TC(1)=1034,1034,17*1033$
$DATA
 PEE=2000,
 TEE=860,
 MAXI=30,
 TEI=845,830,800,760,720,680,640,600,560,520,500,490,450,400,375,350,325,
     300,275,250,230,215,200,190,180,170,160,150,140,130,
 VC(1)=0.298,0.307,0.465,0.793,1.05,1.42,1.92,2.65,3.71,5.26,7.59,9.00,11.17,
       13.00,15.48,18.34,21.80,26.1,31.5,38.3,
 TC(1)=820,819,817,816,815,815,14*814$
```

APPENDIX C – Continued

Program B

NASA-LANGLEY RESEARCH CENTER

01 5	01 7 PROGRAM NO	COMPUTER PROGRAM ABSTRACT	01 14 DATE
LAR	E 1554		10/68

01 20 TITLE OF PROGRAM (61 CHARACTERS MAXIMUM)	PARENT PROGRAM		
Ballistic-Range Normal Shock Program	02 14 CATEGORY	02 15 SITE	02 16 PROGRAM NO

02 26 CATEGORY	02 27 LANGUAGE NO 1	02 32 LANGUAGE NO 2	02 37 KEY WORDS (8 MAXIMUM, SEPARATED BY COMMAS)
R	FØR6M		Ballistic-Range, Static, Shock, Tetrafluoromethane

WHO TO CONTACT ABOUT THE PROGRAM					05 48 STATUS	05 49
05 34 CONTACT	05 28 SITE	05 31 ORGN CODE	05 39 PROJECT NO	05 45 NASA CENTER	A UNDER DEVELOPMENT B OPERATIONAL C COMPLETED	A THIS PROGRAM IS NOT FOR SHARING
K. A. Smith	LAR	11.170	RGL-206		C	

DATES		05 58 REVISION CODE	TIME AND COST FOR DEVELOPMENT			
05 50 INITIATED	05 54 COMPLETED	A REVISION B CANCELLATION	05 59 MANMONTHS (59 60 61 62 63)	05 64 MACHINE HOURS (64 65 66 67 68)	05 69 COMPUTER TYPE	05 74 TOTAL COST (DOLLARS) (74 75 76 77 78 79 80)
10/67	10/68				6000	

ELITE MARGIN | PICA MARGIN

CARD NUMBER	COLUMN 14 ABSTRACT
06	The relations across a normal shock wave in equilibrium
07	tetrafluoromethane are programed to yield the downstream static
08	thermodynamic properties of one-dimensional flow. The inputs
09	are range static temperature, static pressure, and projectile
10	velocity.
11	
12	
13	
14	
15	
16	
17	
18	
19	
20	
21	
22	
23	
24	
25	
26	
27	
28	
29	
30	
31	
32	
33	
34	
35	
36	
37	
38	
39	
40	

APPENDIX C – Continued

Program B – Continued

```
      PROGRAM BLISTC(INPUT,OUTPUT,TAPE5=INPUT,TAPE6=OUTPUT)
      COMMON A2,A3,A4,A5,B2,B3,B4,B5,C2,C3,C4,C5,XKK,R,TREF,VREF,BLIT,XJ
      COMMON D4,Z4,ESS,TUFF,CLOD,GEE,AJA,KX,P2I(30),U2I(30),H2I(30)
      COMMON PT2(30),RHO(30),TE2I(30),VE2I(30),CV2(30),CP2(30),GAM2(30)
      COMMON ACC2(30),XMACH2(30),RORAT(30),TRAT(30),PRAT(30),PTRAT(30)
      COMMON BIGB4,B6,A6,AL
      COMMON /CLUX/ TC,VC,E1,E2
      COMMON/DESP/VOODOO,ZULU
      EXTERNAL FOP
      DIMENSION TC(30),VC(30)
      EQUIVALENCE (C3,G3),(C5,XJ3),(C2,D3)
      DIMENSION TEI(30),VEI(30),PEI(30),VI(30),GAM(30),SPEED(30)
      DIMENSIONXMACH(30),CP(30),CV(30),H(30),VIS(30)
      NAMELIST /DATA/A2,A3,A4,A5,A6,B2,B3,BIGB4,B5,B6,B4,AL,
     1C2,C3,C4,C5,XKK,XJ,R,BLIT,D4,PEE,TEE,GEE,AJA,NUMB,INT,Z4,A,B,
     2DELTX,IEND,TEI,E1,E2,MAXI,TREF,PREF,TZ,TC,VC,THETA,VI,PEI,AI
      PO (XL,AT)=1./EXP(XL*AT)
   99 READ(5,DATA)
      WRITE(6,DATA)
      KX=1
      DELX1=DELTX
      VOODOO=TREF
      ZULU=PREF
      CALL ITR2(SP,A,B,DELTX,FOP,E1,E2,MAXI,ICODE)
      VREF=SP
      WRITE(6,91)VREF
   91 FORMAT(5HOVREF/E14.5)
      DO 111 N=1,IEND
      VOODOO=TEI(N)
      ZULU=PEI(N)
      DELTX=DELX1
      CALL ITR2(SP,A1,B,DELTX,FOP,E1,E2,MAXI,ICODE)
                        WRITE(6,100) ICODE
  100 FORMAT(7HOICODE=I5)
      VEI(N)=SP
      WRITE(6,9) VEI(N)
    9 FORMAT(E20.8)
      CALL EQU3(TEI(N),VEI(N),ANS3)
      H(N)=ANS3+200.
      HO=H(N)+(VI(N)*VI(N))/(2.*GEE*AJA)
      CV(N)=CEV(VEI(N),TEI(N))
```

```
      CP(N)=CEP(VEI(N),TEI(N))+CV(N)
      GAM(N)=CP(N)/CV(N)
      SPEED(N)=SQRT(GAM(N)*PART(VEI(N),TEI(N))*4633.056)
      XMACH(N)=VI(N)/SPEED(N)
      VIS(N)=149.5*(TEI(N)/TZ)*SQRT(TEI(N)/TZ)* 1.22/(TEI(N)/TZ+.22)
      IF(XMACH(N).GT.2..AND.IEND.LT.15)CALL SHOCK(H(N),VI(N),PEI(N),VEI
     2(N),TEI(N))
  111 CONTINUE
      KQ=KX-1
      WRITE(6,52)VEE,PEE,H0,ESS,GAM0,TREF,PREF
   52 FORMAT(3H1V0,15X,2HP0,15X,2HH0,15X,2HS0,15X,5HGAMMA,15X,4HTREF,15X
     2,4HPREF//7E16.6)
      WRITE(6,56)(TEI(N),VEI(N),PEI(N),H(N),XMACH(N),N=1,IEND)
   56 FORMAT(12H0TEMPERATURE,15X,6HVOLUME,15X,8HPRESSURE,15X,8HENTHALPY,
     215X,7HMACH NO///(5E20.6))
      WRITE(6,54)(VI(J),CP(J),CV(J),GAM(J),SPEED(J),VIS(J),J=1,IEND)
   54 FORMAT(9H1VELOCITY,20X,2HCP,20X,2HCV,20X,5HGAMMA,15X,12HACCELERATI
     20N,15X,9HVISCOSITY///(6E21.6))
      IF(IEND.LT.15)WRITE(6,57)(VE2I(K),TE2I(K),P2I(K),U2I(K),XMACH2(K),
     2H2I(K),K=1,KQ)
      IF(IEND.LT.15)WRITE(6,58)(RHO(K),CV2(K),CP2(K),GAM2(K),
     2ACC2(K),K=1,KQ)
      IF(IEND.LT.15)WRITE(6,59)(RORAT(K),TRAT(K),PRAT(K),K=1,KQ)
   57 FORMAT(8H1VOLUME2,20X,12HTEMPERATURE2,12X,9HPRESSURE2,12X,9HVELOCI
     2TY2,12X,8HMACH NO2,12X,9HENTHALPY2///(6E21.5))
   58 FORMAT(5H1RHO2,20X,3HCV2,16X,3HCP2,16X,6HGAMM2,16X,14HSPEED OF SOU
     1ND///(5E21.5))
   59 FORMAT(6H1V2/V1,20X,5HT2/T1,16X,5HP2/P1///(3E21.5))
      GO TO 99
      END
$IBFTC SHOC     DECK,LIST
      SUBROUTINE SHOCK(H,VEL,P,V,T)
      COMMON A2,A3,A4,A5,B2,B3,B4,B5,C2,C3,C4,C5,XKK,R,TREF,VREF,BLIT,XJ
      COMMON D4,Z4,ESS,TUFF,CLOD,GEE,AJA,KX,P2I(30),U2I(30),H2I(30)
      COMMON PT2(30),RHO(30),TE2I(30),VE2I(30),CV2(30),CP2(30),GAM2(30)
      COMMON ACC2(30),XMACH2(30),RORAT(30),TRAT(30),PRAT(30),PTRAT(30)
      COMMON BIGB4,B6,A6,AL
      COMMON /CLUX/ TC,VC,E1,E2
      COMMON/DOPE/A,B,C,PRAY
      COMMON/PRTS/ PXTV,PVTV
      COMMON /RATS/PEE,TEE,PT2ORT(30),P1T2RT(30),T2ORT(30)
      DIMENSION IPIVOT(2),INDEX(2,2)
      DIMENSION TC(30),VC(30)
      DIMENSION HOPE(25),BEG(25),TEMP(25)
      DIMENSION AMAT(2,2),BMAT(2)
```

```
      EQUIVALENCE (C3,G3),(C5,XJ3),(C2,D3)
      EXTERNAL FONC,FOND
      ICHEK=0
      EL=1./144.
      K=KX
      A=H+VEL**2/(50082.)
      B=P+(EL/32.174)*VEL**2/V
      C=VEL/V
 8000 FORMAT(5H1SHOC,5X,2HA=E15.8,5X,2HB=E15.8,5X,2HC=E15.8,
     12HV=E15.8,5X,4HVEL=E15.8)
      WRITE(6,8000) A,B,C,V,VEL
      MAXI=30
      PRAY=TC(K)
      HOPE(1)=VC(K)
   77 DO 59 IND=1,30
C     H(T,V)
      HTV=FOND(HOPE(1))
C     P(T,V)
      PTV=FONC(HOPE(1))
      WRITE(6,9000) HTV,PTV
 9000 FORMAT(6E17.8)
C     PX(T,V)
      PXTV=FONCX(HOPE(1))
C     PV(T,V)
      PVTV=FONCV(HOPE(1))
      WRITE(6,9000) PXTV,PVTV
C     HX(T,V)
      HXTV=FONDX(HOPE(1))
C     HV(T,V)
      HVTV=FONDV(HOPE(1))
      WRITE(6,9000) HXTV,HVTV
      AMAT(2,1)=HXTV
      AMAT(2,2)=HVTV
      AMAT(1,1)=PXTV
      AMAT(1,2)=PVTV
      BMAT(2)=(-HTV)
      BMAT(1)=(-PTV)
      WRITE(6,2000) BMAT,AMAT
      CALL MATINV(AMAT,2,BMAT,1,DETERM,IPIVOT,INDEX,2,ISCALE)
      WRITE(6,2000) BMAT
      WRITE(6,2000) HOPE(1),PRAY,PTV,HTV
 2000 FORMAT(5E20.8)
      DEL1=ABS(BMAT(1)/PRAY )
      DEL2=ABS(BMAT(2)/HOPE(1))
      IF(( DEL1 .LE.E1).AND.(DEL2  .LE.E2))  GO TO 60
```

```
      PRAY=PRAY+BMAT(1)
      HOPE(1)=HOPE(1)+BMAT(2)
   59 CONTINUE
C     TOO MANY ITERATIONS HERE
      WRITE(6,2001)
 2001 FORMAT(15HOMAX ITERATIONS)
      RETURN
   60 CONTINUE
      WRITE(6,1000) PRAY,HOPE(1)
 1000 FORMAT( 7H ROOTS=E15.8,E20.8)
    1 FORMAT(5H HOPE,20X,3HBEG,20X,4HTEMP/3E22.6)
      VE2I(K)=HOPE(1)
      TE2I(K)=PRAY
      P2I(K)=PRES(VE2I(K),TE2I(K))
      U2I(K)=C*VE2I(K)
      CALL EQU3(TE2I(K),VE2I(K),ENTH)
      H2I(K)=ENTH + 200.0
      RHO(K)=1./VE2I(K)
      CV2(K)=CEV(VE2I(K),TE2I(K))
      CP2(K)=CEP(VE2I(K),TE2I(K))+CV2(K)
      GAM2(K)=CP2(K)/CV2(K)
      ACC2(K)=SQRT(ABS(GAM2(K))*ABS(PART(VE2I(K),TE2I(K)))*4633.056)
      XMACH2(K)=U2I(K)/ACC2(K)
      RORAT(K)=VE2I(K)/V
      TRAT(K)=TE2I(K)/T
      PRAT(K)=P2I(K)/P
      RORAT(K)=V/VE2I(K)
      T2CRT(K)=TE2I(K)/TEE
      KX=KX+1
      RETURN
      END
$IBFTC FOND    DECK
      FUNCTION FOND(VE)
      COMMON A2,A3,A4,A5,B2,B3,B4,B5,C2,C3,C4,C5,XKK,R,TREF,VREF,BLIT,XJ
      COMMON D4,Z4,ESS,TUFF,CLOD,GEE,AJA,KX,P2I(30),U2I(30),H2I(30)
      COMMON PT2(30),RHO(30),TE2I(30),VE2I(30),CV2(30),CP2(30),GAM2(30)
      COMMON ACC2(30),XMACH2(30),RORAT(30),TRAT(30),PRAT(30),PTRAT(30)
      COMMON BIGB4,B6,A6,AL
      COMMON/DOPE/A,B,C,PRAY
      EQUIVALENCE (C3,G3),(C5,XJ3),(C2,D3)
      PO (XL,AT)=1./EXP(XL*AT)
      TE=PRAY
      H6 =Z4*(TE-TREF)+B4*(TE**2-TREF**2)/2.+C4*(TE**3-TREF**3)/3.+D4*
     2(TE**4-TREF**4)/4.+(PO(XKK,TE)*(XKK*TE+1.)-PO(XKK,TREF)*(XKK*TREF
     3+1.))*(XJ*D3/(VREF-BLIT)+XJ*G3/(2.*(VREF-BLIT)**2)+XJ*XJ3/(4.*
```

```
     4(VREF-BLIT)**4))+XJ*(VREF*R*(TE-TREF)/(VREF-BLIT)+VREF*(B2*(TE-
     5TREF)+C2*(PO(XKK,TE)-PO(XKK,TREF)))/(VREF-BLIT)**2)+XJ*(VREF*(B3*
     6(TE-TREF)+C3*(PO(XKK,TE)-PO(XKK,TREF)))/(VREF-BLIT)**3)+XJ*(VREF*
     7(B5*(TE-TREF)+C5*(PO(XKK,TE)-PO(XKK,TREF)))/(VREF-BLIT)**5)-(R*TE*
     8(ALOG((VE-BLIT)/(VREF-BLIT))+BLIT/(VREF-BLIT)-BLIT/(VE-BLIT)))*XJ
      H7=H6-(2.*(A2+B2*TE+C2*PO(XKK,TE))*(1./(VREF-BLIT)+BLIT/(2.*(VREF-
     2BLIT)**2)-1./(VE-BLIT)-BLIT/(2.*(VE-BLIT)**2)))*XJ
      H8=H7-(3.*(A3+B3*TE+C3*PO(XKK,TE))*(1./(2.*(VREF-BLIT)**2)+BLIT/(3
     2.*(VREF-BLIT)**3)-1./(2.*(VE-BLIT)**2)-BLIT/(3.*(VE-BLIT)**3)))*XJ
      H9=H8-(4.*A4*(1./(3.*(VREF-BLIT)**3)+BLIT/(4.*(VREF-BLIT)**4)-1./(
     23.*(VE-BLIT)**3)-BLIT/(4.*(VE-BLIT)**4)))*XJ
      H10=H9-((5.*(A5+B5*TE+C5*PO(XKK,TE)))*(1./(4.*(VREF-BLIT)**4)+BLIT
     2/(5.*(VREF-BLIT)**5)-1./(4.*(VE-BLIT)**4)-BLIT/(5.*(VE-BLIT)**5)))
     3*XJ
      H11=H10+TE*R*ALOG((VE-BLIT)/(VREF-BLIT))*XJ
      H12=H11-TE*(B2-XKK*C2*PO(XKK,TE))*(1./(VE-BLIT)-1./(VREF-BLIT))*XJ
      H13=H12-TE*(B3-XKK*C3*PO(XKK,TE))/2.*(1./(VE-BLIT)**2-1./(VREF-BLI
     2T)**2)*XJ
      H14=H13-TE*(B5-XKK*C5*PO(XKK,TE))/4.*(1./(VE-BLIT)**4-1./(VREF-BLI
     2T)**4)*XJ
      FOND=H14+C**2*VE**2/(2.*GEE*AJA)-A   +200.
      EXAL=EXP(AL*VE)                                                    EQU3
      EXAR=EXP(AL*VREF)                                                  EQU3
      TEMP=XJ*VREF*((BIGB4*(TE-TREF)/(VREF-BLIT)**4) +B6*EXAR*(TE-TREF))EQU3
      DUM=BIGB4*TE/(VE-BLIT)**4                                          EQU3
      DUM1=A6*EXAL+B6*TE*EXAL                                            EQU3
      TEMP=TEMP+XJ*VE*(0.5*VE*(-4.*DUM/(VE-BLIT)+AL*DUM1)+ DUM+DUM1)     EQU3
      DUM=BIGB4*TE/(VREF-BLIT)**4                                        EQU3
      DUM1=A6*EXAR+B6*TE*EXAR                                            EQU3
      TEMP=TEMP-XJ*VREF*(0.5*VREF*(-4.*DUM/(VREF-BLIT)+AL*DUM1)+         EQU3
     1DUM+DUM1)                                                          EQU3
      TEMP=TEMP+XJ*(BIGB4*TE*(1./(3.*(VREF-BLIT)**3)-1./(3.*(VE-BLIT)   EQU3
     1**3))+B6*TE*(EXAL-EXAR)/AL)                                        EQU3
      FOND=FOND+TEMP
      RETURN
      END
$IBFTC FONC     DECK
      FUNCTION FONC(VE)
C     EQ. OF STATE FOR NEWTON-RAPHSON                                    FONC
      COMMON A2,A3,A4,A5,B2,B3,B4,B5,C2,C3,C4,C5,XKK,R,TREF,VREF,BLIT,XJ
      COMMON D4,Z4,ESS,TUFF,CLOD,GEE,AJA,KX,P2I(30),U2I(30),H2I(30)
      COMMON PT2(30),RHO(30),TE2I(30),VE2I(30),CV2(30),CP2(30),GAM2(30)
      COMMON ACC2(30),XMACH2(30),RORAT(30),TRAT(30),PRAT(30),PTRAT(30)
      COMMON BIGB4,B6,A6,AL
      EQUIVALENCE (C3,G3),(C5,XJ3),(C2,D3)
```

```
      COMMON/DOPE/A,B,C,PRAY
      PO (XL,AT)=1./EXP(XL*AT)
      EL=1./144.
      TE=PRAY
      POT=PO(XKK,TE)                                                    FONCV
      FONC=R*TE/(VE-BLIT)+(A2+B2*TE+C2*POT)/(VE-BLIT)**2+(A3+B3*TE+     FONC
     1C3*POT)/(VE-BLIT)**3+(A4+BIGB4*TE)/(VE-BLIT)**4+(A5+B5*TE+C5*POT) FONC
     2/(VE-BLIT)**5+(A6+B6*TE)*EXP(AL*VE)+(EL/GEE)*C**2*VE-B            FONC
      RETURN
      END
      FUNCTION FOP(V)                                                   FOP
C     EQN OF STATE-USED TO FIND V AS A FUNCTION OF P+T
      COMMON A2,A3,A4,A5,B2,B3,B4,B5,C2,C3,C4,C5,XKK,R,TREF,VREF,BLIT,XJ
      COMMON D4,Z4,ESS,TUFF,CLOD,GEE,AJA,KX,P2I(30),U2I(30),H2I(30)
      COMMON PT2(30),RHO(30),TE2I(30),VE2I(30),CV2(30),CP2(30),GAM2(30)
      COMMON ACC2(30),XMACH2(30),RORAT(30),TRAT(30),PRAT(30),PTRAT(30)
      COMMON BIGB4,B6,A6,AL
      PO (XL,AT)=1./EXP(XL*AT)
      COMMON/DESP/VOODOO,ZULU
      T=VOODOO
      P=ZULU
      POT=PO(XKK,T)                                                     FOP
      FOP=P-(R*T)/(V-BLIT)-(A2+B2*T+C2*POT)/(V-BLIT)**2-(A3+B3*T+       FOP
     1C3*POT)/(V-BLIT)**3-(A4+BIGB4*T)/(V-BLIT)**4-(A5+B5*T+C5*POT)/    FOP
     2(V-BLIT)**5-(A6-B6*T)*EXP(AL*V)                                   FOP
      RETURN
      END
      FUNCTION CEV(VE,TE)
      COMMON A2,A3,A4,A5,B2,B3,B4,B5,C2,C3,C4,C5,XKK,R,TREF,VREF,BLIT,XJ
      COMMON D4,Z4,ESS,TUFF,CLOD,GEE,AJA,KX,P2I(30),U2I(30),H2I(30)
      COMMON PT2(30),RHO(30),TE2I(30),VE2I(30),CV2(30),CP2(30),GAM2(30)
      COMMON ACC2(30),XMACH2(30),RORAT(30),TRAT(30),PRAT(30),PTRAT(30)
      COMMON BIGB4,B6,A6,AL
      EQUIVALENCE (C3,G3),(C5,XJ3),(C2,D3)
      PO (XL,AT)=1./EXP(XL*AT)
      CEV=Z4+B4*TE+C4*TE**2+D4*TE**3-XJ*(D3*TE*XKK**2*PO(XKK,TE))/(VE-
     2BLIT)-XJ*(G3*TE*XKK**2*PO(XKK,TE))/(2.*(VE-BLIT)**2)-XJ*(XJ3*TE*
     3XKK**2*PO(XKK,TE))/(4.*(VE-BLIT)**4)
      RETURN
      END
      FUNCTION PRES(VE,TE)                                              PRES
C     EQUATION OF STATE
      COMMON A2,A3,A4,A5,B2,B3,B4,B5,C2,C3,C4,C5,XKK,R,TREF,VREF,BLIT,XJ
      COMMON D4,Z4,ESS,TUFF,CLOD,GEE,AJA,KX,P2I(30),U2I(30),H2I(30)
      COMMON PT2(30),RHO(30),TE2I(30),VE2I(30),CV2(30),CP2(30),GAM2(30)
```

```
      COMMON ACC2(30),XMACH2(30),RORAT(30),TRAT(30),PRAT(30),PTRAT(30)
      COMMON BIGB4,B6,A6,AL
      PO (XL,AT)=1./EXP(XL*AT)
      POT=PO(XKK,TE)                                                    PRES
      PRES=R*TE/(VE-BLIT)+(A2+B2*TE+C2*POT)/(VE-BLIT)**2+(A3+B3*TE      PRES
     1+C3*POT)/(VE-BLIT)**3+(A4+BIGB4*TE)/(VE-BLIT)**4+(A5+B5*TE+C5*POT)PRES
     2/(VE-BLIT)**5+(A6+B6*TE)*EXP(AL*VE)                               PRES
      RETURN
      END
      FUNCTION CEP(VE,TE)
C     CP                                                                CEP
      COMMON A2,A3,A4,A5,B2,B3,B4,B5,C2,C3,C4,C5,XKK,R,TREF,VREF,BLIT,XJ
      COMMON D4,Z4,ESS,TUFF,CLOD,GEE,AJA,KX,P2I(30),U2I(30),H2I(30)
      COMMON PT2(30),RHO(30),TE2I(30),VE2I(30),CV2(30),CP2(30),GAM2(30)
      COMMON ACC2(30),XMACH2(30),RORAT(30),TRAT(30),PRAT(30),PTRAT(30)
      COMMON BIGB4,B6,A6,AL
      EQUIVALENCE (C3,G3),(C5,XJ3),(C2,D3)
      PO (XL,AT)=1./EXP(XL*AT)
      DEN=R*TE/(VE-BLIT)**2+2.*(A2+B2*TE+C2*PO(XKK,TE))/(VE-BLIT)**3+3.
     2*(A3+B3*TE+C3*PO(XKK,TE))/(VE-BLIT)**4+4.*A4/(VE-BLIT)**5+5.*
     3(A5+B5*TE+C5*PO(XKK,TE))/(VE-BLIT)**6
      WRITE(6,100) DEN,TE,VE
      EXAL=EXP(AL*VE)                                                   CEP
      DEN=DEN-4.*BIGB4*TE/(VE-BLIT)**5+A6*AL*EXAL+B6*AL*TE*EXAL         CEP
      WRITE(6,100) EXAL,DEN
      XNU=R/(VE-BLIT)+(B2-XKK*C2*PO(XKK,TE))/(VE-BLIT)**2+(B3-XKK*C3*
     2PO(XKK,TE))/(VE-BLIT)**3+(B5-XKK*C5*PO(XKK,TE))/(VE-BLIT)**5
      WRITE(6,100) XNU
      XNU =XNU+BIGB4/(VE-BLIT)**4+B6*EXAL                               CEP
      WRITE(6,100) XNU
      XNUM=TE*XJ*XNU**2
      WRITE(6,100) XNUM
      CEP =XNUM/DEN
      WRITE(6,100) CEP
  100 FORMAT(3E20.8)
      RETURN
      END
      SUBROUTINE EQU3(TE,VE,ANS3)
C     ENTHALPY                                                          EQU3
      COMMON A2,A3,A4,A5,B2,B3,B4,B5,C2,C3,C4,C5,XKK,R,TREF,VREF,BLIT,XJ
      COMMON D4,Z4,ESS,TUFF,CLOD,GEE,AJA,KX,P2I(30),U2I(30),H2I(30)
      COMMON PT2(30),RHO(30),TE2I(30),VE2I(30),CV2(30),CP2(30),GAM2(30)
      COMMON ACC2(30),XMACH2(30),RORAT(30),TRAT(30),PRAT(30),PTRAT(30)
      COMMON BIGB4,B6,A6,AL
      EQUIVALENCE (C3,G3),(C5,XJ3),(C2,D3)
```

```
      PO (XL,AT)=1./EXP(XL*AT)
      ANS3=Z4*(TE-TREF)+B4*(TE**2-TREF**2)/2.+C4*(TE**3-TREF**3)/3.+D4*
     2(TE**4-TREF**4)/4.+(PO(XKK,TE)*(XKK*TE+1.)-PO(XKK,TREF)*(XKK*TREF
     3+1.))*(XJ*D3/(VE-BLIT)+XJ*G3/(2.*(VE-BLIT)**2)+XJ*XJ3/(4.*(VE-
     4BLIT)**4))+XJ*(VE*R*(TE-TREF)/(VE-BLIT)+VE*(B2*(TE-TREF)+C2*(PO
     5(XKK,TE)-PO(XKK,TREF)))/(VE-BLIT)**2)+XJ*(VE*(B3*(TE-TREF)+C3*(PO
     6(XKK,TE)-PO(XKK,TREF)))/(VE-BLIT)**3)+XJ*(VE*(B5*(TE-TREF)+C5*(PO
     7(XKK,TE)-PO(XKK,TREF)))/(VE-BLIT)**5)-(R*TREF*(ALOG((VE-BLIT)/(VR
     8EF-BLIT))+BLIT/(VREF-BLIT)-BLIT/(VE-BLIT)))*XJ-(2.*(A2+B2*TREF+C2
     9*PO(XKK,TREF))*(1./(VREF-BLIT)+BLIT/(2.*(VREF-BLIT)**2)-1./(VE-
     ABLIT)-BLIT/(2.*(VE-BLIT)**2)))*XJ-(3.*(A3+B3*TREF+C3*PO(XKK,TREF
     B))*(1./(2.*(VREF-BLIT)**2)+BLIT/(3.*(VREF-BLIT)**3)-1./(2.*(VE-
     CBLIT)**2)-BLIT/(3.*(VE-BLIT)**3)))*XJ-(4.*A4*(1./(3.*(VREF-BLIT)
     D**3)+BLIT/(4.*(VREF-BLIT)**4)-1./(3.*(VE-BLIT)**3)-BLIT/(4.*(VE-
     EBLIT)**4)))*XJ
      ANS3=ANS3-((5.*(A5+B5*TREF+C5*PO(XKK,TREF)))*(1./(4.*(VREF-BLIT)
     2**4)+BLIT/(5.*(VREF-BLIT)**5)-1./(4.*(VE-BLIT)**4)-BLIT/(5.*(VE-
     3BLIT)**5)))*XJ+TREF*R*ALOG((VE-BLIT)/(VREF-BLIT))*XJ-TREF*(B2-XKK
     4*C2*PO(XKK,TREF))*(1./(VE-BLIT)-1./(VREF-BLIT))*XJ-TREF*(B3-XKK*
     5C3*PO(XKK,TREF))/2.*(1./(VE-BLIT)**2-1./(VREF-BLIT)**2)*XJ-TREF*
     6(B5-XKK*C5*PO(XKK,TREF))/4.*(1./(VE-BLIT)**4-1./(VREF-BLIT)**4)
     7*XJ
      EXAL=EXP(AL*VE)                                                    EQU3
      EXAR=EXP(AL*VREF)                                                  EQU3
      TEMP=XJ*VREF*((BIGB4*(TE-TREF)/(VREF-BLIT)**4) +B6*EXAR*(TE-TREF))EQU3
      DUM=BIGB4*TE/(VE-BLIT)**4                                          EQU3
      DUM1=A6*EXAL+B6*TE*EXAL                                            EQU3
      TEMP=TEMP+XJ*VE*(0.5*VE*(-4.*DUM/(VE-BLIT)+AL*DUM1)+ DUM+DUM1)     EQU3
      DUM=BIGB4*TE/(VREF-BLIT)**4                                        EQU3
      DUM1=A6*EXAR+B6*TE*EXAR                                            EQU3
      TEMP=TEMP-XJ*VREF*(0.5*VREF*(-4.*DUM/(VREF-BLIT)+AL*DUM1)+         EQU3
     1DUM+DUM1)                                                          EQU3
      TEMP=TEMP+XJ*(BIGB4*TE*(1./(3.*(VREF-BLIT)**3)-1./(3.*(VE-BLIT)   EQU3
     1**3))+B6*TE*(EXAL-EXAR)/AL)                                        EQU3
      ANS3=ANS3+TEMP                                                     EQU3
      RETURN
      END
      FUNCTION PART(V,T)
C     PARTIAL P W,R,T, RHO                                               PART
      COMMON A2,A3,A4,A5,B2,B3,B4,B5,C2,C3,C4,C5,XKK,R,TREF,VREF,BLIT,XJ
      COMMON D4,Z4,ESS,TUFF,CLOD,GEE,AJA,RX,P2I(30),U2I(30),H2I(30)
      COMMON PT2(30),RHO(30),TE2I(30),VE2I(30),CV2(30),CP2(30),GAM2(30)
      COMMON ACC2(30),XMACH2(30),RORAT(30),TRAT(30),PRAT(30),PTRAT(30)
      COMMON BIGB4,B6,A6,AL
      EQUIVALENCE (C3,G3),(C5,XJ3),(C2,D3)
```

```
      PO (XL,AT)=1./EXP(XL*AT)
      PART=R*T*V**2/(V-BLIT)**2+4.*A4*V**2/(V-BLIT)**5+2.*V**2*(A2+B2*
     2T+C2*PO(XKK,T))/(V-BLIT)**3+3.*V**2*(A3+B3*T+C3*PO(XKK,T))/(V-BL
     3IT)**4+5.*V**2*(A5+B5*T+C5*PO(XKK,T))/(V-BLIT)**6
      EXAL=EXP(AL*V)                                                    PART
      PART=PART-(V**2)*(-4.*BIGB4*T/(V-BLIT)**5+A6*AL*EXAL+B6*T*AL*EXAL)PART
      RETURN
      END
      FUNCTION FONDX(VE)
C     PARTIAL H W.R.T. T                                                FONDX
      COMMON/PRTS/ PXTV,PVTV
      COMMON A2,A3,A4,A5,B2,B3,B4,B5,C2,C3,C4,C5,XKK,R,TREF,VREF,BLIT,XJ
      COMMON D4,Z4,ESS,TUFF,CLOD,GEE,AJA,KX,P2I(30),U2I(30),H2I(30)
      COMMON PT2(30),RHO(30),TE2I(30),VE2I(30),CV2(30),CP2(30),GAM2(30)
      COMMON ACC2(30),XMACH2(30),RORAT(30),TRAT(30),PRAT(30),PTRAT(30)
      COMMON BIGB4,B6,A6,AL
      COMMON/DOPE/A,B,C,PRAY
      EQUIVALENCE (C3,G3),(C5,XJ3),(C2,D3)
      PO (XL,AT)=1./EXP(XL*AT)
      TE=PRAY
      FONDX=Z4+B4*TE+C4*TE**2-XJ*((D3*TE*(XKK**2)*PO(XKK,TE))/(VE-BLIT))
     1-XJ*((G3*TE*(XKK**2)*PO(XKK,TE))/(2.0*(VE-BLIT)**2))
     2-XJ*((XJ3*TE*(XKK**2)*PO(XKK,TE))/(4.0*(VE-BLIT)**4))
     3+VE*PXTV+D4*TE**3
      EXAR=EXP(AL*VREF)                                                 FONDX
      EXAL=EXP(AL*VE)                                                   FONDX
      DUM=BIGB4/(VE  -BLIT)**4                                          FONDX
      DUM1=B6*EXAL                                                      FONDX
      TEMP=XJ* VE *(DUM+DUM1+VE*(-4.*DUM/(VE-BLIT)+AL*DUM1))            FONDX
      TEMP=TEMP-0.5*XJ*VREF*VREF*(-4.*BIGB4/(VREF-BLIT)**5+B6*AL*EXAR)  FONDX
      FONDX=TEMP+FONDX+XJ*(BIGB4*(1./(3.*(VREF-BLIT)**3)-1./(3.*(VE-    FONDX
     1BLIT)**3))+(B6/AL)*(EXAL-EXAR))
      RETURN
      END
      FUNCTION FONCX(VE)
C     PARTIAL OF P(V,T) W.R.T. T                                        FONCX
      COMMON/PRTS/ PXTV,PVTV
      COMMON A2,A3,A4,A5,B2,B3,B4,B5,C2,C3,C4,C5,XKK,R,TREF,VREF,BLIT,XJ
      COMMON D4,Z4,ESS,TUFF,CLOD,GEE,AJA,KX,P2I(30),U2I(30),H2I(30)
      COMMON PT2(30),RHO(30),TE2I(30),VE2I(30),CV2(30),CP2(30),GAM2(30)
      COMMON ACC2(30),XMACH2(30),RORAT(30),TRAT(30),PRAT(30),PTRAT(30)
      COMMON BIGB4,B6,A6,AL
      EQUIVALENCE (C3,G3),(C5,XJ3),(C2,D3)
      COMMON/DOPE/A,B,C,PRAY
      PO (XL,AT)=1./EXP(XL*AT)
```

```
      EL=1./144.
      TE=PRAY
      FONCX=R /(VE-BLIT)+(B2-C2*XKK*PO(XKK,TE))/(VE-BLIT)**2
     1+(B3-C3*XKK*PO(XKK,TE))/(VE-BLIT)**3 +(B5-C5*XKK*PO(XKK,TE))
     2/(VE-BLIT)**5
      FONCX=FONCX+BIGB4/(VE-BLIT)**4+B6*EXP(AL*VE)                    FONCX
      RETURN
      END
      FUNCTION FONDV(VE)                                              FONDV
C     PARTIAL  H W,R,T, V
      COMMON/PRTS/ PXTV,PVTV
      COMMON A2,A3,A4,A5,B2,B3,B4,B5,C2,C3,C4,C5,XKK,R,TREF,VREF,BLIT,XJ
      COMMON D4,Z4,ESS,TUFF,CLOD,GEE,AJA,KX,P2I(30),U2I(30),H2I(30)
      COMMON PT2(30),RHO(30),TE2I(30),VE2I(30),CV2(30),CP2(30),GAM2(30)
      COMMON ACC2(30),XMACH2(30),RORAT(30),TRAT(30),PRAT(30),PTRAT(30)
      COMMON BIGB4,B6,A6,AL
      COMMON/DOPE/A,B,C,PRAY
      EQUIVALENCE (C3,G3),(C5,XJ3),(C2,D3)
      PO (XL,AT)=1./EXP(XL*AT)
      TE=PRAY
      FONDV=VE*PVTV +TE*PXTV +(C**2)*VE/( GEE*AJA)                    FONDV
      EXAL=EXP(AL*VE)                                                 FONDV
      DUM=BIGB4*TE/(VE-BLIT)**4                                       FONDV
      DUM1=A6*EXAL                                                    FONDV
      DUM2=B6*TE*EXAL                                                 FONDV
      TEMP=2.0*XJ*VE*(-4.*DUM/(VE-BLIT)+AL*(DUM1+DUM2))+XJ*(2.0*(DUM+ FONDV
     1DUM2)+DUM1)                                                     FONDV
      FONDV=FONDV+TEMP+0.5*XJ*VE*VE*(20.*DUM/(VE-BLIT)**2+(AL**2)*    FONDV
     1(DUM1+DUM2))                                                    FONDV
      RETURN
      END
      FUNCTION FONCV(VE)                                              FONCV
C     PARTIAL OF  P(V,T) W,R,T, V
      COMMON/PRTS/ PXTV,PVTV
      COMMON A2,A3,A4,A5,B2,B3,B4,B5,C2,C3,C4,C5,XKK,R,TREF,VREF,BLIT,XJ
      COMMON D4,Z4,ESS,TUFF,CLOD,GEE,AJA,KX,P2I(30),U2I(30),H2I(30)
      COMMON PT2(30),RHO(30),TE2I(30),VE2I(30),CV2(30),CP2(30),GAM2(30)
      COMMON ACC2(30),XMACH2(30),RORAT(30),TRAT(30),PRAT(30),PTRAT(30)
      COMMON BIGB4,B6,A6,AL
      EQUIVALENCE (C3,G3),(C5,XJ3),(C2,D3)
      COMMON/DOPE/A,B,C,PRAY
      PO (XL,AT)=1./EXP(XL*AT)
      EL=1./144.
      TE=PRAY
      FONCV=(-R*TE)/(VE-BLIT)**2-2.*(A2+B2*TE+C2*PO(XKK,TE))/(VE-BLIT)
```

APPENDIX C – Continued

Program B – Concluded

```
     1**3-3.0*(A3+B3*TE+C3*PO(XKK,TE))/(VE-BLIT)**4-4.0*A4/(VE-BLIT)**5
     2-5.0*(A5+B5*TE+C5*PO(XKK,TE))/(VE-BLIT)**6+(EL/GEE)*C**2
      POT=PO(XKK,TE)                                                    FONCV
      FONCV=(-R*TE)/(VE-BLIT)**2-2.0*(A2+B2*TE+C2*POT)/(VE-BLIT)**3     FONCV
     1-3.0*(A3+B3*TE+C3*POT)/(VE-BLIT)**4-4.0*(A4+BIGB4*TE)/(VE-BLIT)**5FONCV
     2-5.0*(A5+B5*TE+C5*POT)/(VE-BLIT)**6+AL*(A6+B6*TE)*EXP(AL*VE)      FONCV
     3+(EL/GEE)*C**2                                                    FONCV
      RETURN
      END
-00
 $DATA A2=-2.162959,A3=4.04057E-3,A4=1.921072E-4,A5=-4.481049E-6,
 XKK=.976E-2,B2=2.135114E-3,B3=1.282818E-5,B4=3.00892783E-4,
 B5=9.062318E-9,XJ=.185053,
 C2=-18.941131,C3=0.539776,C4=-1.30237441E-7,C5=-4.836678E-5,
 R=0.1219336,BLIT=0.15E-2,D4=1.96802894E-11,PEE=0.1026,
 IEND=5,
 VI(1)=3000,3500,4000,4500,5000,
 TC(1)=1344,1610,1910,2250,2600,
 VC(1)=14.9,13.2,12.1,11.7,11.3,
 PEI(1)=5*3.87E-1,
 A1=15,
 TEE=260,GEE=32.174,AJA=778.3,A=.008,B=12000,DELTX=2,
 TREF=820,PREF=1,TZ=409.5,Z4=1.90458084E-2,
 TEI=5*532,E1=.00001,E2=.00001,MAXI=30,NUMB=5,INT=0,
 A6=5.83882E7, BIGB4=-3.918263E-7, AL=-6.61199E2, B6=-9.26392E4,
 PEE=.387$
```

APPENDIX C – Continued

Program C

NASA-LANGLEY RESEARCH CENTER

01 4	01 7 PROGRAM NO	COMPUTER PROGRAM ABSTRACT	01 14 DATE
LAR			10/68

01 20 TITLE OF PROGRAM (61 CHARACTERS MAXIMUM)	PARENT PROGRAM		
	02 14 CATEGORY	02 15 SITE	02 16 PROGRAM NO
Total Conditions Behind Shock			

02 26 CATEGORY	02 27 LANGUAGE NO 1	02 32 LANGUAGE NO 2	02 37 KEY WORDS (8 MAXIMUM SEPARATED BY COMMAS)
R	FØR6M		Shock, Static, Isentropic, Total, Tetrafluoromethane

WHO TO CONTACT ABOUT THE PROGRAM					05 48 STATUS	05 49
05 14 CONTACT	05 28 SITE	05 31 ORGN CODE	05 39 PROJECT NO	05 45 NASA CENTER	☐ A UNDER DEVELOPMENT ☐ B OPERATIONAL ☒ C COMPLETED	☐ A THIS PROGRAM IS NOT FOR SHARING
K. A. Smith	LAR	11.170	RGL-206			

DATES		05 56 REVISION CODE	TIME AND COST FOR DEVELOPMENT			
05 50 INITIATED	05 54 COMPLETED	☐ A REVISION ☐ B CANCELLATION	05 59 MANMONTHS (59 60 61 62 63)	05 64 MACHINE HOURS (64 65 66 67 68)	05 69 COMPUTER TYPE	05 74 TOTAL COST (DOLLARS) (74 75 76 77 78 79 80)
04/68	10/68				6000	

ELITE MARGIN | PICA MARGIN

CARD NUMBER | COLUMN 14

ABSTRACT

With the static conditions behind a given shock in CF_4 known, the total conditions behind this shock are obtained by bringing the flow to rest isentropically. The governing statement in this compression process is that the entropy (stipulated by the static conditions behind the shock) remains constant. The final point in this compression process is stipulated by the total enthalpy which is constant on either side of the shock. The relations for isentropic compressions in equilibrium tetrafluoromethane are programed to yield the total properties of a one-dimensional flow. The static temperature and static specific volume behind a given shock are used as inputs along with the stagnation temperature and pressure, in the case of the expansion problem, and the static temperature, static pressure, and projectile velocity in the case of the ballistic-range problem.

Program C – Continued

```
      PROGRAM PCH(INPUT,OUTPUT,TAPE5=INPUT,TAPE6=OUTPUT,TAPE8)
      COMMON A2,A3,A4,A5,B2,B3,B4,B5,C2,C3,C4,C5,XKK,R,TREF,VREF,BLIT,XJ
      COMMON D4,Z4,ESS,TUFF,CLOD,GEE,AJA,KX,P2I(30),U2I(30),H2I(30)
      COMMON S2,H0
      COMMON PT2(30),RHO(30),TE2I(30),VE2I(30),CV2(30),CP2(30),GAM2(30)
      COMMON ACC2(30),XMACH2(30),RORAT(30),TRAT(30),PRAT(30),PTRAT(30)
      COMMON BIGB4,B6,A6,AL
      COMMON/CLUX/TC ,VC
      COMMON/DESP/VOODOO,ZULU
      EXTERNAL FOP
      DIMENSION TC(30),VC(30)
      DIMENSION P1ORAT(30),T1ORAT(30),REN(30)
      COMMON /RATS/PEE,TEE,PT2ORT(30),P1T2RT(30),T2ORT(30)
      DIMENSION NO(30)
      EQUIVALENCE (C3,G3),(C5,XJ3),(C2,D3)
      PO (XL,AT)=1./EXP(XL*AT)
      DIMENSION TEI(30),VEI(30),PEI(30),VI(30),GAM(30),SPEED(30)
      DIMENSIONXMACH(30),CP(30),CV(30),H(30),VIS(30)
      DIMENSION P2RT(30),P2T(30),P2T1(30),T2TT(30),V2TV(30),S2(30)
      DIMENSION AMAT(2,2),BMAT(2),IPIVOT(2),INDEX(2,2)
      NAMELIST /DATA/A2,A3,A4,A5,A6,B2,B3,BIGB4,B5,B6,B4,AL,
     1C2,C3,C4,C5,XKK,XJ,R,BLIT,D4,PEE,TEE,GEE,AJA,NUMB,INT,Z4,A,B,
     2DELTX,IEND,TEI,E1,E2,MAXI,TREF,PREF,TZ,TC,VC,THETA,
     3VEE,H0,PRAT,XMACH,NO,VEI,VREF,S2,U2I
   99 READ(5,DATA)
      WRITE(6,DATA)
      WRITE(6,88)A2,A3,A4,A5,B2,B3,B4,B5
   88 FORMAT(10H0A2 5 B2 5//8E13.5)
      WRITE(6,89)C2,C3,C4,C5,XKK,XJ,R,BLIT
   89 FORMAT(20H0C2 5  K   J   R   B/8E13.5)
      WRITE(6,90)D4,PEE,TEE,GEE,AJA,NUMB,INT,Z4
   90 FORMAT(23H0D4  P0  T0  G  J  N  I/5E13.5,2I13,E14.5)
      CALL EQU3(TEE,VEE,ANS3)
      DO 1 I=1,IEND
      S2(I)=ENT(VEI(I),TEI(I))
      PRINT 9,S2
    9 FORMAT(4E16.8)
      H0=ANS3+200.+(U2I(I)**2)/(2.0*GEE*AJA)
      PRINT 9,H0
      DO 22 J=1,50
      PRINT 9,VC(I),TC(I)
```

```
C       H(T,V)
        HTV=FOND(VC(I),TC(I))
C       S(T,V)
        STV=ENT(VC(I),TC(I))-S2(I)
C       HSUBT(T,V)
        HST=FONT(VC(I),TC(I))
C       HSUBV(T,V)
        HSV=FONV(VC(I),TC(I))
C       S SUBT(T,V)
        SST=ENTT(VC(I),TC(I))
C       S SUBV(T,V)
        SSV=ENTV(VC(I),TC(I))
C       SET UP MATRICES FOR NEWTON-RAPHSON
        AMAT(1,1)=HST
        AMAT(2,1)=SST
        AMAT(1,2)=HSV
        AMAT(2,2)=SSV
        BMAT(1)=-HTV
        BMAT(2)=-STV
        CALL MATINV(AMAT,2,BMAT,1,DETERM,IPIVOT,INDEX,2,ISCALE)
        DEL1=ABS(BMAT(1)/TC(I))
        DEL2=ABS(BMAT(2)/VC(I))
        PRINT 9,DEL1,DEL2,BMAT
        IF(DEL1.LT.E1.AND.DEL2.LT.E2) GO TO 33
        TC(I)=TC(I)+BMAT(1)
        VC(I)=VC(I)+BMAT(2)
     22 CONTINUE
        PRINT 101
    101 FORMAT(24HOMAX.ITERATIONS EXCEEDED)
     33 PRINT 100,NO(I),PRAT(I),VEI(I),TEI(I),XMACH(I),
       1VC(I),TC(I)
    100 FORMAT(I5,6E18.8)
C       P(V,T)
        P2T(I)=FONC(VC(I),TC(I))
        P2RT(I)=P2T(I)/PEE
        P2T1(I)=P2RT(I)/PRAT(I)
        T2TT(I)=TC(I)/TEE
        V2TV(I)=VC(I)/VEE
      1 CONTINUE
        PRINT 102,H0,S0
    102 FORMAT(4H1H0=E15.8,5X,3HS0=E15.8//1H0,10X,3HT2T,17X,3HV2T,17X,
       13HP2T,18X,2HS2)
        PRINT 103,(TC(I),VC(I),P2T(I),S2(I),I=1,IEND)
    103 FORMAT(4E20.8)
        PRINT 104
```

```
  104 FORMAT(1H1,10X,6HP2T/P0,14X,6HP2T/P1,14X,6HT2T/T0,14X,6HV2T/V0)
      PRINT 103,(P2RT(I),P2T1(I),T2TT(I),V2TV(I),I=1,IEND)
      WRITE(8) IEND
      WRITE(8) (XMACH(I),P2RT(I),P2T1(I),I=1,IEND)
      END FILE 8
      GO TO 99
      END
      FUNCTION ENT(VEE,TEE)
C     ENTROPY                                                          ENT
      COMMON A2,A3,A4,A5,B2,B3,B4,B5,C2,C3,C4,C5,XKK,R,TREF,VREF,BLIT,XJ
      COMMON D4,Z4,ESS,TUFF,CLOD,GEE,AJA,KX,P2I(30),U2I(30),H2I(30)
      COMMON S2,H0
      COMMON PT2(30),RHO(30),TE2I(30),VE2I(30),CV2(30),CP2(30),GAM2(30)
      COMMON ACC2(30),XMACH2(30),RORAT(30),TRAT(30),PRAT(30),PTRAT(30)
      COMMON BIGB4,B6,A6,AL
      DIMENSION S2(30)
      EQUIVALENCE (C3,G3),(C5,XJ3),(C2,D3)
      PO (XL,AT)=1./EXP(XL*AT)
      ESS1=Z4*ALOG(TEE/TREF)+B4*(TEE-TREF)+C4*(TEE**2-TREF**2)/2.
      ESS2=ESS1+D4*(TEE**3-TREF**3)/3.+XJ*D3*XKK/(VREF-BLIT)*(PO(XKK,TEE
     2)-PO(XKK,TREF))
      ESS3=ESS2+XJ*G3*XKK/(2.*(VREF-BLIT)**2)*(PO(XKK,TEE)-PO(XKK,TREF))
      ESS4=ESS3+XJ*XJ3*XKK/(4.*(VREF-BLIT)**4)*(PO(XKK,TEE)-PO(XKK,TREF)
     2)
      ESS5=ESS4+(R*ALOG((VEE-BLIT)/(VREF-BLIT)))*XJ
      ESS6=ESS5-(B2-XKK*C2*PO(XKK,TEE))*(1./(VEE-BLIT)-1./(VREF-BLIT))*X
     2J
      ESS7=ESS6-(B3-XKK*C3*PO(XKK,TEE))/2.*(1./(VEE-BLIT)**2-1./(VREF-BL
     2IT)**2)*XJ
      ENT=ESS7-(B5-XKK*C5*PO(XKK,TEE))/4.*(1./(VEE-BLIT)**4-1./(VREF-BLI
     2T)**4)*XJ
      EXAL=EXP(AL*VEE)                                                 ENT
      EXAR=EXP(AL*VREF)                                                ENT
      ENT=ENT+XJ*(BIGB4*(1./(3.*(VREF-BLIT)**3)-1./(3.*(VEE-BLIT)**3))  ENT
     1+B6*(EXAL-EXAR)/AL)                                              ENT
      ENT=ENT+0.848
      RETURN
      END
      FUNCTION FOND(VF,TE)
C     ENTHALPY FOR NEWTON-RAPHSON                                      FOND
      COMMON A2,A3,A4,A5,B2,B3,B4,B5,C2,C3,C4,C5,XKK,R,TREF,VREF,BLIT,XJ
      COMMON D4,Z4,ESS,TUFF,CLOD,GEE,AJA,KX,P2I(30),U2I(30),H2I(30)
      COMMON S2,H0
      COMMON PT2(30),RHO(30),TE2I(30),VE2I(30),CV2(30),CP2(30),GAM2(30)
      COMMON ACC2(30),XMACH2(30),RORAT(30),TRAT(30),PRAT(30),PTRAT(30)
```

```
      COMMON BIGB4,B6,A6,AL
      DIMENSION S2(30)
      EQUIVALENCE (C3,G3),(C5,XJ3),(C2,D3)
      P0 (XL,AT)=1./EXP(XL*AT)
      H6 =Z4*(TE-TREF)+B4*(TE**2-TREF**2)/2.+C4*(TE**3-TREF**3)/3.+D4*
     2(TE**4-TREF**4)/4.+(P0(XKK,TE)*(XKK*TE+1.)-P0(XKK,TREF)*(XKK*TREF
     3+1.))*(XJ*D3/(VREF-BLIT)+XJ*G3/(2.*(VREF-BLIT)**2)+XJ*XJ3/(4.*
     4(VREF-BLIT)**4))+XJ*(VREF*R*(TE-TREF)/(VREF-BLIT)+VREF*(B2*(TE-
     5TREF)+C2*(P0(XKK,TE)-P0(XKK,TREF)))/(VREF-BLIT)**2)+XJ*(VREF*(B3*
     6(TE-TREF)+C3*(P0(XKK,TE)-P0(XKK,TREF)))/(VREF-BLIT)**3)+XJ*(VREF*
     7(B5*(TE-TREF)+C5*(P0(XKK,TE)-P0(XKK,TREF)))/(VREF-BLIT)**5)-(R*TE*
     8(ALOG((VE-BLIT)/(VREF-BLIT))+BLIT/(VREF-BLIT)-BLIT/(VE-BLIT)))*XJ
      H7=H6-(2.*(A2+B2*TE+C2*P0(XKK,TE))*(1./(VREF-BLIT)+BLIT/(2.*(VREF-
     2BLIT)**2)-1./(VE-BLIT)-BLIT/(2.*(VE-BLIT)**2)))*XJ
      H8=H7-(3.*(A3+B3*TE+C3*P0(XKK,TE))*(1./(2.*(VREF-BLIT)**2)+BLIT/(3
     2.*(VREF-BLIT)**3)-1./(2.*(VE-BLIT)**2)-BLIT/(3.*(VE-BLIT)**3)))*XJ
      H9=H8-(4.*A4*(1./(3.*(VREF-BLIT)**3)+BLIT/(4.*(VREF-BLIT)**4)-1./(
     23.*(VE-BLIT)**3)-BLIT/(4.*(VE-BLIT)**4)))*XJ
      H10=H9-((5.*(A5+B5*TE+C5*P0(XKK,TE)))*(1./(4.*(VREF-BLIT)**4)+BLIT
     2/(5.*(VREF-BLIT)**5)-1./(4.*(VE-BLIT)**4)-BLIT/(5.*(VE-BLIT)**5)))
     3*XJ
      H11=H10+TE*R*ALOG((VE-BLIT)/(VREF-BLIT))*XJ
      H12=H11-TE*(B2-XKK*C2*P0(XKK,TE))*(1./(VE-BLIT)-1./(VREF-BLIT))*XJ
      H13=H12-TE*(B3-XKK*C3*P0(XKK,TE))/2.*(1./(VE-BLIT)**2-1./(VREF-BLI
     2T)**2)*XJ
      H14=H13-TE*(B5-XKK*C5*P0(XKK,TE))/4.*(1./(VE-BLIT)**4-1./(VREF-BLI
     2T)**4)*XJ
      FOND=H14-H0+200.0
      EXAL=EXP(AL*VE)                                                    EQU3
      EXAR=EXP(AL*VREF)                                                  EQU3
      TEMP=XJ*VREF*((BIGB4*(TE-TREF)/(VREF-BLIT)**4) +B6*EXAR*(TE-TREF))EQU3
      DUM=BIGB4*TE/(VE-BLIT)**4                                          EQU3
      DUM1=A6*EXAL+B6*TE*EXAL                                            EQU3
      TEMP=TEMP+XJ*VE*(0.5*VE*(-4.*DUM/(VE-BLIT)+AL*DUM1)+ DUM+DUM1)     EQU3
      DUM=BIGB4*TE/(VREF-BLIT)**4                                        EQU3
      DUM1=A6*EXAR+B6*TE*EXAR                                            EQU3
      TEMP=TEMP-XJ*VREF*(0.5*VREF*(-4.*DUM/(VREF-BLIT)+AL*DUM1)+         EQU3
     1DUM+DUM1)                                                          EQU3
      TEMP=TEMP+XJ*(BIGB4*TE*(1./(3.*(VREF-BLIT)**3)-1./(3.*(VE-BLIT)    EQU3
     1**3))+B6*TE*(EXAL-EXAR)/AL)                                        EQU3
      FOND=FOND+TEMP                                                     FOND
      RETURN
      END
      FUNCTION  ENTV(V,T)
C     PARTIAL  S W.R.T. V                                                ENTV
```

```
      COMMON A2,A3,A4,A5,B2,B3,B4,B5,C2,C3,C4,C5,XKK,R,TREF,VREF,BLIT,XJ
      COMMON D4,Z4,ESS,TUFF,CLOD,GEE,AJA,KX,P2I(30),U2I(30),H2I(30)
      COMMON S2,H0
      COMMON PT2(30),RHO(30),TE2I(30),VE2I(30),CV2(30),CP2(30),GAM2(30)
      COMMON ACC2(30),XMACH2(30),RORAT(30),TRAT(30),PRAT(30),PTRAT(30)
      COMMON BIGB4,B6,A6,AL
      DIMENSION S2(30)
      PO(XL,AT)=1.0/EXP(XL*AT)
      VM=V-BLIT
      SUM=(R/(V-BLIT))+(B2-XKK*C2*PO(XKK,T))/(VM**2)
      SUM=SUM+(B3-XKK*C3*PO(XKK,T))/(VM**3)
      ENTV=SUM+(B5-XKK*C5*PO(XKK,T))/(VM**5)
      ENTV=ENTV+XJ*(BIGB4/(V-BLIT)**4 +B6*EXP(AL*V))                    ENTV
      RETURN
      END
      FUNCTION   ENTT(V,T)
      COMMON A2,A3,A4,A5,B2,B3,B4,B5,C2,C3,C4,C5,XKK,R,TREF,VREF,BLIT,XJ
      COMMON D4,Z4,ESS,TUFF,CLOD,GEE,AJA,KX,P2I(30),U2I(30),H2I(30)
      COMMON S2,H0
      COMMON PT2(30),RHO(30),TE2I(30),VE2I(30),CV2(30),CP2(30),GAM2(30)
      COMMON ACC2(30),XMACH2(30),RORAT(30),TRAT(30),PRAT(30),PTRAT(30)
      COMMON BIGB4,B6,A6,AL
      DIMENSION S2(30)
      EQUIVALENCE (C3,G3),(C5,XJ3),(C2,D3)
      PO(XL,AT) =1.0/EXP(XL*AT)
      XK2=XKK*XKK
      VERB=VREF-BLIT
      VIB=V-BLIT
      POT=PO(XKK,T)
      DUM=(Z4/T)+B4+C4*T+D4*(T**2)-XJ*XK2*POT*
     1(D3/VERB+G3/(2.*(VERB**2)) + XJ3/(4.0*(VERB**4)))
      DUM=DUM-C2*XK2*POT*((1./VIB)-(1./VERB))
      ENTT=DUM-0.5*C3*XK2*POT*((1./(VIB**2))-(1./(VERB**2)))
     1-0.25*XK2*POT*C5*((1./(VIB**4))-(1./(VERB**4)))
      RETURN
      END
      FUNCTION FONT(VE,TE)                                              FONDX
C     PARTIAL H W.R.T. T
      COMMON A2,A3,A4,A5,B2,B3,B4,B5,C2,C3,C4,C5,XKK,R,TREF,VREF,BLIT,XJ
      COMMON D4,Z4,ESS,TUFF,CLOD,GEE,AJA,KX,P2I(30),U2I(30),H2I(30)
      COMMON S2,H0
      COMMON PT2(30),RHO(30),TE2I(30),VE2I(30),CV2(30),CP2(30),GAM2(30)
      COMMON ACC2(30),XMACH2(30),RORAT(30),TRAT(30),PRAT(30),PTRAT(30)
      COMMON BIGB4,B6,A6,AL
      DIMENSION S2(30)
```

```
      EQUIVALENCE (C3,G3),(C5,XJ3),(C2,D3)
      PO (XL,AT)=1./EXP(XL*AT)
      POT=PO(XKK,TE)
      VER=VREF-BLIT
      VIB=VE-BLIT
      WVB=1./VIB
      WVR=1./VER
      B2C2=B2-C2*XKK*POT
      B3C3=B3-C3*XKK*POT
      B5C5=B5-C5*XKK*POT
      VR2=WVR*WVR
      VR3=VR2*WVR
      VR5=VR2*VR3
      VB2=WVB*WVB
      VB3=WVB*VB2
      VB5=VB2*VB3
      XK2=XKK*XKK
      FONT =Z4+B4*TE+C4*TE**2-XJ*((D3*TE*(XKK**2)*PO(XKK,TE))/(VE-BLIT))
     1-XJ*((G3*TE*(XKK**2)*PO(XKK,TE))/(2.0*(VE-BLIT)**2))
     2-XJ*((XJ3*TE*(XKK**2)*PO(XKK,TE))/(4.0*(VE-BLIT)**4))
     3+XJ *VREF*(R*WVR+B2C2*VR2+B3C3*VR3+B5C5*VR5)-XJ *(R*(ALOG(VIB*WVR)
     4+BLIT*(WVR-WVB))+2.0*B2C2*(WVR+0.5*BLIT*VR2-WVB-0.5*BLIT*VB2)
     D+3.0*B3C3*(0.5*VR2+BLIT*VR3/3.0-0.5*VB2-BLIT*VB3/3.0)
     E+5.0*B5C5*(0.25*VR2*VR2+BLIT*0.2*VR5-0.25*VB2*VB2-0.2*BLIT*VB5))
     5+XJ *(R*ALOG(VIB*WVR)-B2C2*(WVB-WVR)-B3C3*(VB2-VR2)-B5C5*(VB2*VB2
     6-VR2*VR2))-XJ*TE*XK2*POT*(C2*(WVB-WVR)+0.5*C3*(VB2-VR2)
     7+0.25*C5*(VB2*VB2-VR2*VR2))+D4*(TE**3)
      EXAR=EXP(AL*VREF)                                                    FONDX
      EXAL=EXP(AL*VE)                                                      FONDX
      DUM=BIGB4/(VE  -BLIT)**4                                             FONDX
      DUM1=B6*EXAL                                                         FONDX
      TEMP=XJ* VE *(DUM+DUM1+VE*(-4.*DUM/(VE-BLIT)+AL*DUM1))               FONDX
      TEMP=TEMP-0.5*XJ*VREF*VREF*(-4.*BIGB4/(VREF-BLIT)**5+B6*AL*EXAR)     FONDX
      FONT =TEMP+FONT +XJ*(BIGB4*(1./(3.*(VREF-BLIT)**3)-1./(3.*(VE-       FONDX
     1BLIT)**3))+(B6/AL)*(EXAL-EXAR))
      RETURN
      END
      FUNCTION FONV(V,T)
C     PARTIAL  H W,R,T, V                                                   FONDV
      PO (XL,AT)=1./EXP(XL*AT)
      COMMON A2,A3,A4,A5,B2,B3,B4,B5,C2,C3,C4,C5,XKK,R,TREF,VREF,BLIT,XJ
      COMMON D4,Z4,ESS,TUFF,CLOD,GEE,AJA,KX,P2I(30),U2I(30),H2I(30)
      COMMON S2,H0
      COMMON PT2(30),RHO(30),TE2I(30),VE2I(30),CV2(30),CP2(30),GAM2(30)
      COMMON ACC2(30),XMACH2(30),RORAT(30),TRAT(30),PRAT(30),PTRAT(30)
```

```
      COMMON BIGB4,B6,A6,AL
      DIMENSION S2(30)
      VIB=1./(V-BLIT)
      V2=VIB*VIB
      V3=VIB*V2
      V4=V2*V2
      V5=V2*V3
      V6=V3*V3
      POT=PO(XKK,T)
      DUM=R*T*(VIB+BLIT*V2)+2.0*(A2+B2*T+C2*POT)*(V2+BLIT*V3)
      DUM=DUM+3.0*(A3+B3*T+C3*POT)*(V3+BLIT*V4)+4.0*A4*(V4+BLIT*V5)
      DUM=-XJ *(DUM+5.0*(A5+B5*T+C5*POT)*(V5+BLIT*V6))
      DUM1=XJ *T*(R*VIB+(B2-XKK*C2*POT)*V2+(B3-XKK*C3*POT)*V3
     1+(B5-XKK*C5*POT)*V5)
      FONV=DUM+DUM1
      EXAL=EXP(AL*V )
      DUM=BIGB4*T /(V -BLIT)**4
      DUM1=A6*EXAL                                                    FONDV
      DUM2=B6*T *EXAL
      TEMP=2.0*XJ*V *(-4.*DUM/(V -BLIT)+AL*(DUM1+DUM2))+XJ*(2.0*(DUM+ FONDV
     1DUM2)+DUM1)                                                     FONDV
      FONV =FONV +TEMP+0.5*XJ*V *V *(20.*DUM/(V -BLIT)**2+(AL**2)*    FONDV
     1(DUM1+DUM2))                                                    FONDV
      RETURN
      END
      FUNCTION FONC(VE,TE)
C     EQ. OF STATE FOR NEWTON-RAPHSON                                 FONC
      COMMON A2,A3,A4,A5,B2,B3,B4,B5,C2,C3,C4,C5,XKK,R,TREF,VREF,BLIT,XJ
      COMMON D4,Z4,ESS,TUFF,CLOD,GEE,AJA,KX,P2I(30),U2I(30),H2I(30)
      COMMON S2,HO
      COMMON PT2(30),RHO(30),TE2I(30),VE2I(30),CV2(30),CP2(30),GAM2(30)
      COMMON ACC2(30),XMACH2(30),RORAT(30),TRAT(30),PRAT(30),PTRAT(30)
      COMMON BIGB4,B6,A6,AL
      DIMENSION S2(30)
      EQUIVALENCE (C3,G3),(C5,XJ3),(C2,D3)
      PO (XL,AT)=1./EXP(XL*AT)
      EL=1./144.
      POT=PO(XKK,TE)
      FONC=R*TE/(VE-BLIT)+(A2+B2*TE+C2*POT)/(VE-BLIT)**2+(A3+B3*TE+   FONC
     1C3*POT)/(VE-BLIT)**3+(A4+BIGB4*TE)/(VE-BLIT)**4+(A5+B5*TE+C5*POT) FONC
     2/(VE-BLIT)**5+(A6+B6*TE)*EXP(AL*VE)
      RETURN
      END
      SUBROUTINE EQU3(TE,VE,ANS3)
C     ENTHALPY                                                        EQU3
```

```
      COMMON A2,A3,A4,A5,B2,B3,B4,B5,C2,C3,C4,C5,XKK,R,TREF,VREF,BLIT,XJ
      COMMON D4,Z4,ESS,TUFF,CLOD,GEE,AJA,KX,P2I(30),U2I(30),H2I(30)
      COMMON S2,H0
      COMMON PT2(30),RHO(30),TE2I(30),VE2I(30),CV2(30),CP2(30),GAM2(30)
      COMMON ACC2(30),XMACH2(30),RORAT(30),TRAT(30),PRAT(30),PTRAT(30)
      COMMON BIGB4,B6,A6,AL
      EQUIVALENCE (C3,G3),(C5,XJ3),(C2,D3)
      DIMENSION S2(30)
      PO (XL,AT)=1./EXP(XL*AT)
      ANS3=Z4*(TE-TREF)+B4*(TE**2-TREF**2)/2.+C4*(TE**3-TREF**3)/3.+D4*
     2(TE**4-TREF**4)/4.+(PO(XKK,TE)*(XKK*TE+1.)-PO(XKK,TREF)*(XKK*TREF
     3+1.))*(XJ*D3/(VE-BLIT)+XJ*G3/(2.*(VE-BLIT)**2)+XJ*XJ3/(4.*(VE-
     4BLIT)**4))+XJ*(VE*R*(TE-TREF)/(VE-BLIT)+VE*(B2*(TE-TREF)+C2*(PO
     5(XKK,TE)-PO(XKK,TREF)))/(VE-BLIT)**2)+XJ*(VE*(B3*(TE-TREF)+C3*(PO
     6(XKK,TE)-PO(XKK,TREF)))/(VE-BLIT)**3)+XJ*(VE*(B5*(TE-TREF)+C5*(PO
     7(XKK,TE)-PO(XKK,TREF)))/(VE-BLIT)**5)-(R*TREF*(ALOG((VE-BLIT)/(VR
     8EF-BLIT))+BLIT/(VREF-BLIT)-BLIT/(VE-BLIT)))*XJ-(2.*(A2+B2*TREF+C2
     9*PO(XKK,TREF))*(1./(VREF-BLIT)+BLIT/(2.*(VREF-BLIT)**2)-1./(VE-
     ABLIT)-BLIT/(2.*(VE-BLIT)**2)))*XJ-(3.*(A3+B3*TREF+C3*PO(XKK,TREF
     B))*(1./(2.*(VREF-BLIT)**2)+BLIT/(3.*(VREF-BLIT)**3)-1./(2.*(VE-
     CBLIT)**2)-BLIT/(3.*(VE-BLIT)**3)))*XJ-(4.*A4*(1./(3.*(VREF-BLIT)
     D**3)+BLIT/(4.*(VREF-BLIT)**4)-1./(3.*(VE-BLIT)**3)-BLIT/(4.*(VE-
     EBLIT)**4)))*XJ
      ANS3=ANS3-((5.*(A5+B5*TREF+C5*PO(XKK,TREF)))*(1./(4.*(VREF-BLIT)
     2**4)+BLIT/(5.*(VREF-BLIT)**5)-1./(4.*(VE-BLIT)**4)-BLIT/(5.*(VE-
     3BLIT)**5)))*XJ+TREF*R*ALOG((VE-BLIT)/(VREF-BLIT))*XJ-TREF*(B2-XKK
     4*C2*PO(XKK,TREF))*(1./(VE-BLIT)-1./(VREF-BLIT))*XJ-TREF*(B3-XKK*
     5C3*PO(XKK,TREF))/2.*(1./(VE-BLIT)**2-1./(VREF-BLIT)**2)*XJ-TREF*
     6(B5-XKK*C5*PO(XKK,TREF))/4.*(1./(VE-BLIT)**4-1./(VREF-BLIT)**4)
     7*XJ
      EXAL=EXP(AL*VE)                                                    EQU3
      EXAR=EXP(AL*VREF)                                                  EQU3
      TEMP=XJ*VREF*((BIGB4*(TE-TREF)/(VREF-BLIT)**4) +B6*EXAR*(TE-TREF))EQU3
      DUM=BIGB4*TE/(VE-BLIT)**4                                          EQU3
      DUM1=A6*EXAL+B6*TE*EXAL                                            EQU3
      TEMP=TEMP+XJ*VE*(0.5*VE*(-4.*DUM/(VE-BLIT)+AL*DUM1)+ DUM+DUM1)     EQU3
      DUM=BIGB4*TE/(VREF-BLIT)**4                                        EQU3
      DUM1=A6*EXAR+B6*TE*EXAR                                            EQU3
      TEMP=TEMP-XJ*VREF*(0.5*VREF*(-4.*DUM/(VREF-BLIT)+AL*DUM1)+         EQU3
     1DUM+DUM1)                                                          EQU3
      TEMP=TEMP+XJ*(BIGB4*TE*(1./(3.*(VREF-BLIT)**3)-1./(3.*(VE-BLIT)   EQU3
     1**3))+B6*TE*(EXAL-EXAR)/AL)                                        EQU3
      ANS3=ANS3+TEMP                                                     EQU3
      RETURN
      END
```

```
$DATA A2=-2.162959,A3=4.04057E-3,A4=1.921072E-4,A5=-4.481049E-6,
XKK=.976E-2,B2=2.135114E-3,B3=1.282818E-5,B4=3.00892783E-4,
B5=9.062318E-9,XJ=.185053,
C2=-18.941131,C3=0.539776,C4=-1.30237441E-7,C5=-4.836678E-5,
R=0.1219336,BLIT=0.15E-2,D4=1.96802894E-11,PEE=0.1026,
TEE=260,GEE=32.174,AJA=778.3,A=.008,B=12000,DELTX=2,
TREF=820,PREF=1,TZ=409.5,Z4=1.90458084E-2,
TEI=5*532,E1=.00001,E2=.00001,MAXI=30,NUMB=5,INT=0,
IEND=8,
PEE=1,
TEE=532,
NO(1)=1,2,3,4,5,6,7,8,9,
TEI(1)=8*532, VEI(1)=8*167.6025, PRAT(1)=8*.387,
U2I(1)=1500,2000,2500,3000,3500,4000,4500,5000,
VEE=167.6025,
IEND=5,
XMACH(1)=5.091384,5.939948,6.788512,7.637076,8.485639,
U2I(1)=3000,3500,4000,4500,5000,
VEI(1)=14.914,12.9277,11.5794,10.6234,9.91826,
TEI(1)=1338.31,1583.63,1856.79,2159.55,2492.32,
PRAT(1)=5*1,
VEE=167.6025,
VREF=99.836,
VC(1)=14.28,12.45,11.19,10.30,9.63,
TC(1)=1343.8,1589,1862.2,2165.2,2498.3,
A6=5.83882E7, BIGB4=-3.918263E-7, AL=-6.61199E2, B6=-9.26392E4,
PEE= 1500,TEE=1460,VEE=1.261555E-1,
IEND=10,
XMACH(1)=3.089560,
XMACH(2)=      3.479019,3.858785,4.260383,4.694284,5.174292,5.720277,
6.191075,6.736399,7.156523,
U2I(1)=10*0,
TEI(1)=1447.50,1448.53,1449.12,1449.86,1450.16,1450.52,1451.19,1451.11,
1451.28,1451.45,
VEI(1)=.8249,1.5895,3.1313,6.5190,14.3189,33.2188,81.6414,166.849,
354.500,600.403,
PRAT(1)=1.434844E-2,=.823559E-3,2.386169E-3,9.339631E-4,3.475275E-4,
1.221556E-4,4.019784E-5,1.659644E-5,6.500796E-6,3.360228E-6,
VC(1)=.70,1.4,2.9,6.0,10.0,28.5,77.0,160.0,340.0,575.0,
TC(1)=1457,9*1456,
$
$DATA
PEE= 1500,TEE=1260,VEE=1.082684E-1,
IEND=10,
```

```
XMACH(1)=3.029506,
XMACH(2)=      3.489537,4.030964,4.474187,4.795870,5.145822,5.532728,
5.968807,6.472110,7.137680,
U2I(1)=10*0,
TEI(1)=1244.78,1245.55,1246.21,1246.63,1246.90,1247.03,1247.25,1247.43,
1247.56,1247.71,
VEI(1)=.6301,1.3328,3.3944,7.3098,12.5770,22.2018,40.2732,75.2171,
145.113,312.293,
PRAT(1)=1.672006E-2,5.892466E-3,1.714149E-3,6.400267E-4,3.214062E-4,
1.567887E-4,7.400530E-5,3.361859E-5,1.458690E-5,5.446754E-6,
VC(1)=.55,1.20,3.0,6.9,9.5,18.5,36.0,70.0,138.0,300.0,
TC(1)=1254,2*1253,7*1252,
$
$DATA
PEE= 1500,TEE=1060,VEE=8.976947E-2,
IEND=10,
XMACH(1)=3.053911,
XMACH(2)=      3.490262,3.796251,4.120834,4.471057,4.856265,5.289648,
5.791031,6.392466,7.150918,
U2I(1)=10*0,
TEI(1)=1040.84,1040.68,1040.77,1040.86,1041.02,1041.27,1041.45,1041.56,
1041.76,1041.86,
VEI(1)=.5294,1.0502,1.7285,2.9351,5.1406,9.2934,17.3738,33.7041,68.2717,
145.883,
PRAT(1)=1.618625E-2,6.173591E-3,3.145939E-3,1.559022E-3,7.489170E-4,
3.47178E-4,1.543437E-4,6.520451E-5,2.580923E-5,9.349361E-6,
VC(1)=.48,.89,1.6,2.7,4.85,9.0,16.85,30.0,64.0,140.0,
TC(1)=1049,1048,2*1047,6*1046,
$
$DATA
PEE= 1500,TEE=860,VEE=7.014380E-2,
IEND=11,
XMACH(1)=3.002326,
XMACH(2)=      3.201444,3.844078,4.248112,4.706308,5.246122,5.696985,
6.072574,6.417008,6.813756,7.281658,
U2I(1)=11*0,
TEI(1)=833.158,832.331,830.975,830.705,830.630,830.710,830.793,830.844,
830.890,830.902,830.965,
VEI(1)=.3744,.5006,1.3143,2.3821,4.5076,8.9480,14.9496,22.0079,30.4224,
42.6999,61.0630,
PRAT(1)=1.857906E-2,1.215165E-2,3.146945E-3,1.40197E-3,5.931171E-4,
2.350020E-4,1.168208E-4,6.857934E-5,4.366940E-5,2.704147E-5,1.616425E-5,
VC(1)=.36,.49,1.2,2.1,4.1,7.8,12.0,19.0,27.0,38.0,57.0,
TC(1)=840,838,836,8*835,
$
```

Program D

NASA-LANGLEY RESEARCH CENTER

01 4	01 7 PROGRAM NO	COMPUTER PROGRAM ABSTRACT	01 14 DATE
LAR	D 3000		10/29/68

01 20 TITLE OF PROGRAM (61 CHARACTERS MAXIMUM)

Hypersonic Nozzle Contours for Tetrafluoromethane

PARENT PROGRAM

02 14 CATEGORY	02 15 SITE	02 16 PROGRAM NO
R	LAR	D0700

02 26 CATEGORY	02 27 LANGUAGE NO 1	02 12 LANGUAGE NO 2	02 37 KEY WORDS (8 MAXIMUM SEPARATED BY COMMAS)
R	FØR6M		Tetrafluoromethane, Nozzle Contour, Displacement Thickness

WHO TO CONTACT ABOUT THE PROGRAM

05 14 CONTACT	05 28 SITE	05 31 ORGN CODE	05 39 PROJECT NO	05 45 NASA CENTER
L. R. Boney	LAR	11.160	RGL-168	

05 48 STATUS: ☐ A UNDER DEVELOPMENT ☒ B OPERATIONAL ☐ C COMPLETED

05 49: ☐ A THIS PROGRAM IS NOT FOR SHARING

DATES		05 58 REVISION CODE	TIME AND COST FOR DEVELOPMENT			
05 50 INITIATED	05 54 COMPLETED	☐ A REVISION ☐ B CANCELLATION	05 59 MANMONTHS (59 60 61 62 63)	05 64 MACHINE HOURS (64 65 66 67 68)	05 69 COMPUTER TYPE	05 74 TOTAL COST (DOLLARS) (74 75 76 77 78 79 80)
10/66	10/68				6000	

ELITE MARGIN | PICA MARGIN

CARD NUMBER | COLUMN 14 | ABSTRACT

This program calculates the turbulent boundary-layer displacement thickness along a tetrafluoromethane inviscid nozzle contour. The flow properties at the edge of the inviscid region are supplied by Parts I and II of the program listed in NASA TN D-1622 which calculates the inviscid contour of a hypersonic nozzle for a real gas. The format of this program is identical with Part III of the parent program (NASA TN D-1622) which is restricted to a gas composed of diatomic or linear polyatomic molecules whose vibrational energy modes display harmonic oscillator characteristics having only one fundamental frequency. The shape parameter, the skin-friction coefficient, and the momentum thickness are calculated at each point along the inviscid contour. An iterative procedure determines the value of the displacement thickness which is added to the inviscid contour to give a better approximation of the physical wall. Finally a second-order interpolation is employed to locate points on the physical wall at desired increments.

```
$IBFTC 7001     LIST,REF,DECK,M94
C      P-700.1                                                                  0010
CLRB                                                                            0020
C      PART III COMPUTES BOUNDARY LAYER USING                                   0030
C           WALL POINTS PUNCHED BY PART II                                      0040
       EXTERNAL FOFX
       DIMENSIONTHBI(10),GI(10)
       COMMONTHBI,GI,NOTH
       DIMENSION FS(2),SUM(2),ANS(2),X(2000),Y(2000),W(2000),RRT(2000),         0050
      1THF(2000),TI(2000),SVY(2000),SVDELT(2000),DELS(2000),YY(2000)            0060
       COMMON  OPT     , TI      , RRI     , T0      , THB     , QSUM           0070
       COMMON  QW      , EN      , ERR     , UI      , HW      , R              0080
       COMMON  HT      , CON1    , CON2    , CON     , T       , H              0090
       COMMON  Q       , FR      , FPR     , H3      , HWS     , K              0100
       COMMON  RHOI    , QI      , X       , Y       , W       , RRT            0110
       COMMON  THF     , SVY     , SVDELT  , DELS    , YY      , RHOT           0120
       COMMON  VE      , R1      , C1      , D1      , E1      , THI            0130
       COMMON  GC      , OMEGA   , TW      , XM      , TLTG    , JLIM           0140
       COMMON  DEBUG   , N       , L       , ACASE   , ALPHA   , BETA           0150
       COMMON  GAM     , TAU     , PR      , TT1G    , X1      , Y1             0160
       COMMON  EM1     , W1      , RRT1    , THF1    , TI1     , TLTI           0170
       COMMON  TT11    , THETA   , DXB     , DU      , DR      , DY             0180
       COMMON  PI      , EMU     , RETH    , TEMP    , FT      , FTPR           0190
       COMMON  H1      , DSDEL   , THDEL   , TAW     , ALP     , CW             0200
       COMMON  C2      , C3      , C4      , FTT     , FTTPR   , H2             0210
       COMMON  CF2     , DSTH    , DTDX    , YPD     , DEL     , DP             0220
       COMMON  CP      , BP      , AP      , HI                                 0230
C      DIMENSION FS(2),SUM(2),ANS(2),X(2000),Y(2000),W(2000),RRT(2000),         0240
C     1THF(2000),TI(2000),SVY(2000),SVDELT(2000),DELS(2000),YY(2000)            0250
C      COMMON OPT                                                               0260
C      COMMONTI,RRI,T0,THB,QSUM,QW,EN,ERR,UI,HW,R,HT,CON1,CON2,                 0270
C     1CON,T,H,Q,FR,FPR,H3,HWS,K,RHOI,QI,X,Y,W,RRT,THF,SVY,SVDELT,DELS,YY       0280
C     2                    ,RHOT,VE,R1,C1,D1,E1,THI,GC,                        0290
C     3    OMEGA,TW,     XM,TLTG,JLIM,DEBUG,N,L,ACASE,ALPHA,                   0300
C     4BETA,GAM,TAU,PR,TT1G,X1,Y1,EM1,W1,RRT1,THF1,TI1,                        0310
C     5                              TLTI,TT11,THETA,DXB,DU,                   0320
C     6DR,DY,         PI,EMU,RETH,TEMP,FT,FTPR,H1,  DSDEL,                     0330
C     7THDEL,TAW,ALP,CW,C2,C3,C4,FTT,FTTPR,H2,CF2,DSTH,                        0340
C     8DTDX,YPD,DEL                                                            0350
C     9         ,DP,CP,BP,AP,     HI                                           0360
    1 WRITE (6,25)                                                              0370
   25 FORMAT(1H 6X5HACASE13X4HRHOT14X2HVE15X2HR115X2HC115X2HD1                   0380
     115X2HE1/7X3HTHI15X2HGC15X1HR15X3HTHB                                      0390
     213X5HOMEGA14X2HTW14X3HERR/8X2HXM14X4HTLTG                                 0400
     312X5HALPHA13X4HBETA13X3HGAM14X3HTAU15X2HPR/                               0410
     47X4HTT1G14X2HT015X2HAP15X2HBP15X2HCP15X2HDP15X2HHT)                       0420
  103 FORMAT(1H 7E17.8)                                                         0430
  100 FORMAT(1H06E17.8/6E17.8)                                                  0440
```

```
      CALLFINP(4,THBI,GI,NOTH,NOTHM)
      CALLFINP(39,RHOT,VE,R1,C1,D1,E1,TH1,GC,R,THB,OMEGA,                    0450
     1TW,ERR,XM,TLTG,JLIM,DEBUG,N,L,ACASE,ALPHA,BETA,GAM,                    0460
     2TAU,PR,TT1G,T0,AP,BP,CP,DP,HT,APP,BPP,CPP,YSTAR,                       0470
     3OPT,DIFN,DIFD)                                                         0480
      THB=THBI(NOTHM)
      WRITE (6,103)ACASE,RHOT,VE,R1,C1,D1,E1,THI,GC,R,THB,OMEGA,TW,ERR,X     0490
     1M,TLTG,ALPHA,BETA,GAM,TAU,PR,TT1G                          ,T0,AP,B    0500
     2P,CP,DP,HT                                                             0510
   26 FORMAT(1H 8X1HX16X1HY14X5HTHETA13X4HCF/2                               0520
     114X1HN14X6HTH/DEL/5X7HY+DELST11X5HDELST13X3HDEL                        0530
     214X4HRETH13X4HTLTI10X9HDELST/DEL)                                      0540
      J=JLIM                                                                 0550
C     SUBROUTINE BIRD READS BINARY CARDS CONTAINING X,Y,M,W,RHO/RHOT,         0560
C        THETA,T                                                             0570
C          LIMIT OF 2000 CARDS                                               0580
C     READ IN WALL POINTS EXIT TO THROAT                                     0590
C     MULTIPLY X AND Y BY XM AND STORE THROAT TOEXIT                         0600
 1000 CALLBIRD(X1,TI1)                                                       0610
      X(J)=X1*XM                                                             0620
      Y(J)=Y1*XM                                                             0630
      W(J)=W1                                                                0640
      RRT(J)=RRT1                                                            0650
      THF(J)=THF1                                                            0660
      TI(J)=TI1                                                              0670
      SVY(J)=Y(J)                                                            0680
   50 SVDELT(J)=0                                                            0690
      J=J-1                                                                  0700
      IF(J)81,81,1000                                                        0710
   81 TLTI=TLTG                                                              0720
      TT11=TT1G                                                              0730
      THETA=THI                                                              0740
      WRITE (6,26)                                                           0750
      CALL SLITE (1)                                                         0760
    2 DO80J=1,JLIM                                                           0770
      K=J                                                                    0780
      RHOI=RRT(J)*RHOT                                                       0790
      UI=W(J)*VE                                                             0800
      PI=R1*TI(J)*RHOI                                                       0810
      EMU=(C1*(TI(J)**1.5))/((TI(J)**D1)+E1)                                 0820
C     EQUATION B10                                                           0830
      IF(PI-20000.0)203,203,204                                              0840
  203 QI=1.0                                                                 0850
      GOTO4                                                                  0860
  204 QI=PI*(PI*(PI*(TAU)+GAM)+BETA)+ALPHA                                   0870
    4 IF(THB/TT11-24.0)120,120,101                                           0880
  101 FT=VE*VE-QI*(8.*TT11*R)
      FTPR=-QI*8.*R
      GOTO102                                                                0910
  120 SEM=0
      REM=0
```

```
      DO1201I=1,NOTH
      TEM=EXP(THBI(I)/TT11)
      SEM=GI(I)*THBI(I)/(TEM-1.)+SEM
 1201 REM=GI(I)*THBI(I)*THBI(I)*TEM/(TEM-1.)**2+REM
      FT=VE*VE-QI*(8.*TT11*R+2.*R*SEM)
      FTPR=-QI*(8.*R+2.*R*REM/(TT11*TT11))
  102 H1=-FT/FTPR                                                    0960
      TT11=TT11+H1                                                   0970
      IF(ABS(H1/TT11)-ERR)5,5,4                                      0980
C     EQUATION B16                                                   0990
    5 IF(CPP)400,401,400                                             1000
  401 TW=TT11                                                        1010
      GOTO402                                                        1020
  400 TW=(CPP-APP*(SVY(J)/YSTAR)**1.8)/(1.0+BPP*(SVY(J)/YSTAR)**1.8) 1030
C     EQUATION B11                                                   1040
  402 IF(PI-20000.0)205,205,206                                      1050
  205 QW=1.0                                                         1060
      GOTO207                                                        1070
  206 QW=PI*(PI*(PI*(DP)+CP)+BP)+AP                                  1080
  207 IF(THB/TW-24.0)104,104,105                                     1090
  105 HWS=4.*TW/TO
      GOTO106                                                        1110
  104 SEM=0
      DO1041I=1,NOTH
      TEM=EXP(THBI(I)/TW)
 1041 SEM=GI(I)*THBI(I)/(TEM-1.)+SEM
      HWS=4.*TW/TO+SEM/TO
  106 IF(THB/TI(J)-24.0)107,107,108                                  1130
  108 HI=4.*TI(J)/TO
      GOTO109                                                        1150
  107 SEM=0
      DO1071I=1,NOTH
      TEM=EXP(THBI(I)/TI(J))
 1071 SEM=GI(I)*THBI(I)/(TEM-1.)+SEM
      HI=4.*TI(J)/TO+SEM/TO
  109 QSUM=(QI-QW)/(HI-HWS)                                          1170
      IF(THB/TW-24.0)110,110,111                                     1180
  111 HW=HWS*QW
      GOTO112                                                        1200
  110 HW=HWS*QW
  112 RET=(RHOI*UI)/(EMU*12.0)                                       1220
  503 RETH=RET*THETA                                                 1230
C     EQUATION B5                                                    1240
      EN=1.77*.43429448*ALOG(RETH)-.38-200.0/RETH                    1250
      CALL SLITET(1,K000FX)                                          1260
       GO TO(511,502),K000FX                                         1270
  502 IF(ABS(EN-ENP)-DIFN)500,500,501                                1280
  511 CALL SLITE (1)                                                 1290
  501 RRI=.125                                                       1300
C     SUBROUTINE GAUSS INTEGRATION 5 INTERVALS AND 32 POINTS PERINTERVAL 1310
      A=0.
```

```
      B=1.                                                              1320
      NOFN=2                                                            1330
      CALL GAUSS(N,L,A,B,NOFN, S,FS(1),SUM(1),ANS(1),FOFX)              1340
C     DELTA STAR/DELTA                                                  1350
      DSDEL=1.0-ANS(1)                                                  1360
C     THETA/DELTA                                                       1370
      THDEL=1.0-DSDEL-ANS(2)                                            1380
      TAW=(PR**.33333333)*(TT11-TI(J))+TI(J)                            1390
      ALP=(1.0+OMEGA)/(EN+1.0)                                          1400
      CW=TW/TI(J)                                                       1410
      C2=(TW-TAW)/TI(J)                                                 1420
      C3=(20.0*EN*THDEL/RETH)**(1.0/(EN+1.0))                           1430
      C4=(TAW-TI(J))/TI(J)                                              1440
    7 FTT=CW-C2*C3*(TLTI**ALP)-C4*C3*C3*(TLTI**(2.0*ALP))-TLTI          1450
      FTTPR=-ALP*C2*C3*(TLTI**(ALP-1.0))-2.0*ALP*C4*C3*C3*              1460
     1  (TLTI**(2.0*ALP-1.0))-1.0                                       1470
      H2=-FTT/FTTPR                                                     1480
C     EQUATION B14                                                      1490
C     TL/TI                                                             1500
      TLTI=TLTI+H2                                                      1510
      IF(ABS(H2/TLTI)-ERR)6,6,7                                         1520
C     EQUATION B13                                                      1530
C     CF/2                                                              1540
    6 CF2=(1.0/(20.0*EN))*C3*C3*((TLTI)**((1.0+2.0*OMEGA-EN)            1550
     1    /(EN+1.0)))                                                  1560
C     DELTA STAR/THETA                                                  1570
      DSTH=DSDEL/THDEL                                                  1580
  500 DELS(J)=DSTH*THETA                                                1590
      YPD=SVY(J)+DELS(J)                                                1600
      DEL=DELS(J)/DSDEL                                                 1610
      WRITE (6,100)X(J),Y(J),THETA,CF2,EN,THDEL,YPD,DELS(J),DEL,RETH,TLT1620
     1I,DSDEL                                                           1630
      YY(J)=Y(J)                                                        1640
      Y(J)=YPD                                                          1650
      IF(J-1)504,505,504                                                1660
  505 DELSP=DELS(J)                                                     1670
      GOTO509                                                           1680
  504 DXB=(X(J)-X(J-1))/COS(THF(J-1))                                   1690
      DU=VE*(W(J)-W(J-1))                                               1700
      DR=RHOT*(RRT(J)-RRT(J-1))                                         1710
      DY=Y(J)-Y(J-1)                                                    1720
C     D THETA/D X                                                       1730
      DTDX=CF2P-THETAP*(((2.0+DSTHP)*DU)/(UIP*DXB)+DR/(RHOIP*DXB)       1740
     1 +DY/(Y(J-1)*DXB))                                                1750
      THETA=THETAP+(DTDX)*DXB                                           1760
      CALL SLITET(1,K000FX)                                             1770
       GO TO(508,506),K000FX                                            1780
  506 IF(ABS((DELS(J)-DELSP)/SVY(J))-DIFD)509,509,508                   1790
  508 DELSP=DELS(J)                                                     1800
      ENP=EN                                                            1810
      GOTO503                                                           1820
```

```
  509 Y(J+1)=Y(J+1)+DELS(J)                                                1810
      CF2P=CF2                                                             1820
      THETAP=THETA                                                         1830
      DSTHP=DSTH                                                           1840
      UIP=UI                                                               1850
      RHOIP=RHOI                                                           1860
  510 CALL SLITE (1)                                                       1870
   80 CONTINUE                                                             1880
 1001 XINT=0                                                               1890
      WRITE (6,514)                                                        1900
C     USE SECOND ORDER INTERPOLATION TO FIND GIVEN POINTS                  1910
C     DX=.10 IF Y LESS THAN 1.                                             1920
C     DX=.25 IF Y GREATER THAN 1. AND LESS THAN5.                          1930
C     DX=.50 IF Y GREATER THAN 5.                                          1940
 1005 CALL FTLUP(XINT,YINT,2,JLIM,X(1),YY(1))                              1950
      WRITE (6,513)XINT,YINT                                               1960
      IF(YINT-YY(JLIM))1006,1,1
 1006 IF(YINT-1.0)1002,1009,1009                                           1980
 1002 XINT=XINT+.1                                                         1990
      GO TO 1005                                                           2000
 1009 IF(YINT-5.0)1003,1004,1004                                           2010
 1003 XINT=XINT+.25                                                        2020
      GO TO 1005                                                           2030
 1004 XINT=XINT+.5                                                         2040
      GO TO 1005                                                           2050
  513 FORMAT(1H 2F12.4)                                                    2060
  514 FORMAT(1H 6X1HX11X1HY)                                               2070
      END                                                                  2080
$IBFTC FOFX     LIST,REF,DECK,M94
      SUBROUTINEFOFX(S,FS)                                                 0010
      DIMENSIONTHBI(10),GI(10)
      COMMONTHBI,GI,NOTH
      DIMENSION FS(2),SUM(2),ANS(2),X(2000),Y(2000),W(2000),RRT(2000),     0020
     1THF(2000),TI(2000),SVY(2000),SVDELT(2000),DELS(2000),YY(2000)        0030
      COMMON  OPT    , TI     , RRI    , TO     , THB    , QSUM           0040
      COMMON  QW     , EN     , ERR    , UI     , HW     , R              0050
      COMMON  HT     , CON1   , CON2   , CON    , T      , H              0060
      COMMON  Q      , FR     , FPR    , H3     , HWS    , K              0070
      COMMON  RHOI   , QI     , X      , Y      , W      , RRT            0080
      COMMON  THF    , SVY    , SVDELT , DELS   , YY     , RHOT           0120
      COMMON  VE     , R1     , C1     , D1     , E1     , THI            0130
      COMMON  GC     , OMEGA  , TW     , XM     , TLTG   , JLIM           0140
      COMMON  DEBUG  , N      , L      , ACASE  , ALPHA  , BETA           0150
      COMMON  GAM    , TAU    , PR     , TT1G   , X1     , Y1             0160
      COMMON  EM1    , W1     , RRT1   , THF1   , TI1    , TLTI           0170
      COMMON  TT11   , THETA  , DXB    , DU     , DR     , DY             0180
      COMMON  PI     , EMU    , RETH   , TEMP   , FT     , FTPR           0190
      COMMON  H1     , DSDEL  , THDEL  , TAW    , ALP    , CW             0200
      COMMON  C2     , C3     , C4     , FTT    , FTTPR  , H2             0210
      COMMON  CF2    , DSTH   , DTDX   , YPD    , DEL    , DP             0220
      COMMCN  CP     , BP     , AP     , HI                               0230
```

```
C      DIMENSION FS(2),SUM(2),ANS(2),X(2000),Y(2000),W(2000),RRT(2000),      0100
C     1THF(2000),TI(2000),SVY(2000),SVDELT(2000),DELS(2000),YY(2000)         0110
C      COMMON OPT                                                            0120
C      COMMONTI,RRI,T0,THB,QSUM,QW,EN,ERR,UI,HW,R,HT,CON1,CON2,              0130
C     1CON,T,H,Q,FR,FPR,H3,HWS,K,RHOI,QI,X,Y,W,RRT,THF,SVY,SVDELT,DELS,YY    0140
       CON1=((UI*UI)/(R*T0))                                                0150
       CON2=S**(1.0/EN)                                                     0160
       CON=CON1*(HW*(1.0-CON2)/CON1+HT*CON2/CON1-.5*CON2*CON2)              0170
C      ITERATE FOR RHO/RHOI                                                 0180
    11 T=TI(K)/RRI                                                          0190
C      IF EXPONENTIAL GREATER THAN 24. OMIT TERM                            0200
C      EQUATION 89                                                          0210
       IF(THB/T-24.0)113,113,114                                            0220
   114 H=4.*T/T0                                                            0240
       GO TO 1152
   113 SEM=0
       DO1131I=1,NOTH
       TEM=EXP(THBI(I)/T)
  1131 SEM=GI(I)*THBI(I)/(TEM-1.)+SEM
       H=4.*T/T0+SEM/T0
  1152 IF(OPT)115,1150,115                                                  0260
  1150 Q=QI                                                                 0270
       GO TO 1151                                                           0280
   115 Q=(QSUM)*(H-HWS)+QW                                                  0290
C      IF EXPONENTIAL GREATER THAN 24. OMIT TERM                            0300
  1151 IF(THB*RRI/TI(K)-24.0)116,116,117                                    0310
   117 FR=Q*4.*TI(K)/(T0*RRI)-CON
       FPR=-4.*Q*TI(K)/(T0*RRI*RRI)
       GO TO 118                                                            0340
   116 SEM=0
       REM=0
       DO1161I=1,NOTH
       TEM=EXP(THBI(I)*RRI/TI(K))
       SEM=GI(I)*THBI(I)/(TEM-1.)+SEM
  1161 REM=GI(I)*THBI(I)*THBI(I)*TEM/
      1(TEM-1.)**2+REM
       FR=Q*(4.*TI(K)/(T0*RRI)+SEM/T0)-CON
       FPR=Q*(-4.*TI(K)/(T0*RRI*RRI)-REM/
      1(T0*TI(K)))
   118 H3=-FR/FPR                                                           0390
C      EQUATION B12                                                         0400
       RRIN=RRI+H3                                                          0410
       IF(RRIN)125,125,126                                                  0420
   125 RRI=RRI*.5                                                           0430
       GO TO 11                                                             0440
   126 RRI=RRIN                                                             0450
       IF(ABS(H3/RRI)-ERR)10,10,11                                          0460
    10 FS(1)=RRI*(S**(1.0/EN))                                              0470
    40 FS(2)=RRI*(S**(2.0/EN))                                              0480
       HOLD=S                                                               0490
       HOLD2=FS(1)                                                          0500
```

Program D – Concluded

```
    74 HOLD3=FS(2)                                                          0510
   100 FORMAT(1H 7E17.8)                                                    0520
       RETURN                                                               0530
       END                                                                  0540
$DATA
J1=0,N1=2341,N1127,N3322,N1653,F
J2=0,N1=1,N2,N3,N4,F
J3=4835,J4=2835$
N1=12.451,N2=4193.95,N3=17.55,N4=7.4866E-7,N5=1.0,N6=251.17,N7=.0001,
N8=1.,N9=565.,N11=.6,N12=660.,N13=.00005,N14=.20527,N15=1.,N21=1.,N22=0,
N23=0,N24=0,N25=.76,N26=1460.,N27=455.,N28=1.,N29=0,N30=0,N31=0,
N32=34.2,N33=0,N34=0,N35=1374.,N36=1.,N37=0,N38=.01,N39=.001,
N10=0,N16=388835,N17=0,N18=32835,N19=5835,N20=5.$
```

REFERENCES

1. Hayes, Wallace D.; and Probstein, Ronald F.: Hypersonic Flow Theory. Academic Press, Inc., 1959.

2. Anon.: Comparative Studies of Conceptual Design and Qualification Procedures for a Mars Probe/Lander. Volume V: Subsystem and Technical Analyses – Book 2: Aeromechanics and Thermal Control. AVSSD-0006-66-RR (Contract NAS 1-5224), AVCO Corp., May 11, 1966.

3. Lomax, Harvard; and Inouye, Mamoru: Numerical Analysis of Flow Properties About Blunt Bodies Moving at Supersonic Speeds in an Equilibrium Gas. NASA TR R-204, 1964.

4. Nagamatsu, H. T.; Geiger, R. E.; and Sheer, R. E., Jr.: Real Gas Effects In Flow Over Blunt Bodies at Hypersonic Speeds. J. Aero/Space Sci., vol. 27, no. 4, Apr. 1960, pp. 241-251.

5. Chapman, Dean R.: Some Possibilities of Using Gas Mixtures Other Than Air in Aerodynamic Research. NACA Rep. 1259, 1956. (Supersedes NACA TN 3226.)

6. George, Albert R.: Exploratory Studies of a Low γ, High Mach Number Wind Tunnel Using "Freon 14" as the Working Fluid. AFOSR 1876, U.S. Air Force, Dec. 1961.

7. Mak, Wing; and Zakkay, Victor: A Facility for Hypersonic Flow Simulation Over Blunt-Nosed Bodies. ARL 67-0143, U.S. Air Force, July 1967. (Available from DDC as AD 660574.)

8. Jones, Robert A.; Bushnell, Dennis M.; and Hunt, James L.: Experimental Flow Field and Heat-Transfer Investigation of Several Tension Shell Configurations at a Mach Number of 8. NASA TN D-3800, 1967.

9. Krumins, Maigonis V.: Drag and Stability of Mars Probe/Lander Shapes. J. Spacecraft Rockets, vol. 4, no. 8, Aug. 1967, pp. 1052-1057.

10. South, Jerry C., Jr.: Calculation of Axisymmetric Supersonic Flow Past Blunt Bodies With Sonic Corners, Including a Program Description and Listing. NASA TN D-4563, 1968.

11. Levin, George M.; Evans, Dallas E.; and Stevens, Victor, eds.: NASA Engineering Models of the Mars Atmosphere for Entry Vehicle Design. NASA TN D-2525, 1964.

12. Zeleznik, Frank J.; and Gordon, Sanford: A General IBM 704 or 7090 Computer Program for Computation of Chemical Equilibrium Compositions, Rocket Performance, and Chapman-Jouguet Detonations. NASA TN D-1454, 1962.

13. Ridyard, Herbert W.; and Storer, Elsie M.: Stagnation-Point Shock Detachment of Blunt Bodies in Supersonic Flow. J. Aerospace Sci. (Readers' Forum), vol. 29, no. 6, June 1962, pp. 751-752.

14. Van Dyke, Milton D.; and Gordon, Helen D.: Supersonic Flow Past a Family of Blunt Axisymmetric Bodies. NASA TR R-1, 1959.

15. Fink, M. R.; Clark, J. W.; and Miller, D. P.: Approximate Method for Calculating Flow Fields Around Blunt-Nosed Slender Bodies at Hypersonic Speeds. Transactions of the Sixth Symposium on Ballistic Missile and Aerospace Technology, Vol. IV, DCAS-TDR-62-40, U.S. Air Force, Aug. 1961, pp. 423-456. (Available from DDC as AD-329289.)

16. McBride, Bonnie J.; Heimel, Sheldon; Ehlers, Janet G.; and Gordon, Sanford: Thermodynamic Properties to 6000° K for 210 Substances Involving the First 18 Elements. NASA SP-3001, 1963.

17. Edmonds, P. D.; and Lamb, J.: Vibrational Relaxation Times of a Number of Polyatomic Gases Derived From Measurements of Acoustic Absorption. Proc. Phys. Soc. (London), vol. 72, pt. 6, no. 468, Dec. 1, 1958, pp. 940-948.

18. Herzfeld, Karl F.; and Litovitz, Theodore A.: Absorption and Dispersion of Ultrasonic Waves. Academic Press, 1959.

19. Morris, James F.: Physico-Chemical Reactions During Nozzle Flow. The Chemistry of Propellants, S. S. Penner and J. Ducarme, eds., Pergamon Press, 1960, pp. 410-490.

20. Landau, L.; and Teller, E.: Theory of Sound Dispersion. Phys. Zeitschr. der Sowjetunion, vol. 10, no. 1, 1936, pp. 34-43.

21. Chari, Nallan Chakravartula Satyanarayana: Thermodynamic Properties of Carbon Tetrafluoride. Ph. D. Thesis, Univ. of Mich., 1960.

22. Johnson, Charles B.; Boney, Lillian R.; Ellison, James C.; and Erickson, Wayne D.: Real-Gas Effects on Hypersonic Nozzle Contours With a Method of Calculation. NASA TN D-1622, 1963.

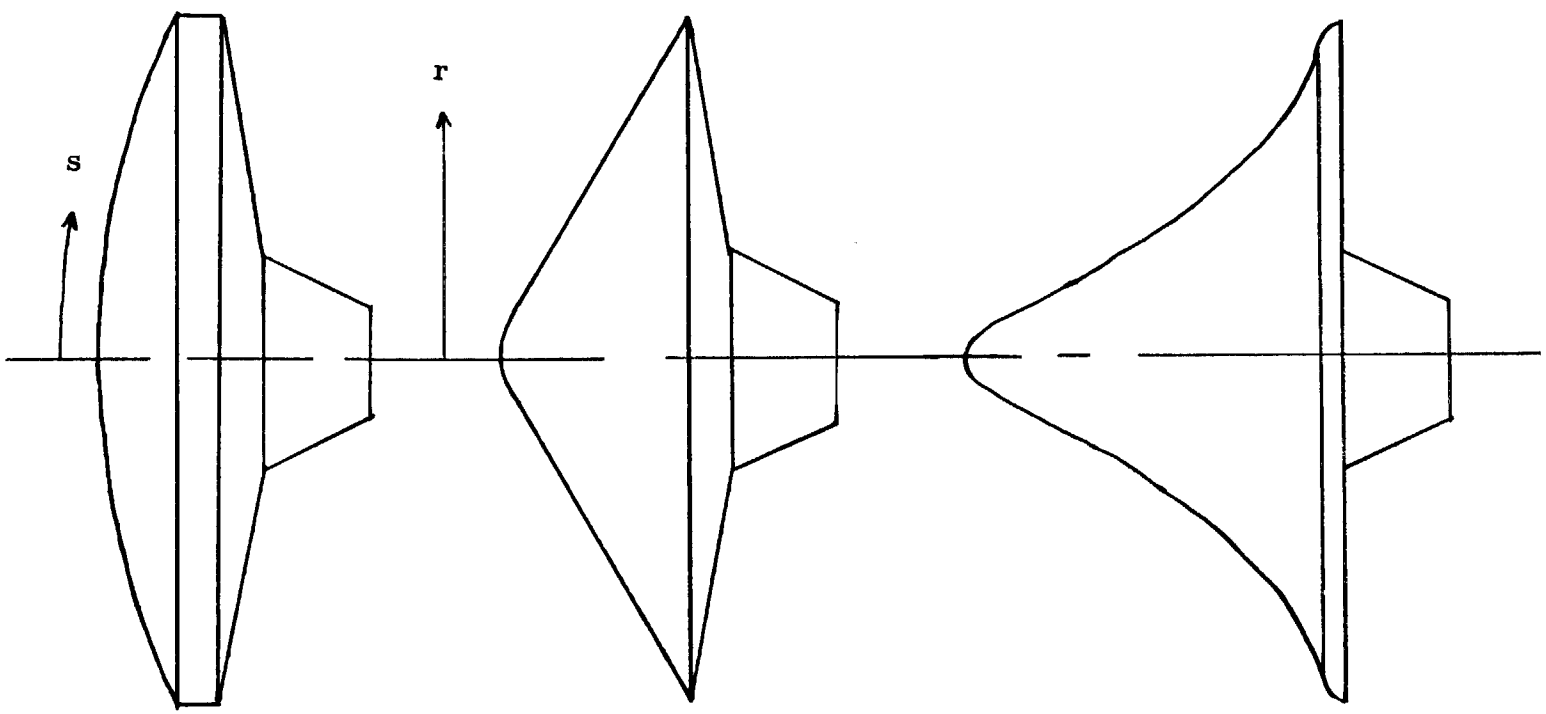

Figure 1.- Three candidate high-drag configurations.

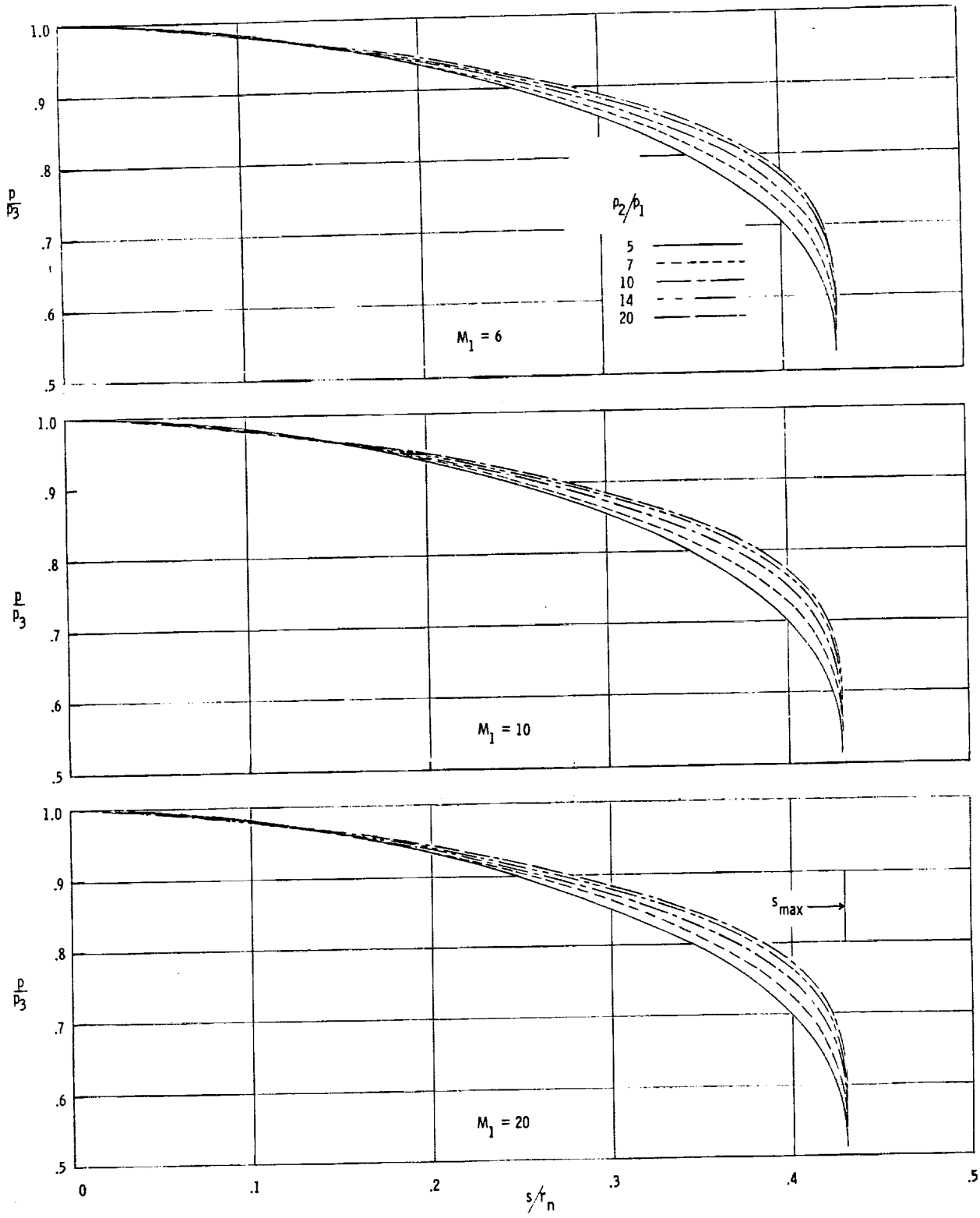

Figure 2.- Ideal-gas pressure distribution about spherical segment.

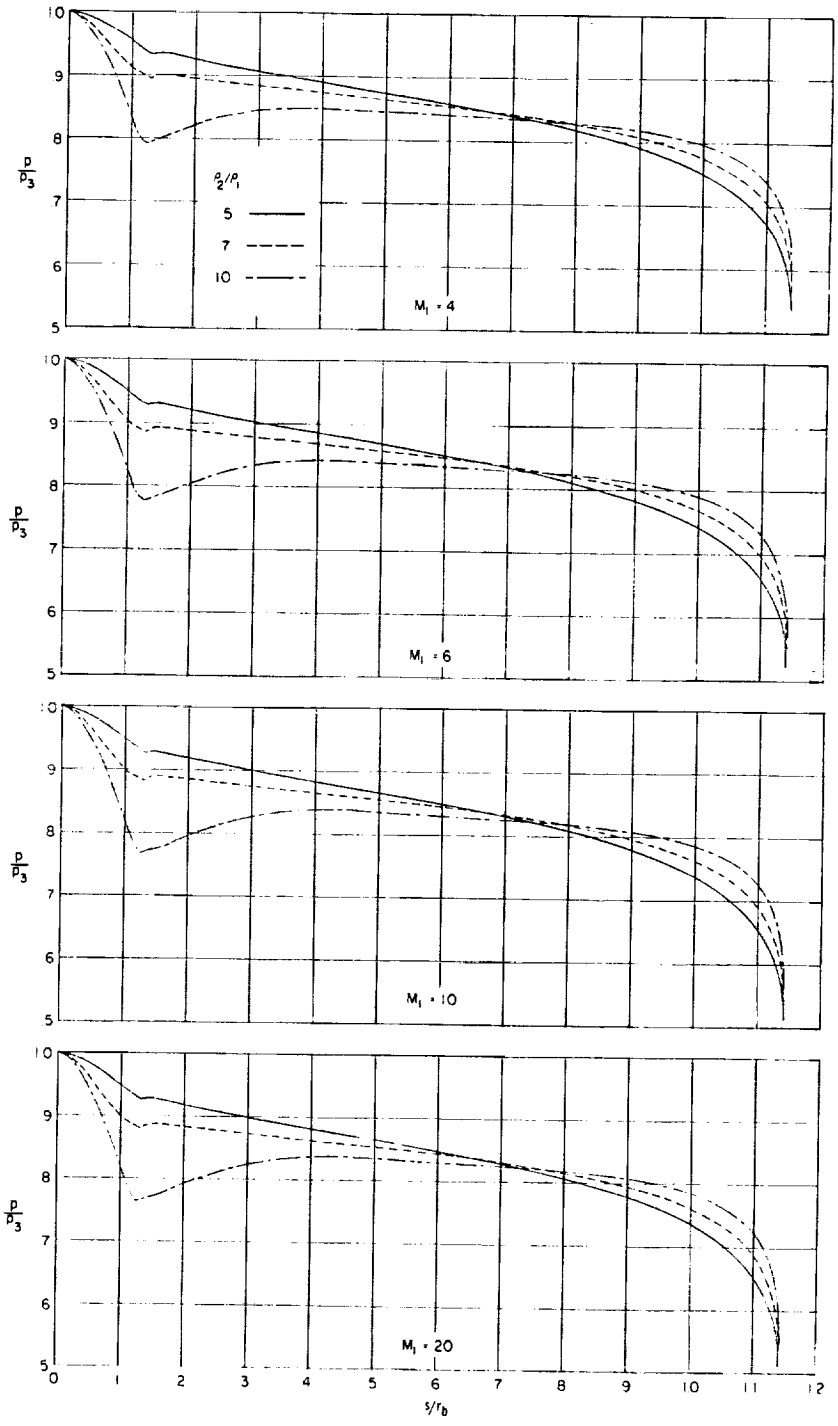

(a) 120^0 cone.

Figure 3.- Ideal-gas pressure distribution about 120^0 and 140^0 cones.

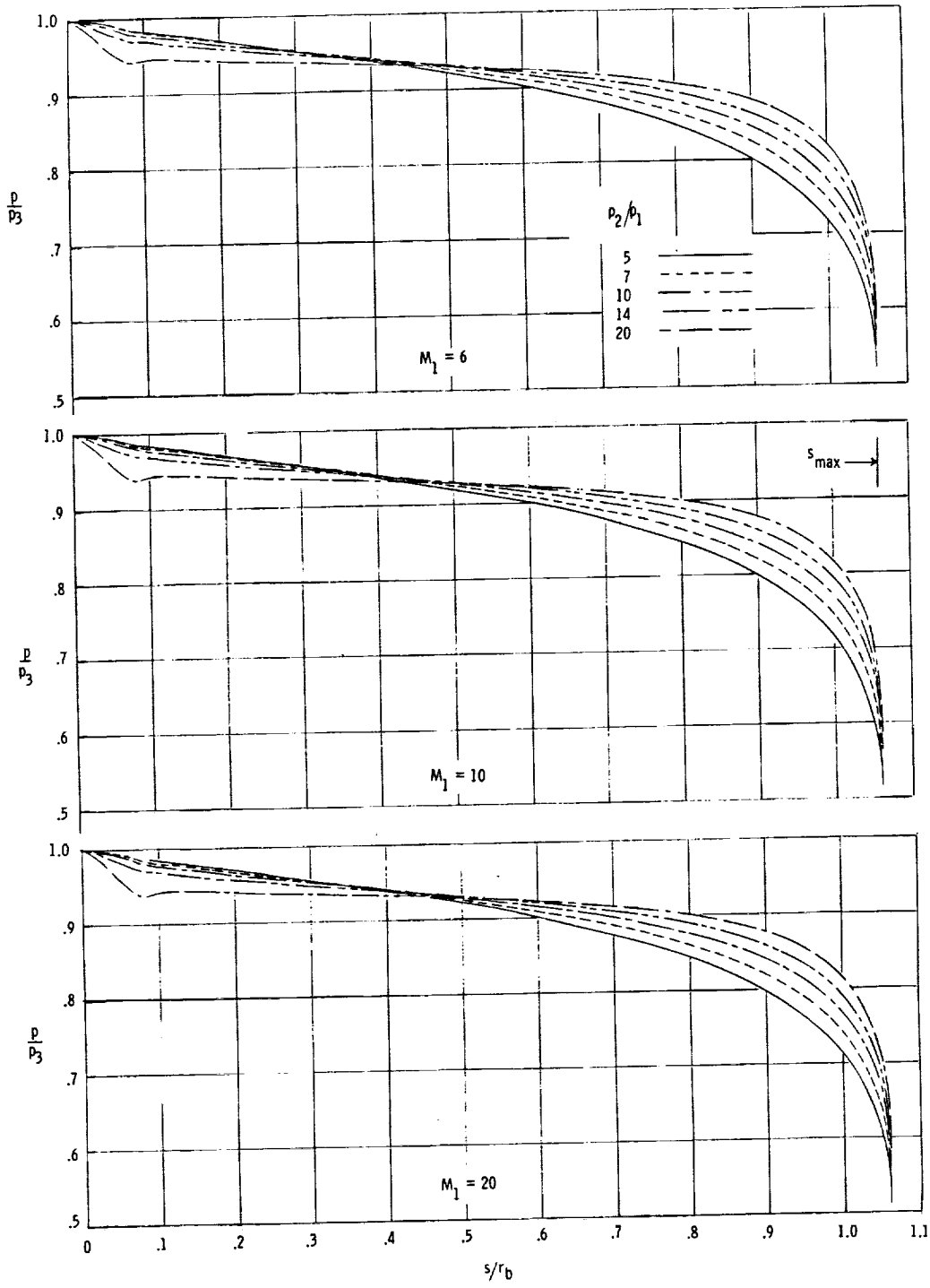

(b) 140° cone.

Figure 3.- Concluded.

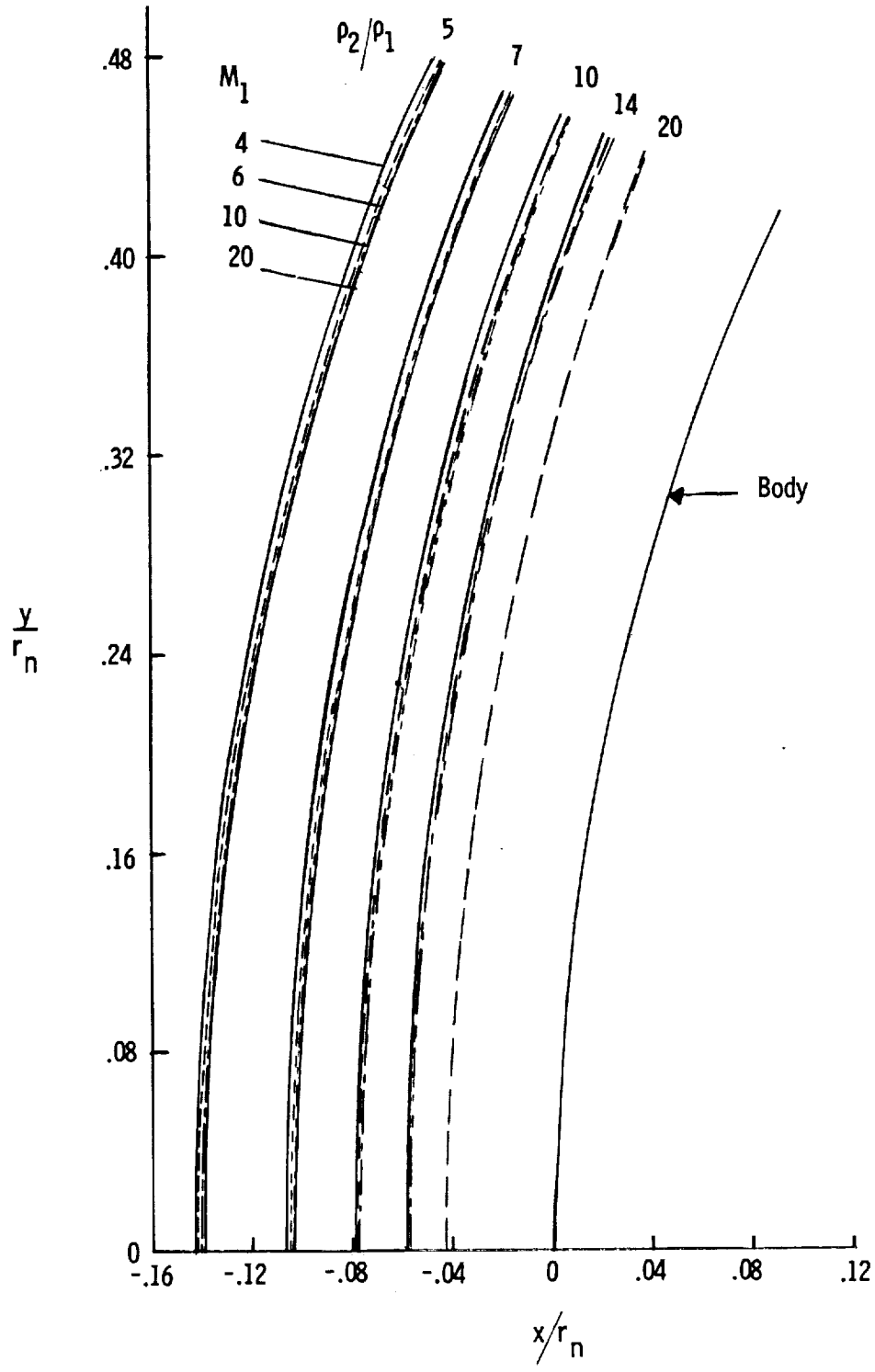

Figure 4.- Shock shape of spherical segment.

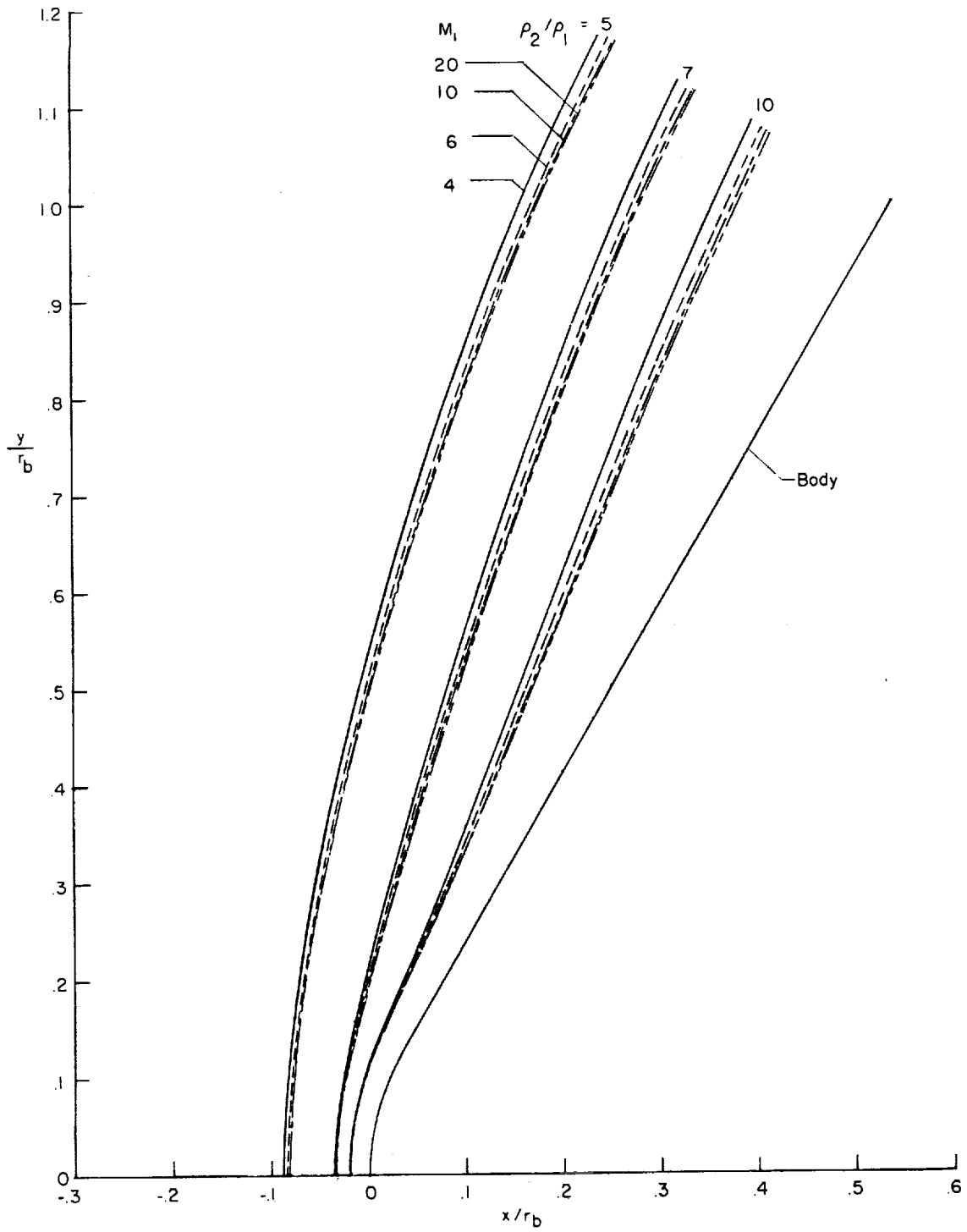

(a) 120^0 cone.

Figure 5.- Shock shape of 120^0 and 140^0 cones.

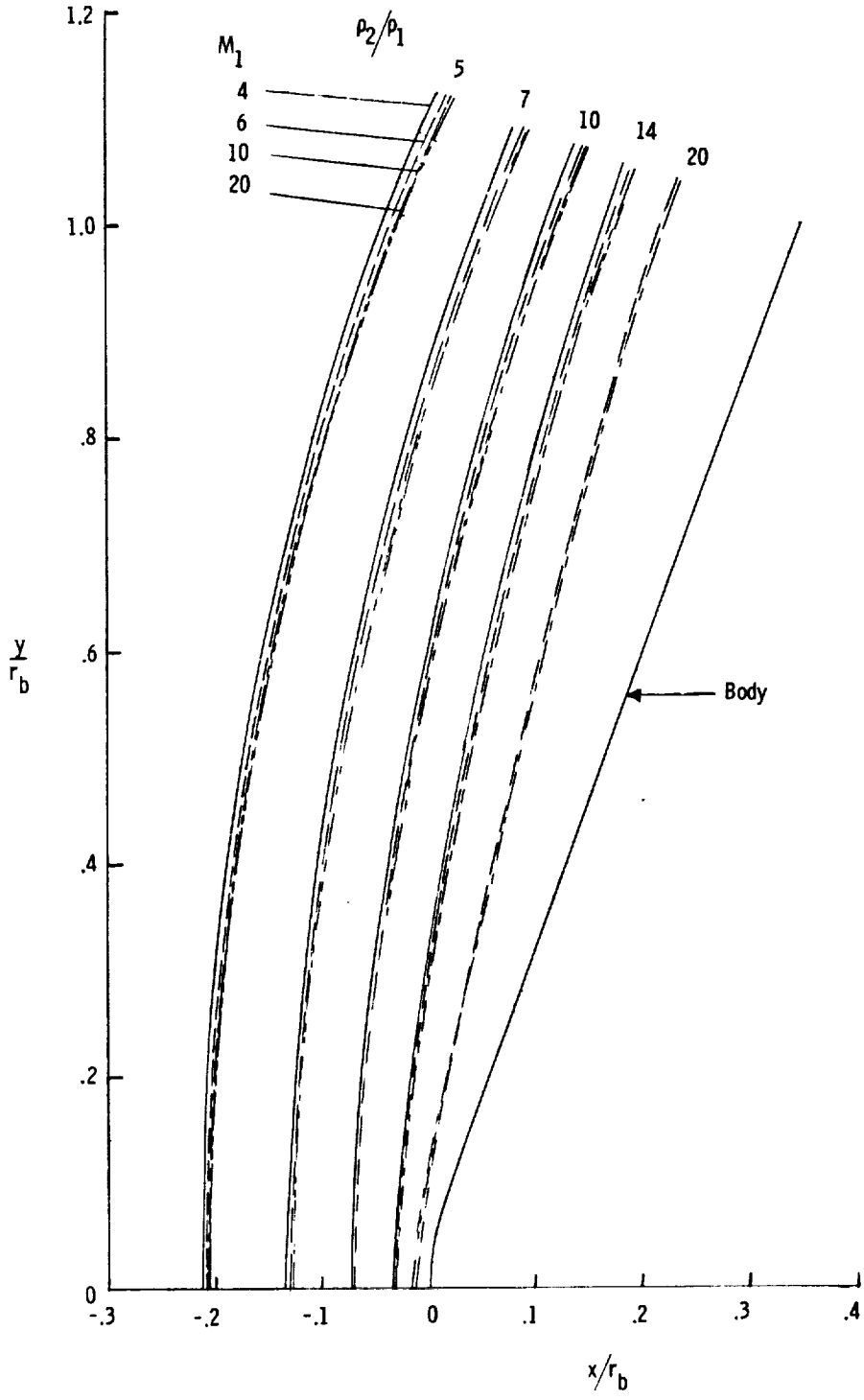

(b) 140^0 cone.

Figure 5.- Concluded.

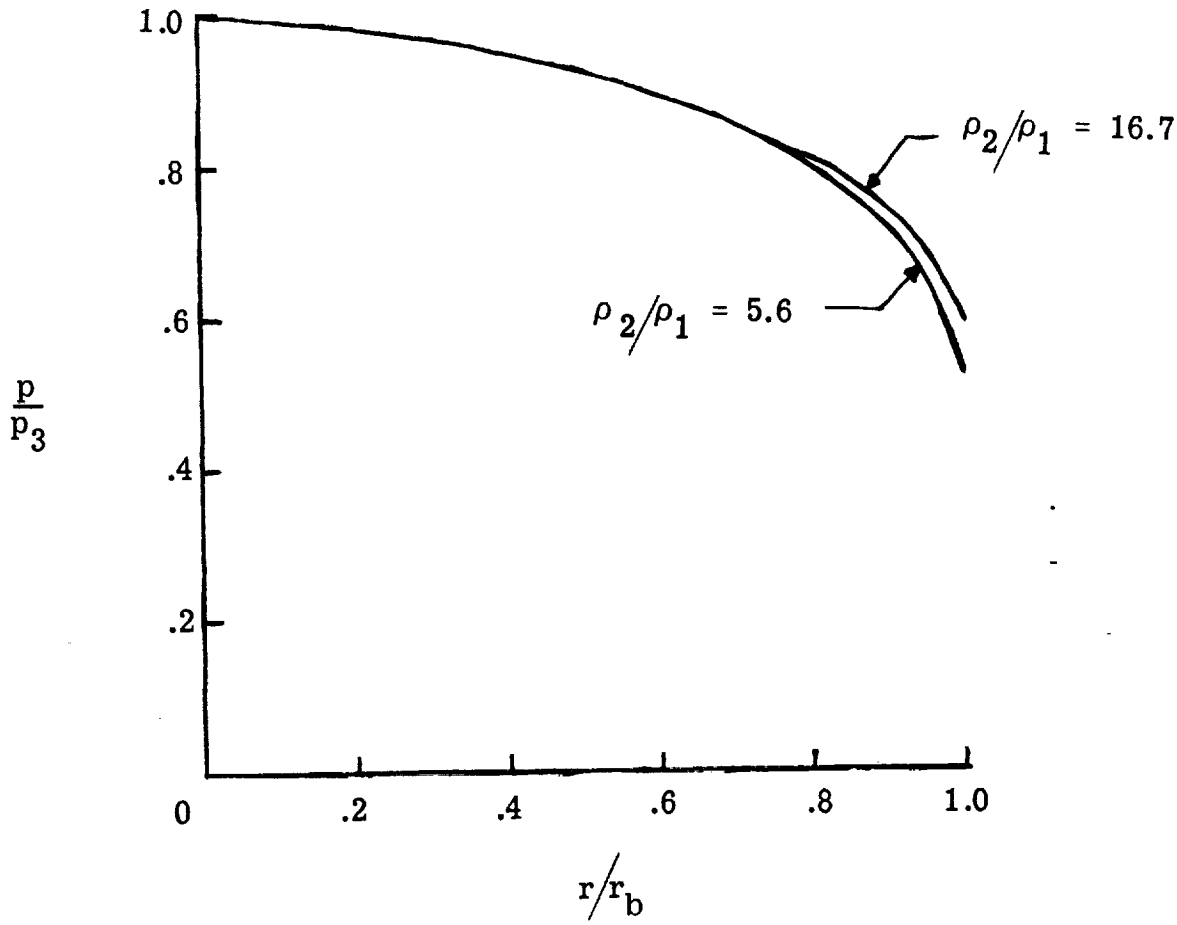

Figure 6.- Calculated pressure distribution for spherical segment (from ref. 2).

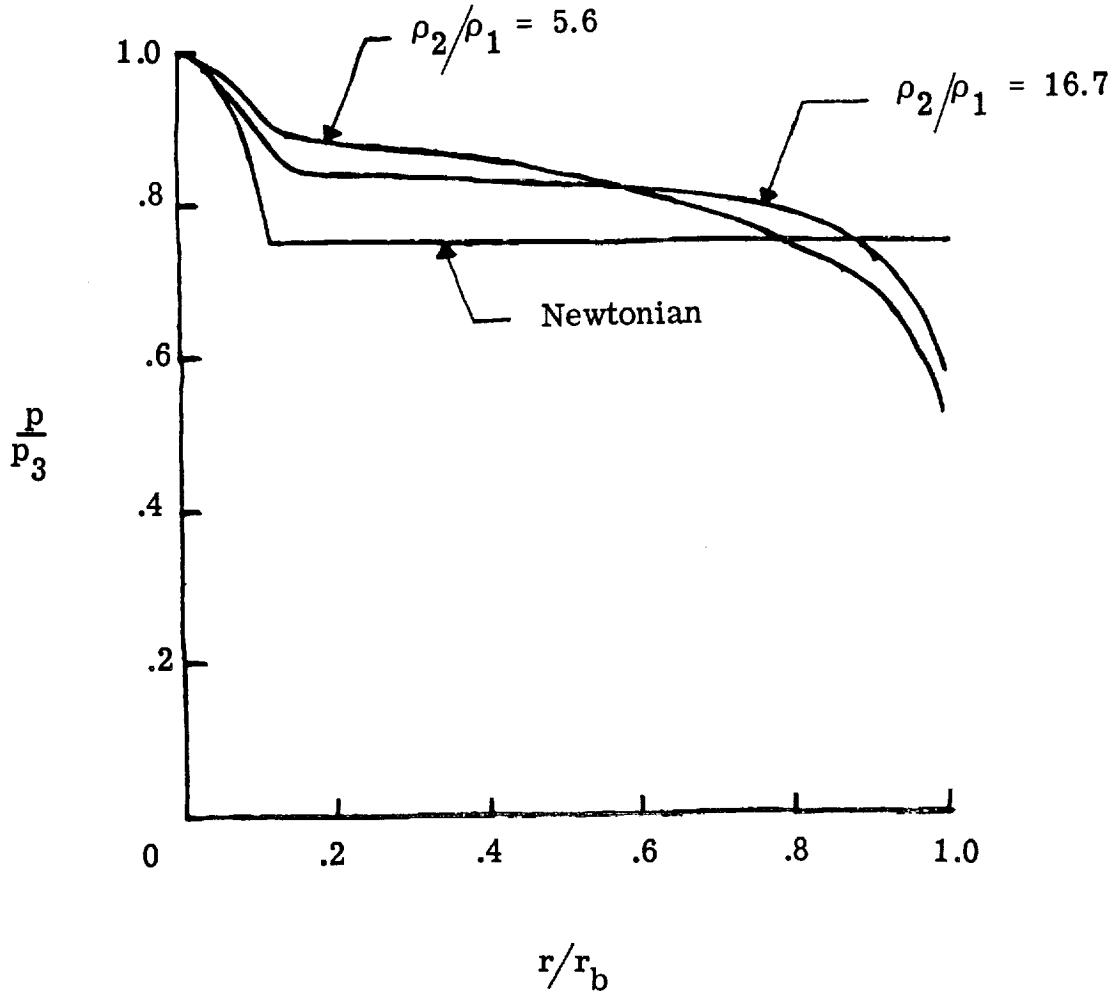

Figure 7.- Calculated pressure distribution for blunt cone (from ref. 2).

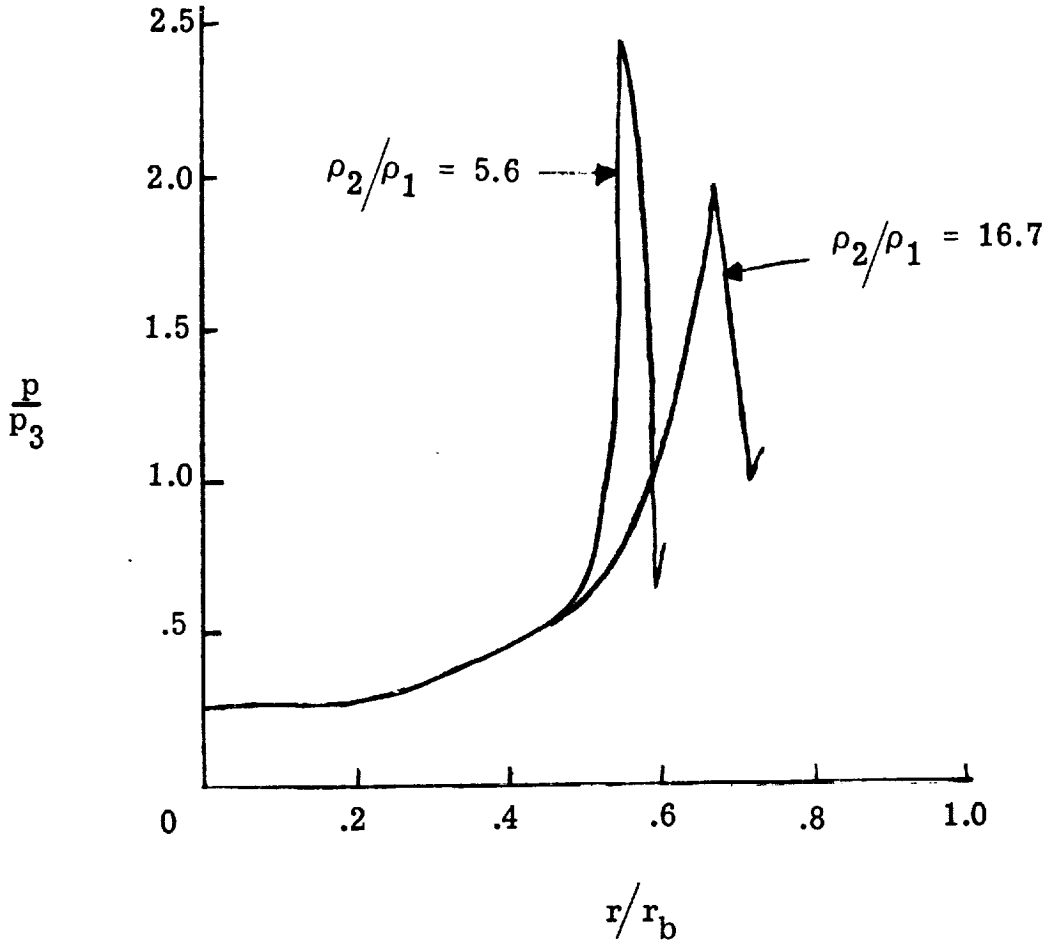

Figure 8.- Calculated pressure distribution for tension shell (from ref. 2).

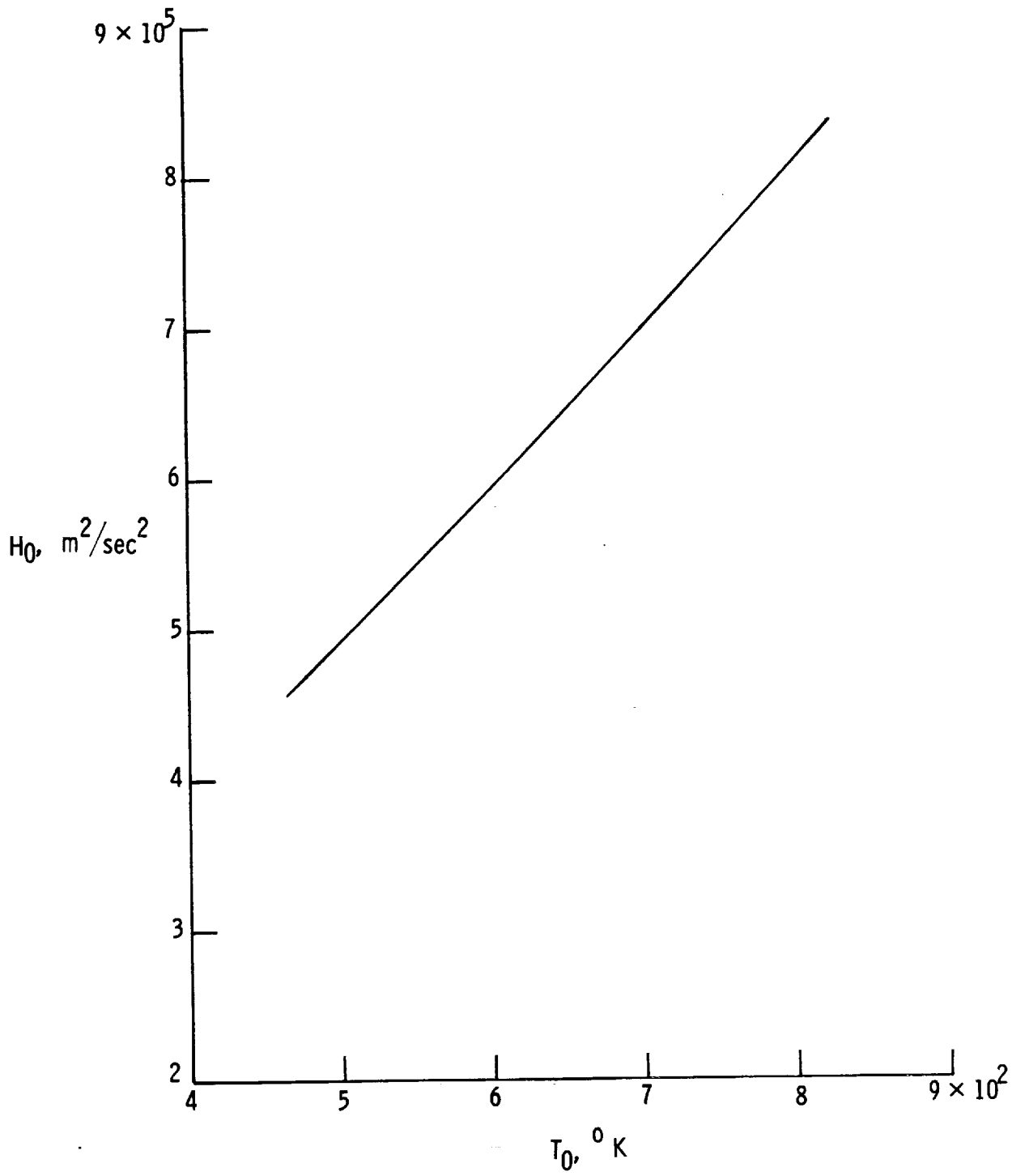

Figure 9.- Total enthalpy of CF_4. (Independent of stagnation pressure from 1034 to 1724 N/cm^2.)

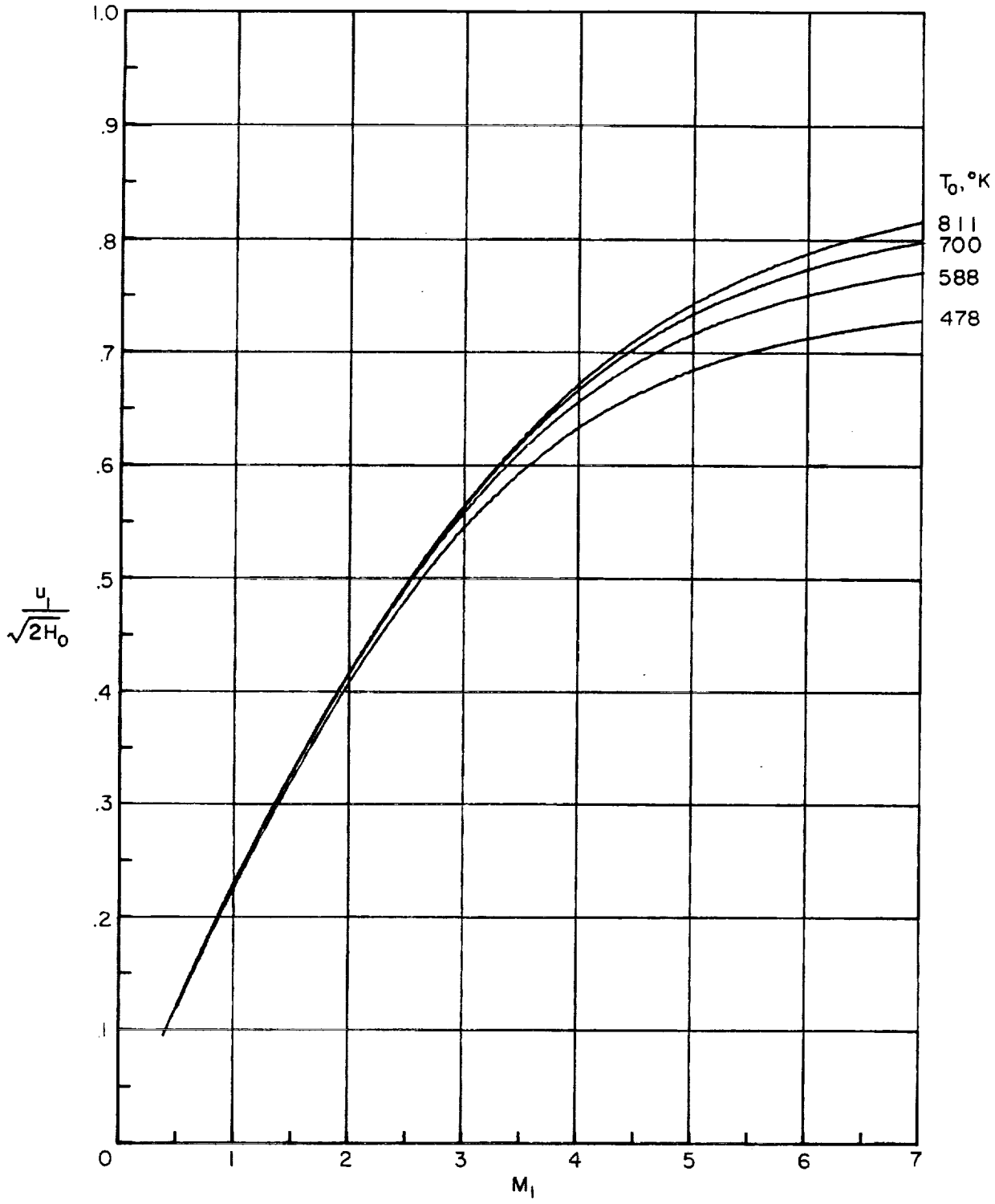

Figure 10.- Variation of free-stream velocity with Mach number. (Independent of stagnation pressure from 1034 to 1724 N/cm^2.)

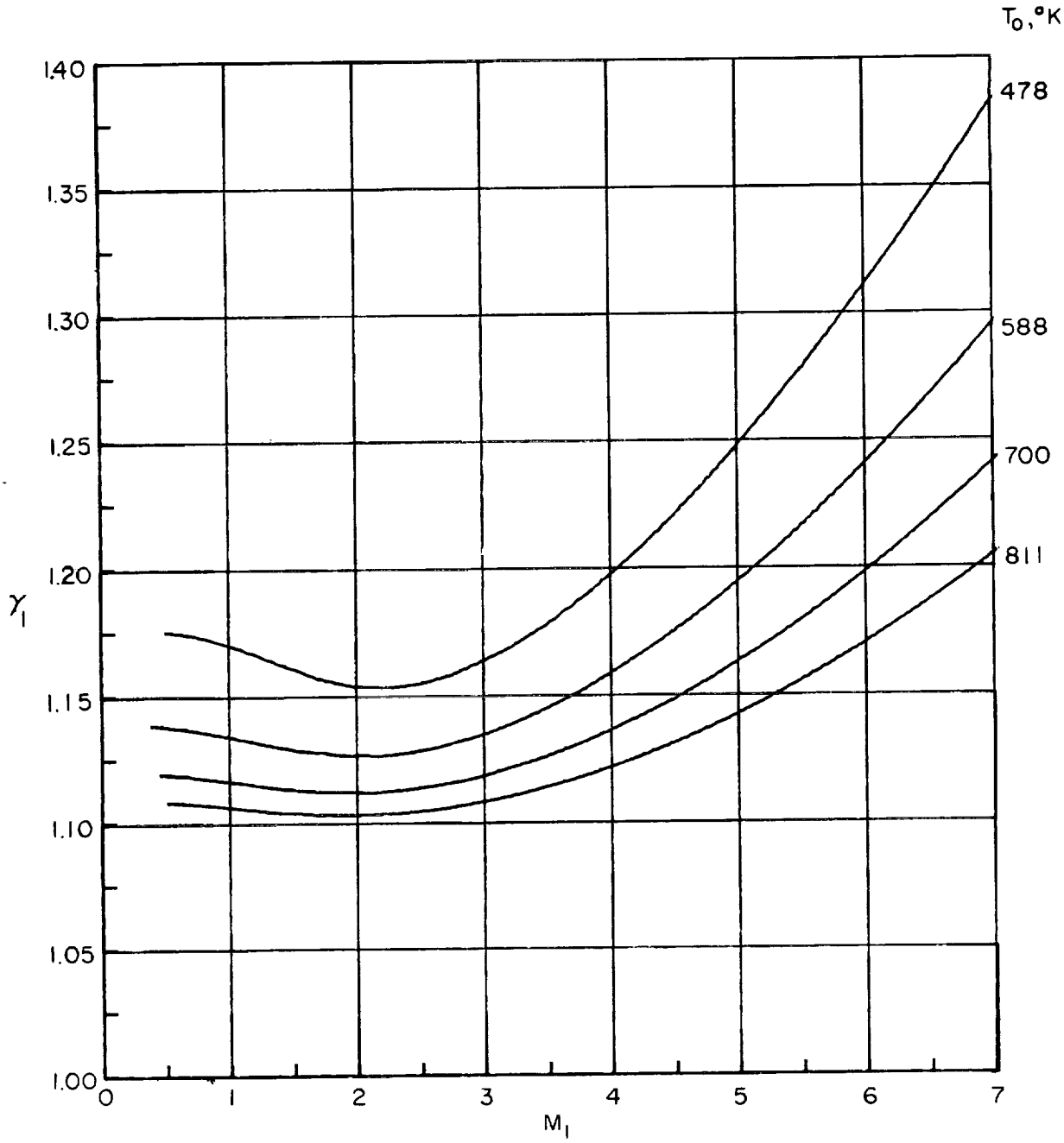

(a) $p_0 = 1034$ N/cm^2.

Figure 11.- Variation of free-stream specific-heat ratio with Mach number.

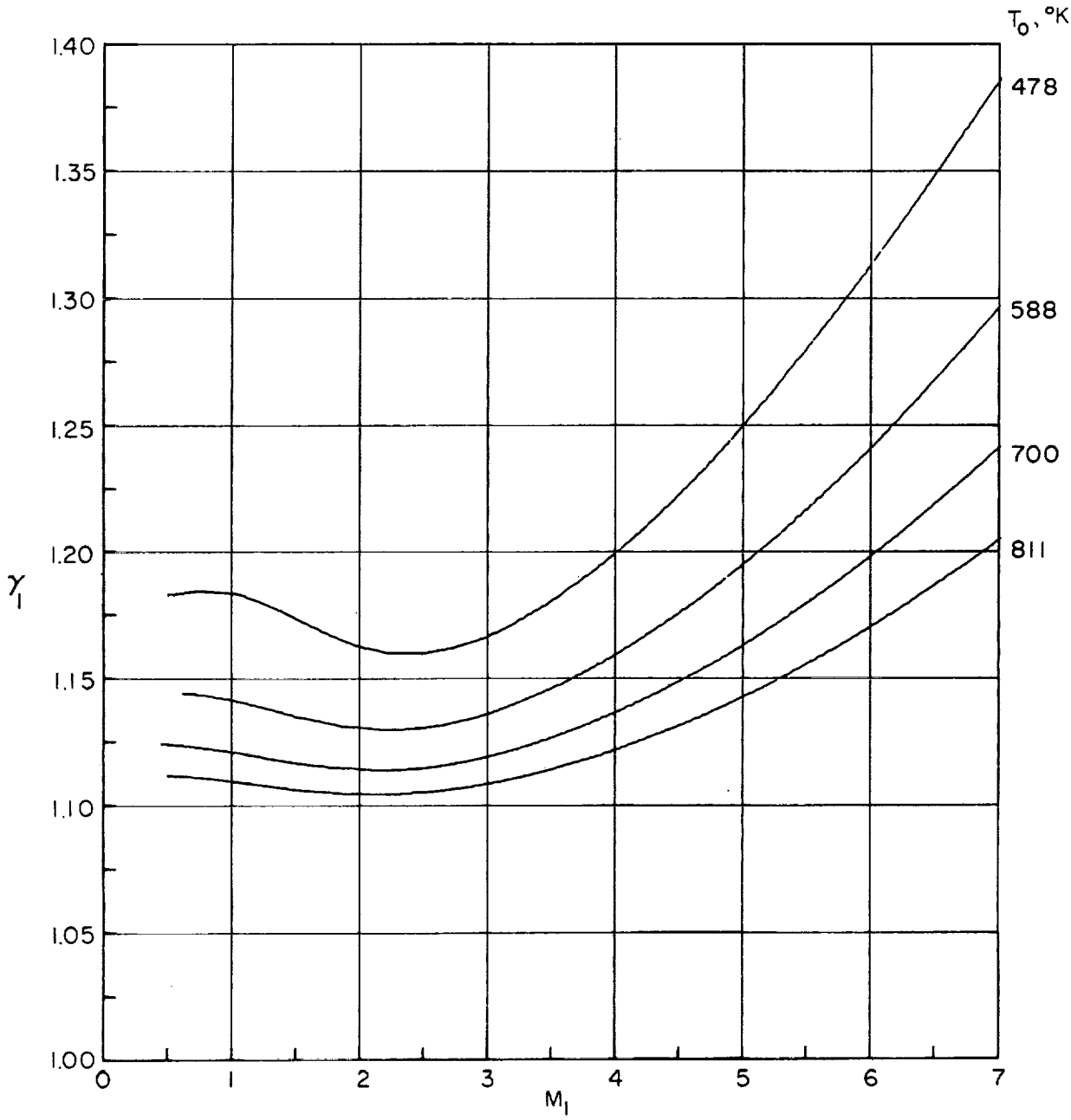

(b) p_0 = 1378 N/cm^2.

Figure 11.- Continued.

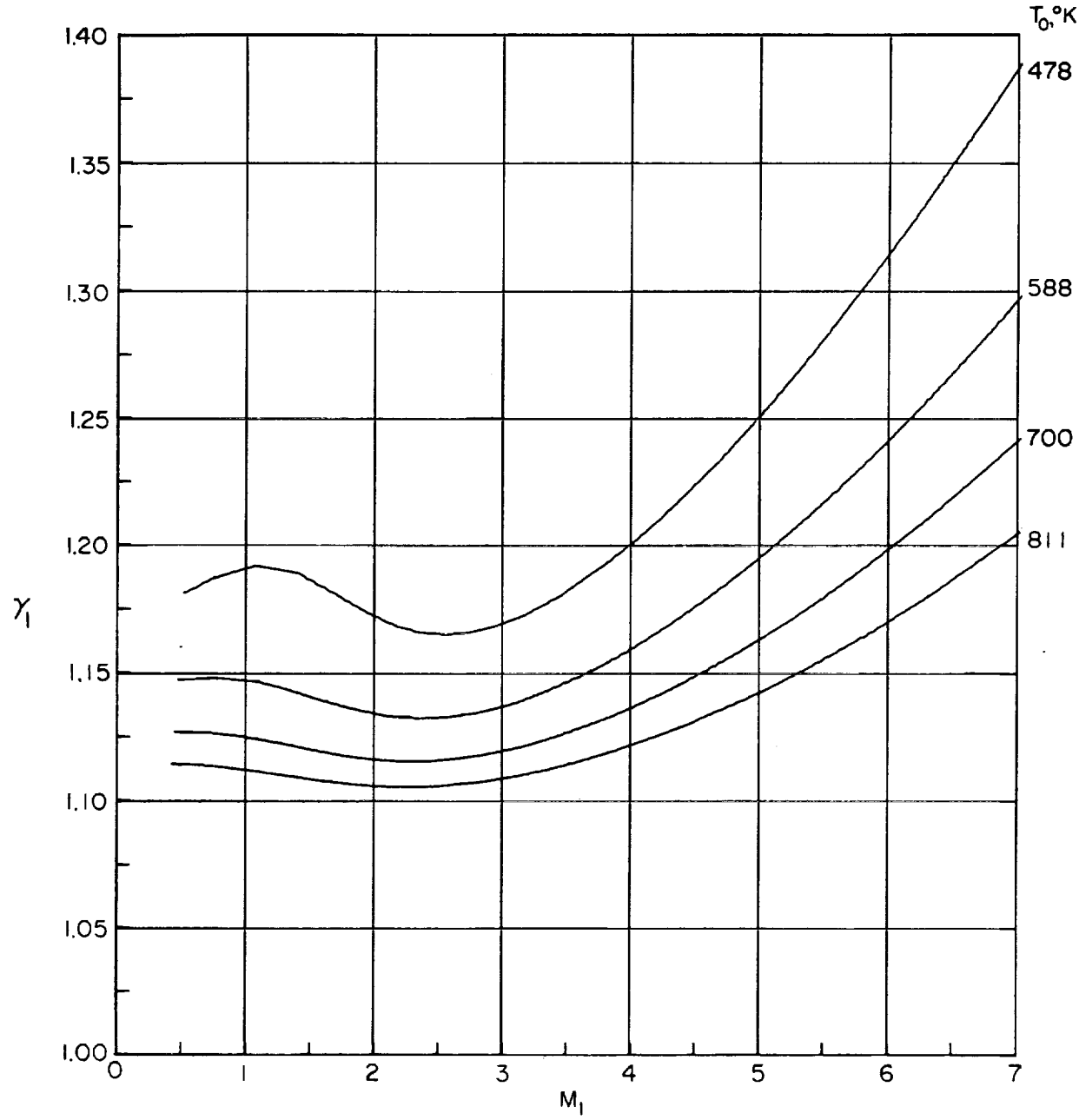

(c) $p_0 = 1724$ N/cm^2.

Figure 11.- Concluded.

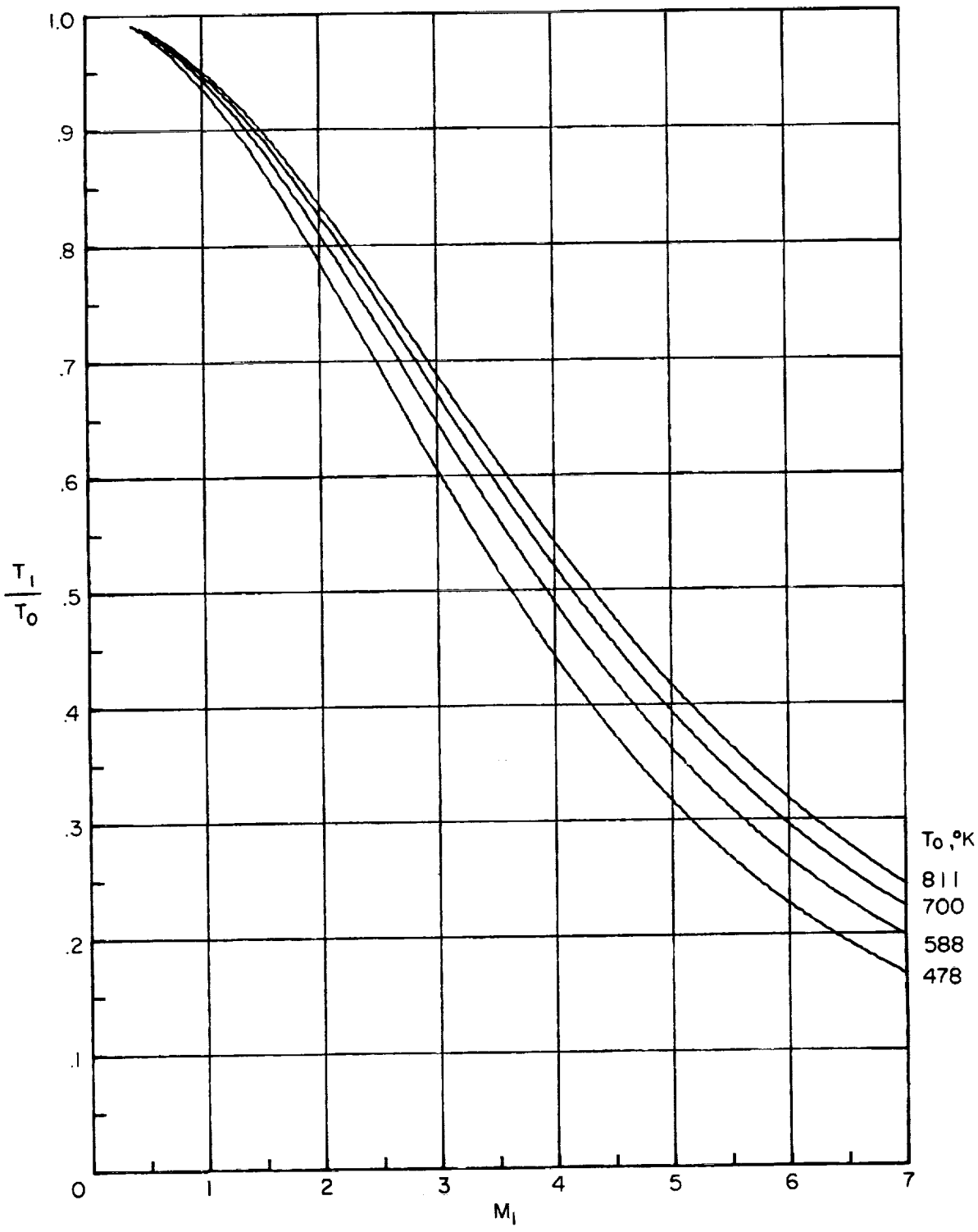

Figure 12.- Variation of ratio of free-stream static temperature to stagnation temperature with Mach number. (Independent of stagnation pressure from 1034 to 1724 N/cm^2.)

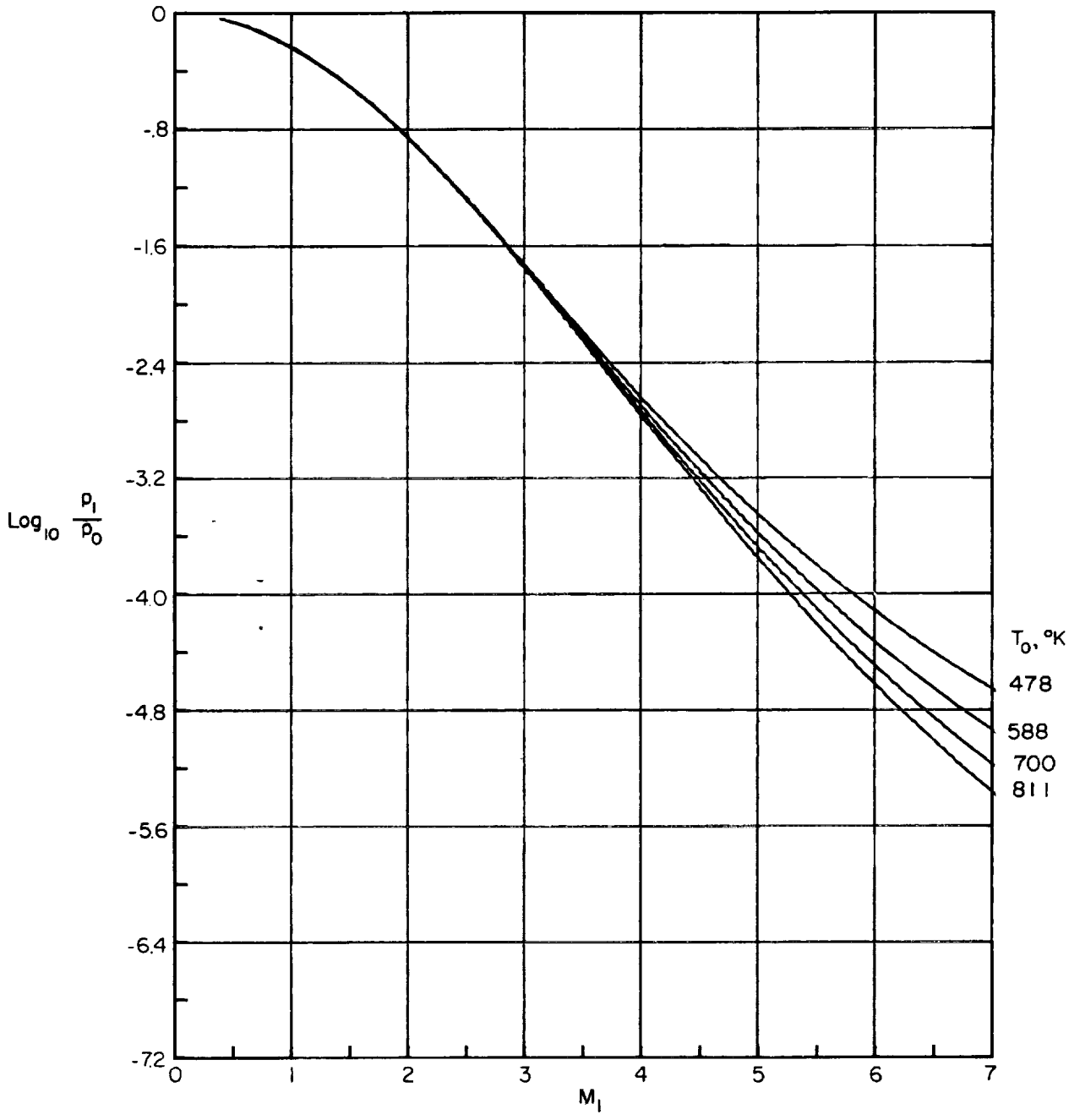

Figure 13.- Variation of ratio of free-stream static pressure to stagnation pressure with Mach number. (Independent of stagnation pressure from 1034 to 1724 N/cm^2.)

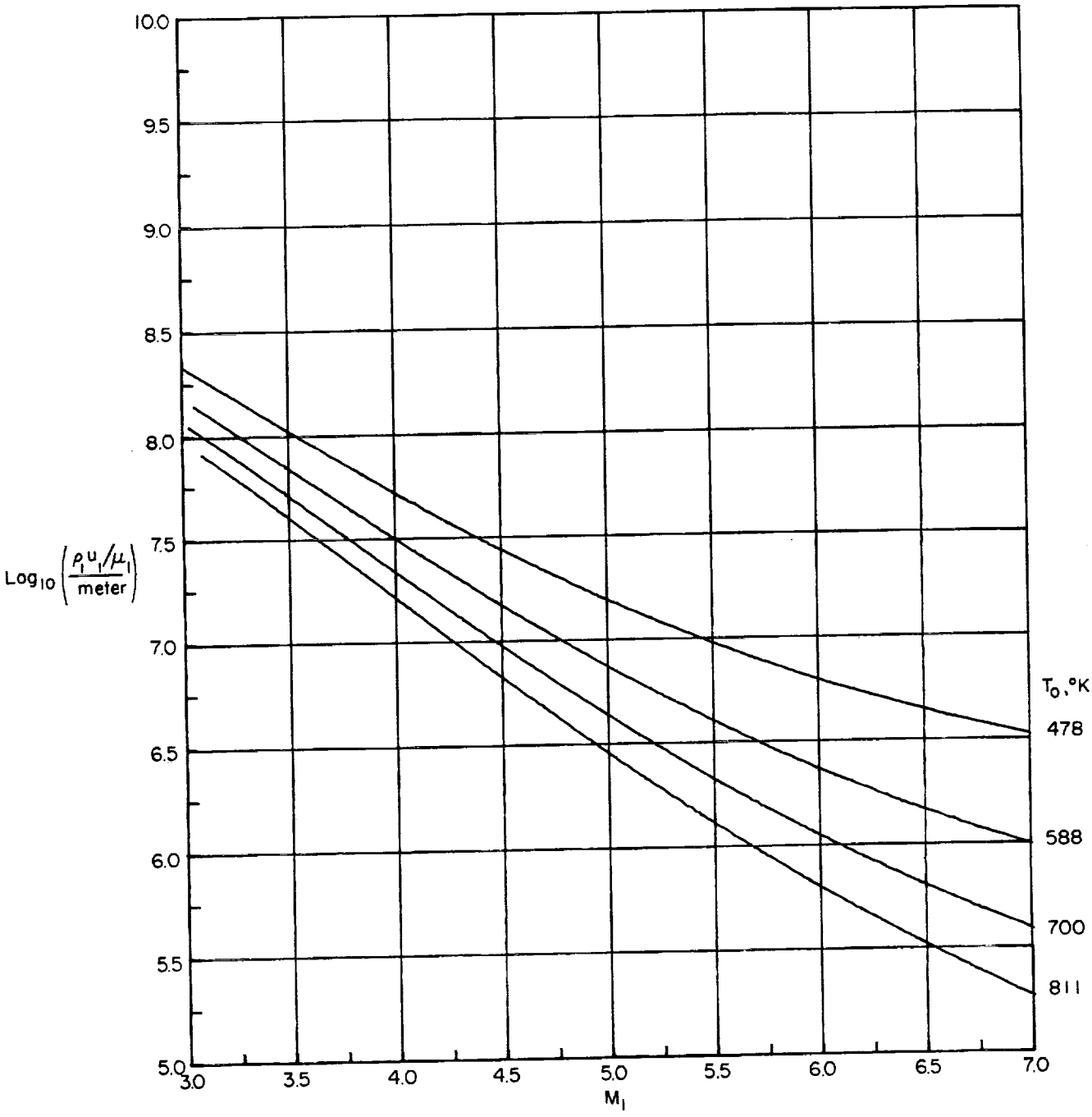

(a) $p_0 = 1034$ N/cm^2.

Figure 14.- Variation of free-stream Reynolds number with Mach number.

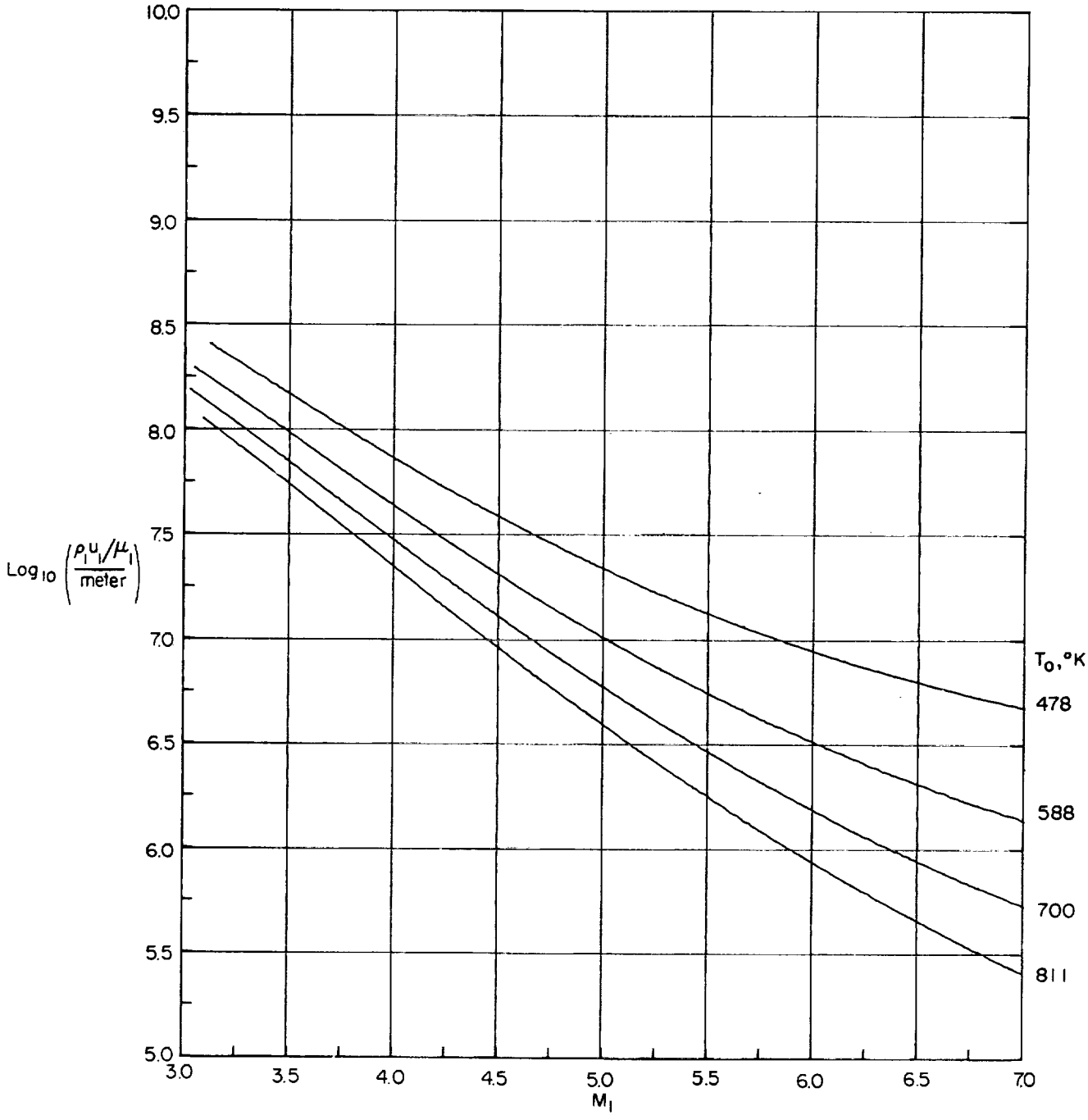

(b) $p_0 = 1378$ N/cm^2.

Figure 14.- Continued.

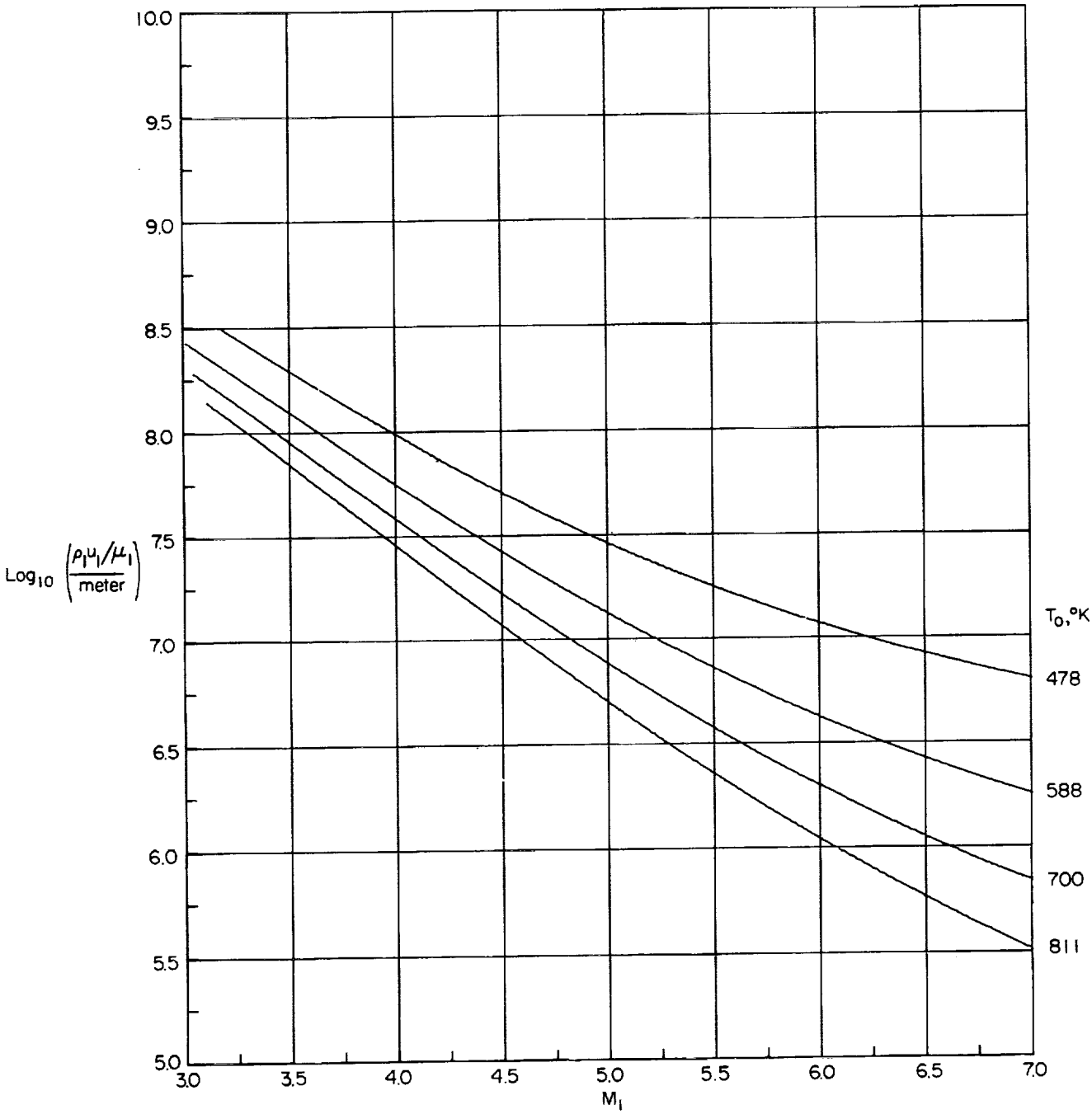

(c) $p_0 = 1724$ N/cm^2.

Figure 14.- Concluded.

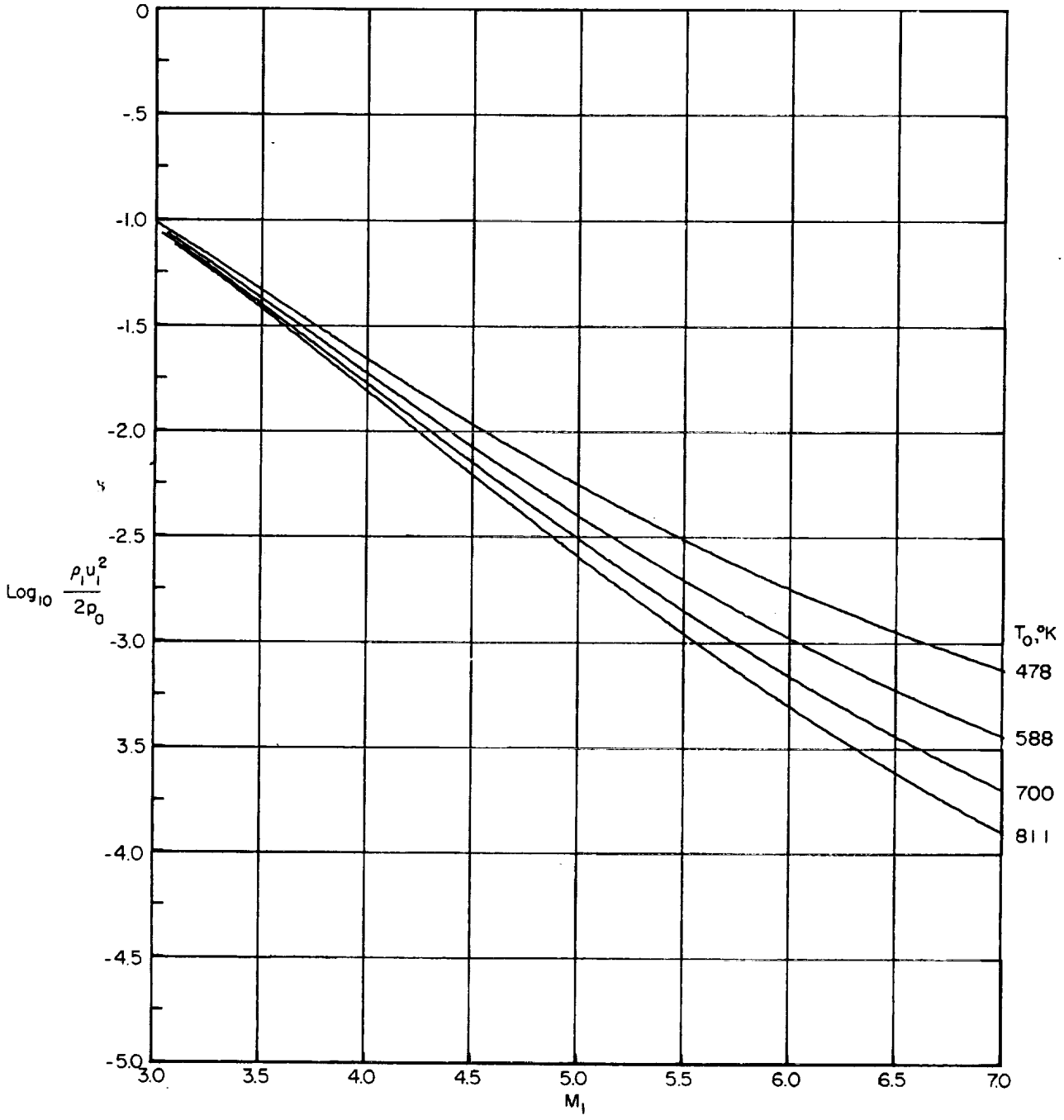

Figure 15.- Variation of ratio of free-stream dynamic pressure to stagnation pressure with Mach number. (Independent of stagnation pressure from 1034 to 1724 N/cm2.)

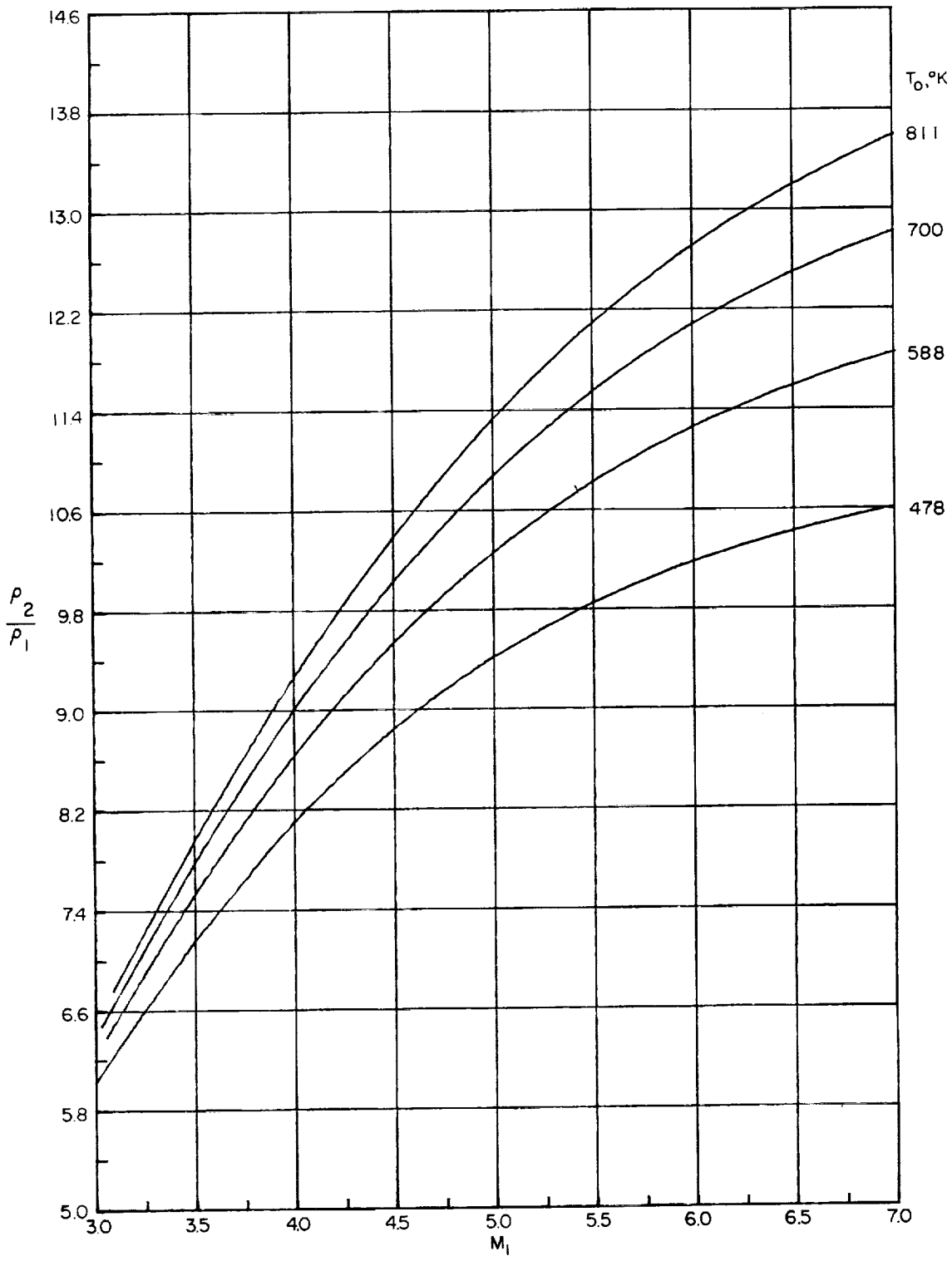

Figure 16.- Variation of density ratio across normal shock with Mach number. (Independent of stagnation pressure from 1034 to 1724 N/cm^2.)

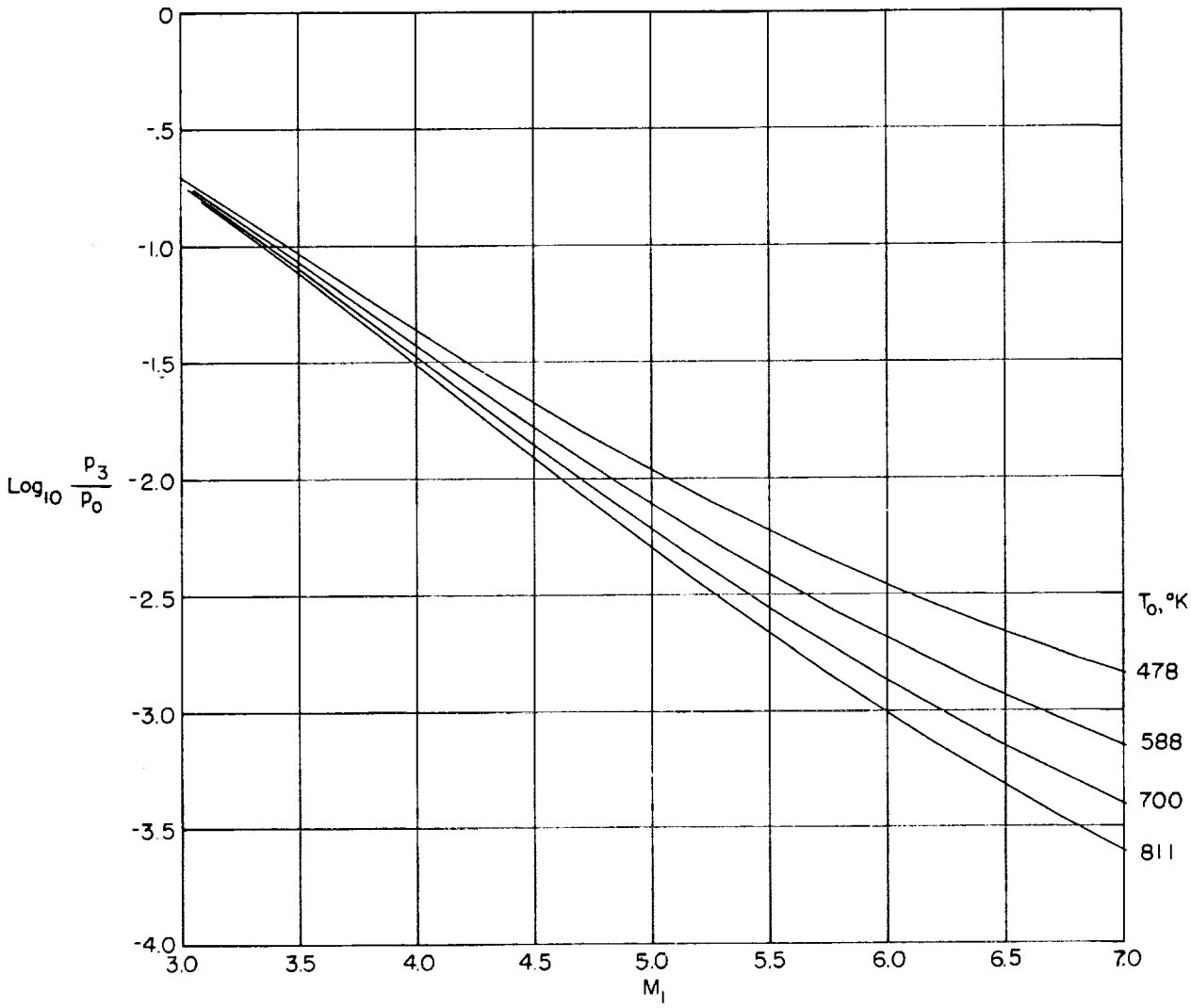

Figure 17.- Variation of ratio of total pressure behind a normal shock to free-stream total pressure with Mach number. (Independent of stagnation pressure from 1034 to 1724 N/cm^2.)

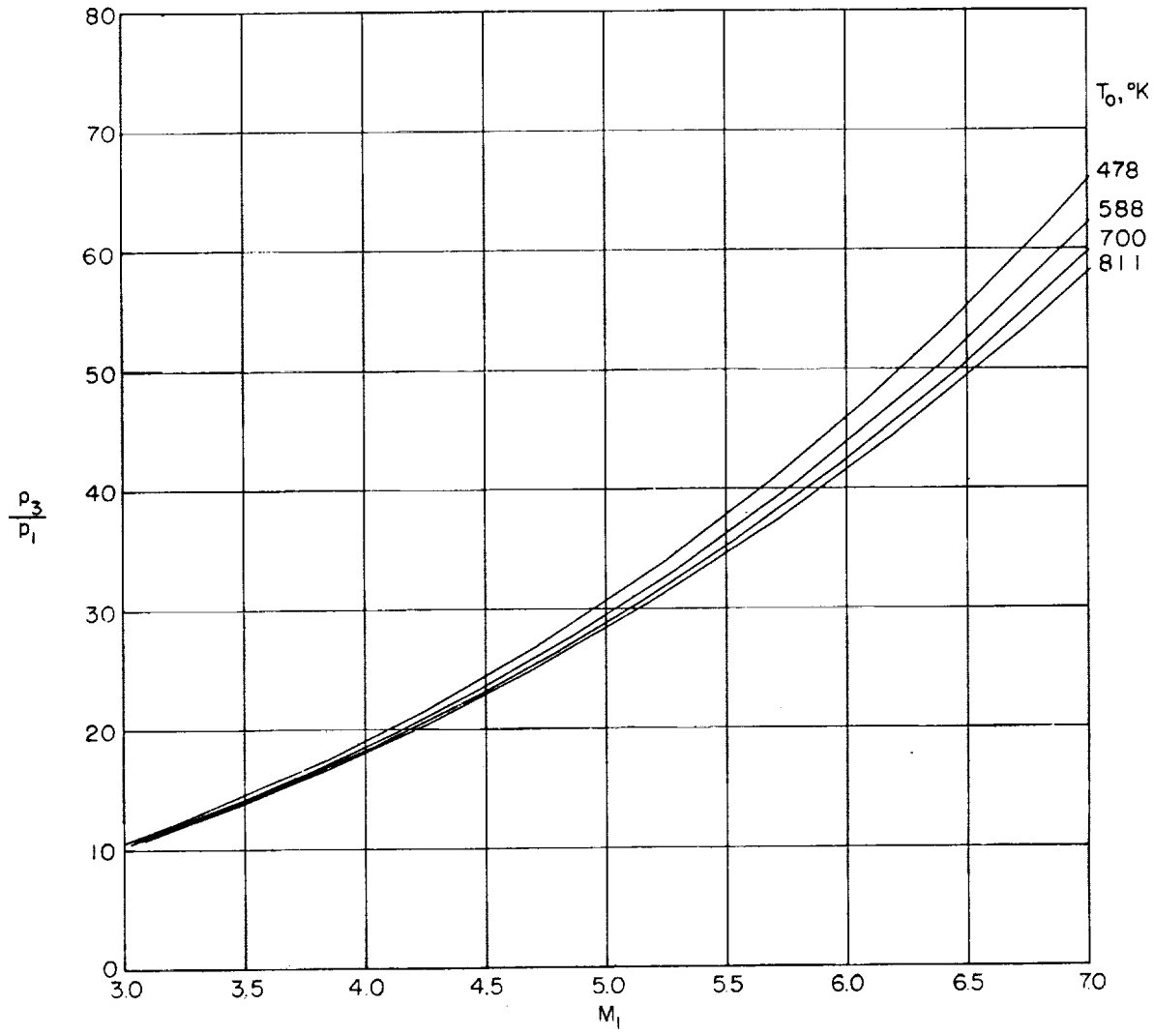

Figure 18.- Variation of ratio of total pressure behind a normal shock to the free-stream static pressure with Mach number. (Independent of stagnation pressure from 1034 to 1724 N/cm^2.)

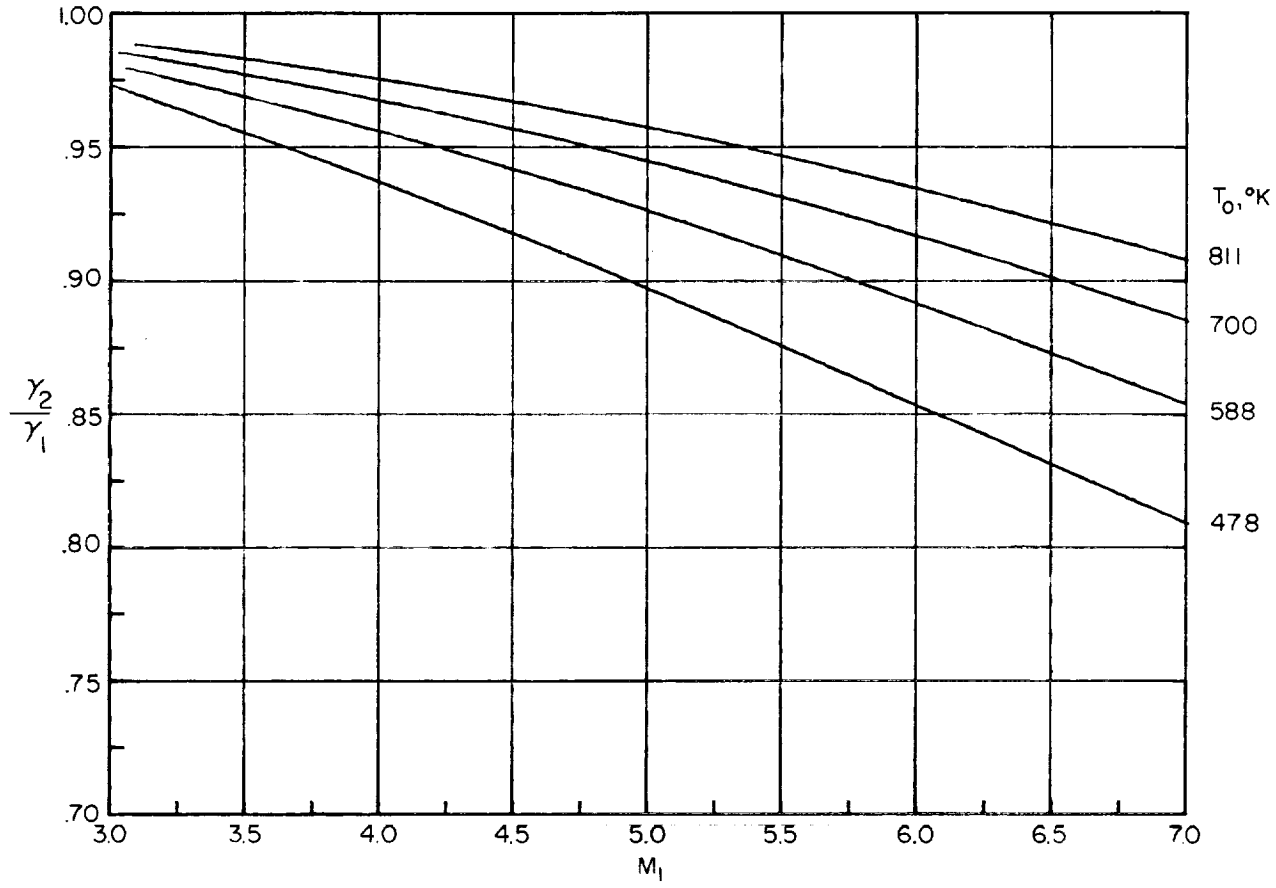

Figure 19.- Variation of γ_2/γ_1 with Mach number. (Independent of stagnation pressure from 1034 to 1724 N/cm^2.)

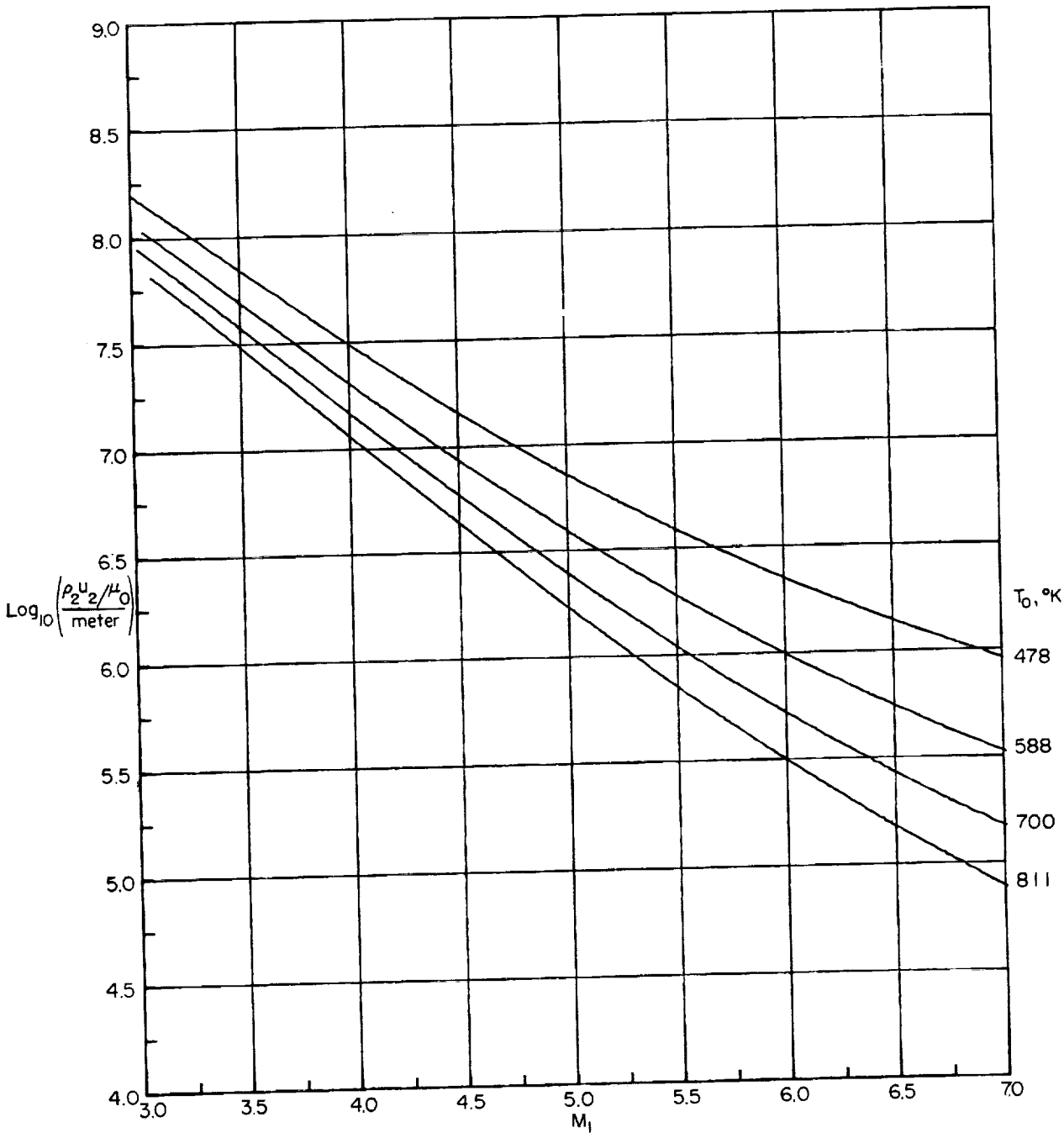

(a) $p_0 = 1034$ N/cm^2.

Figure 20.- Variation of Reynolds number behind normal shock with Mach number.

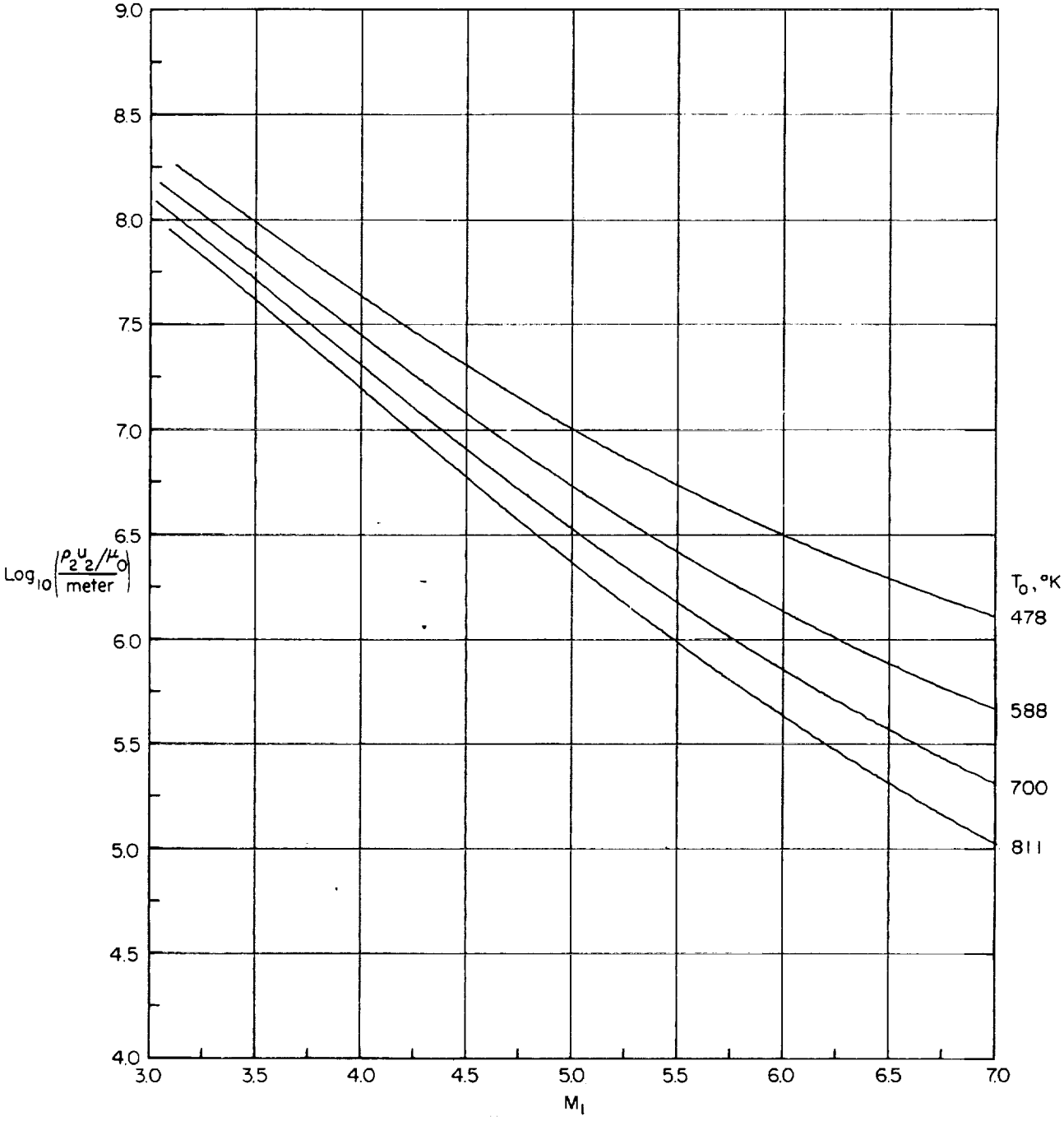

(b) $p_0 = 1378$ N/cm^2.

Figure 20.- Continued.

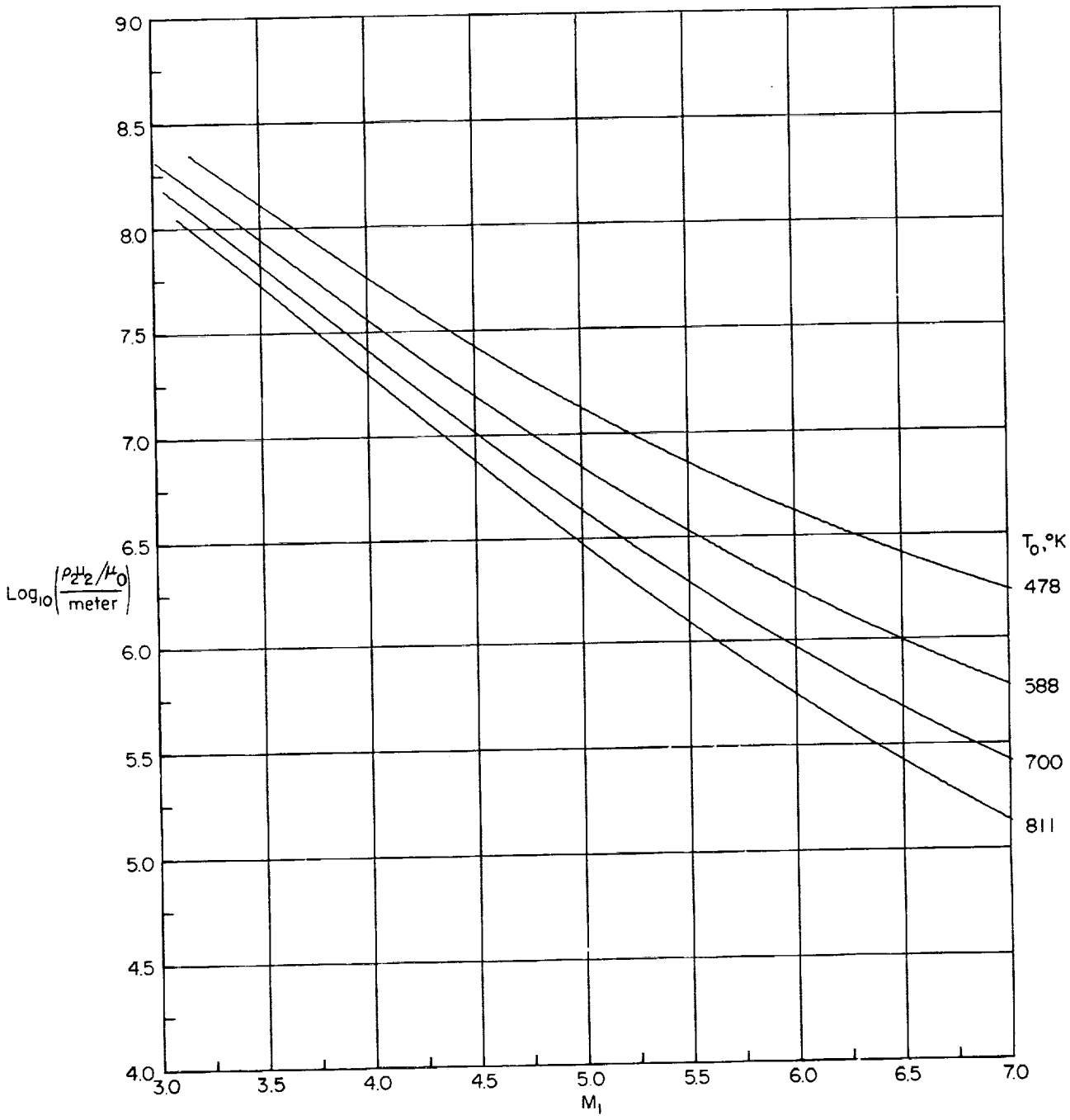

(c) $p_0 = 1724$ N/cm^2.

Figure 20.- Concluded.

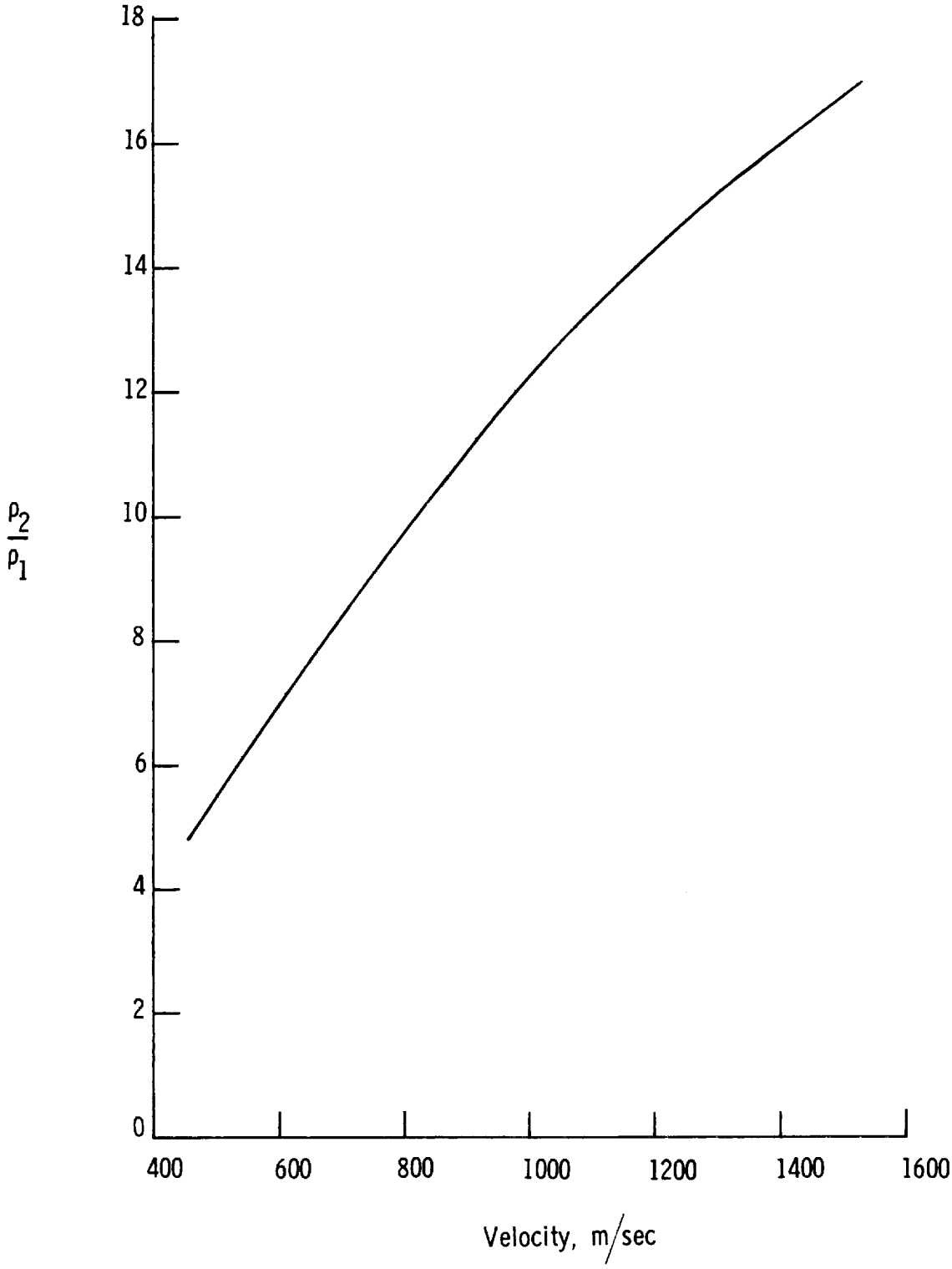

Figure 21.- Ballistic-range shock density ratio.

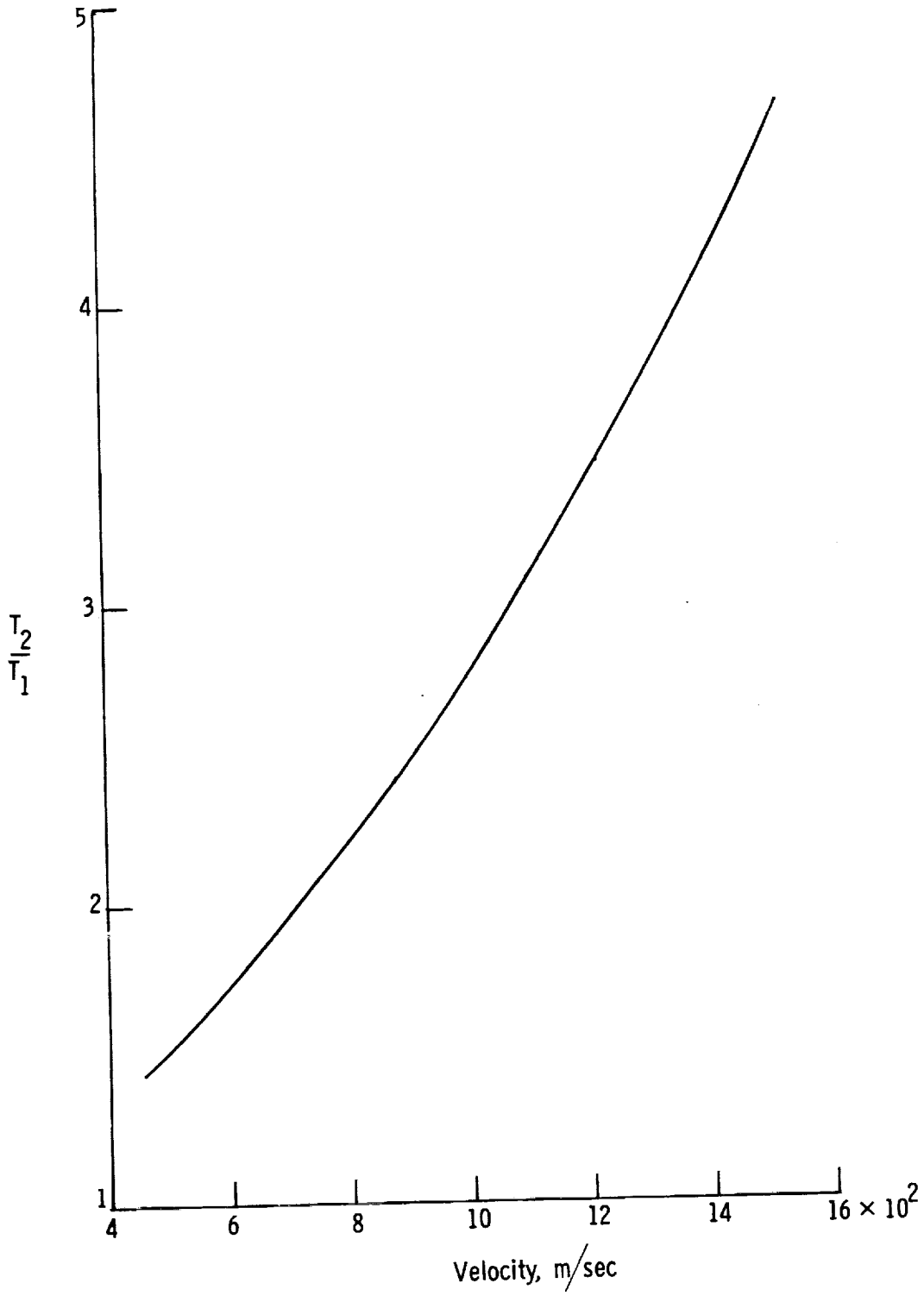

Figure 22.- Ballistic-range static-temperature ratio.

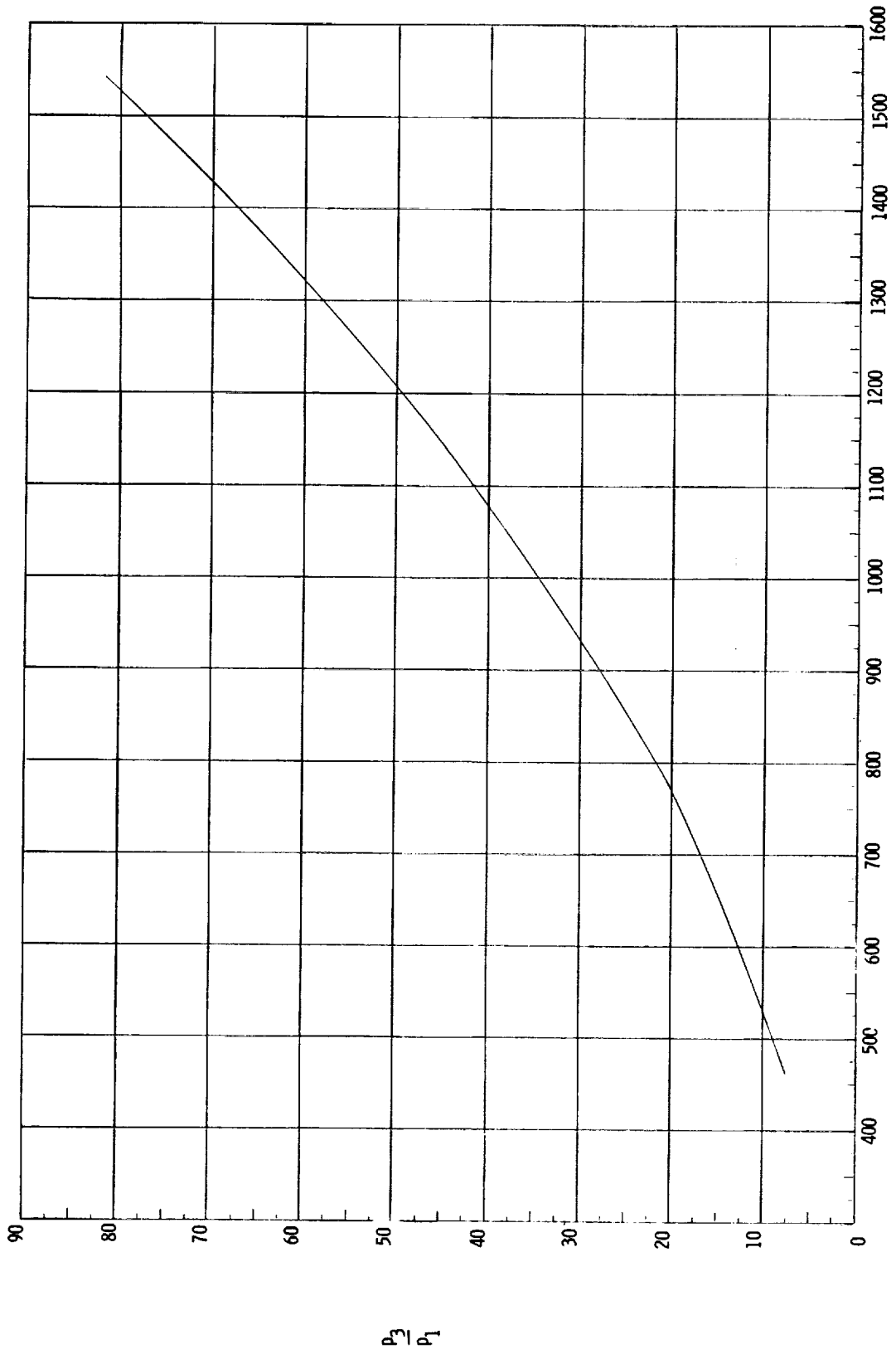

Figure 23.- Ratio of stagnation pressure behind shock to free-stream static pressure in ballistic range.

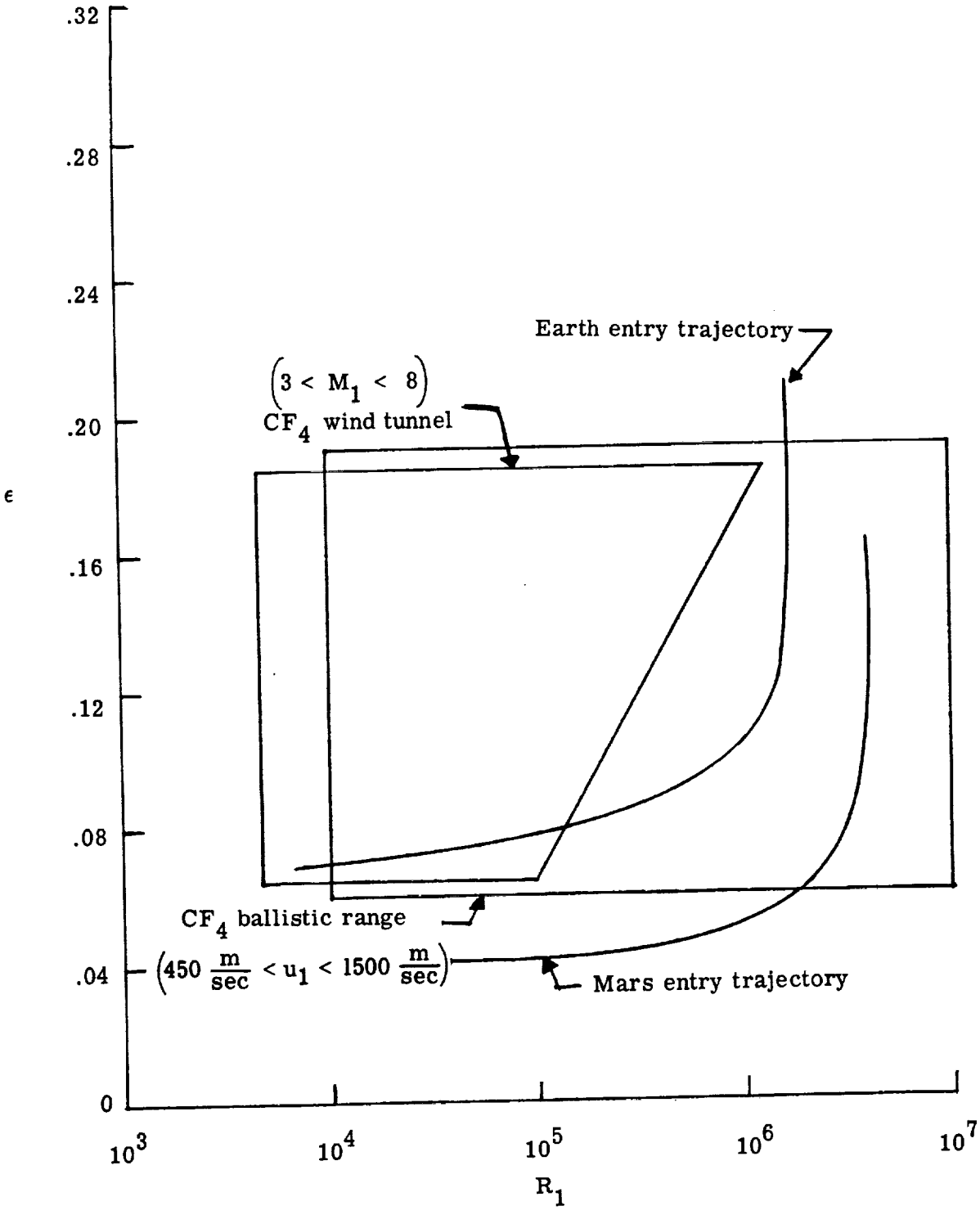

Figure 24.- Density ratio capability with CF_4.

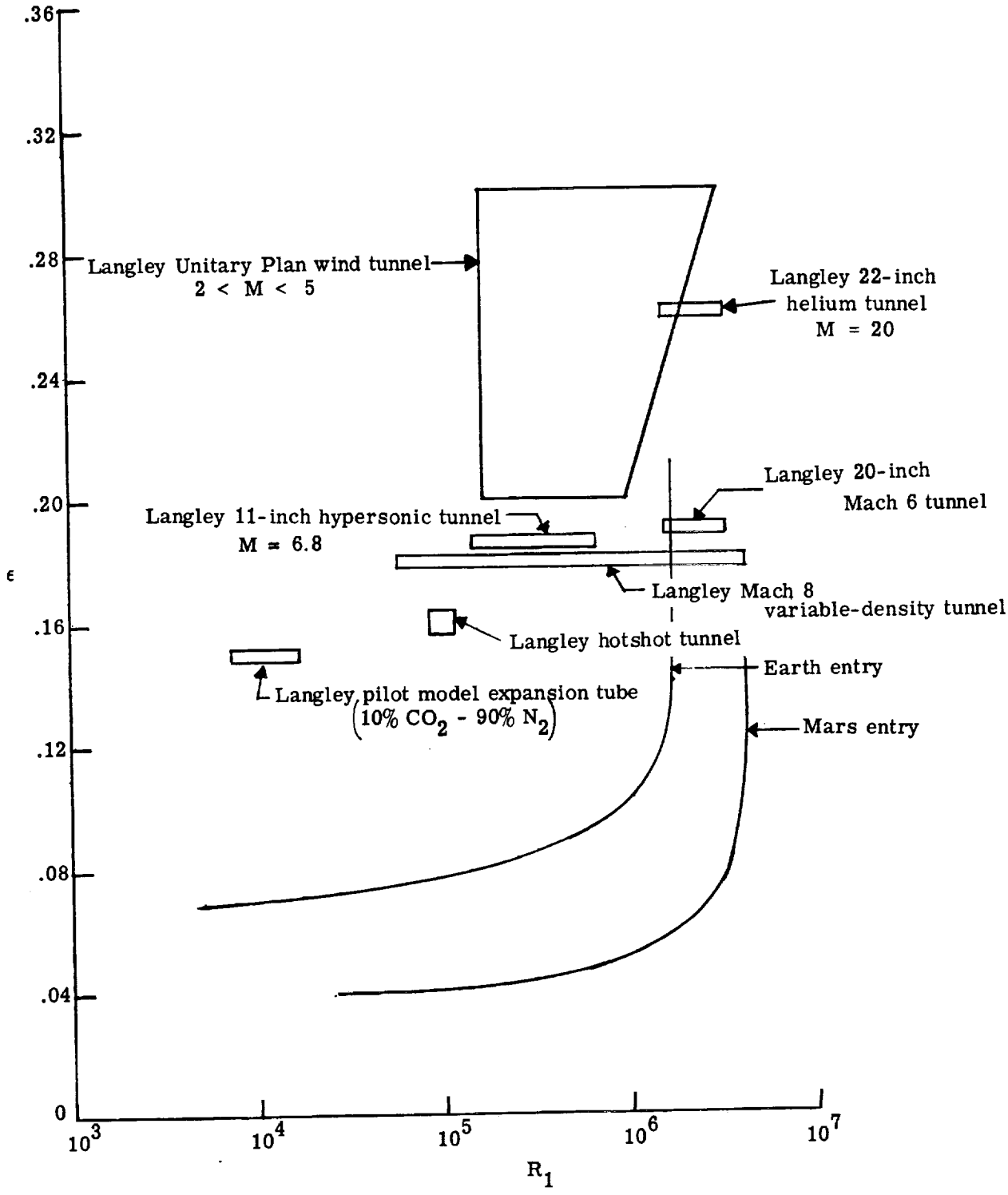

Figure 25.- Density-ratio simulation capability of several facilities.

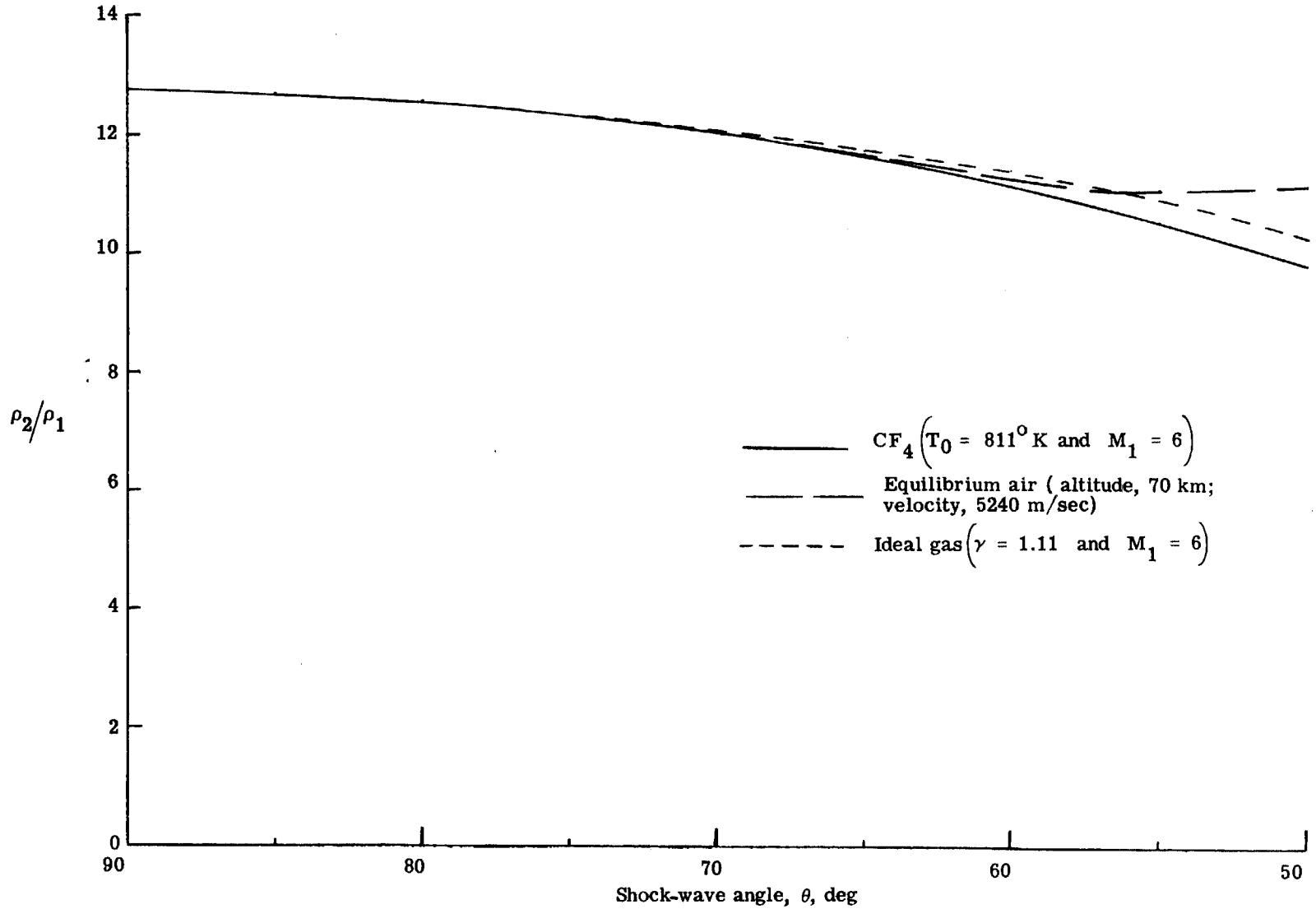

Figure 26.- Variation of shock density ratio with shock-wave inclination angle.

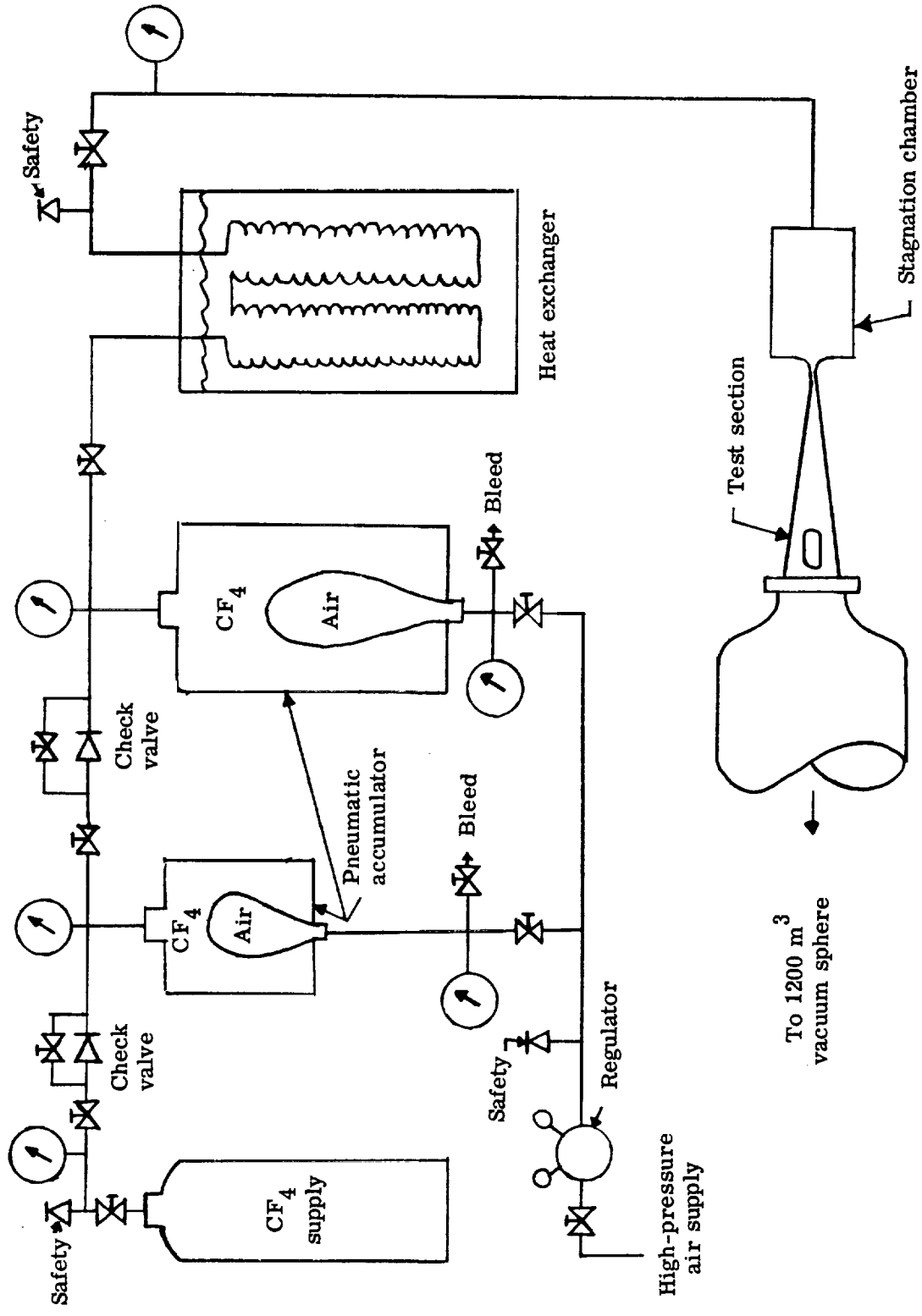

Figure 27.- Schematic diagram of CF_4 tunnel.

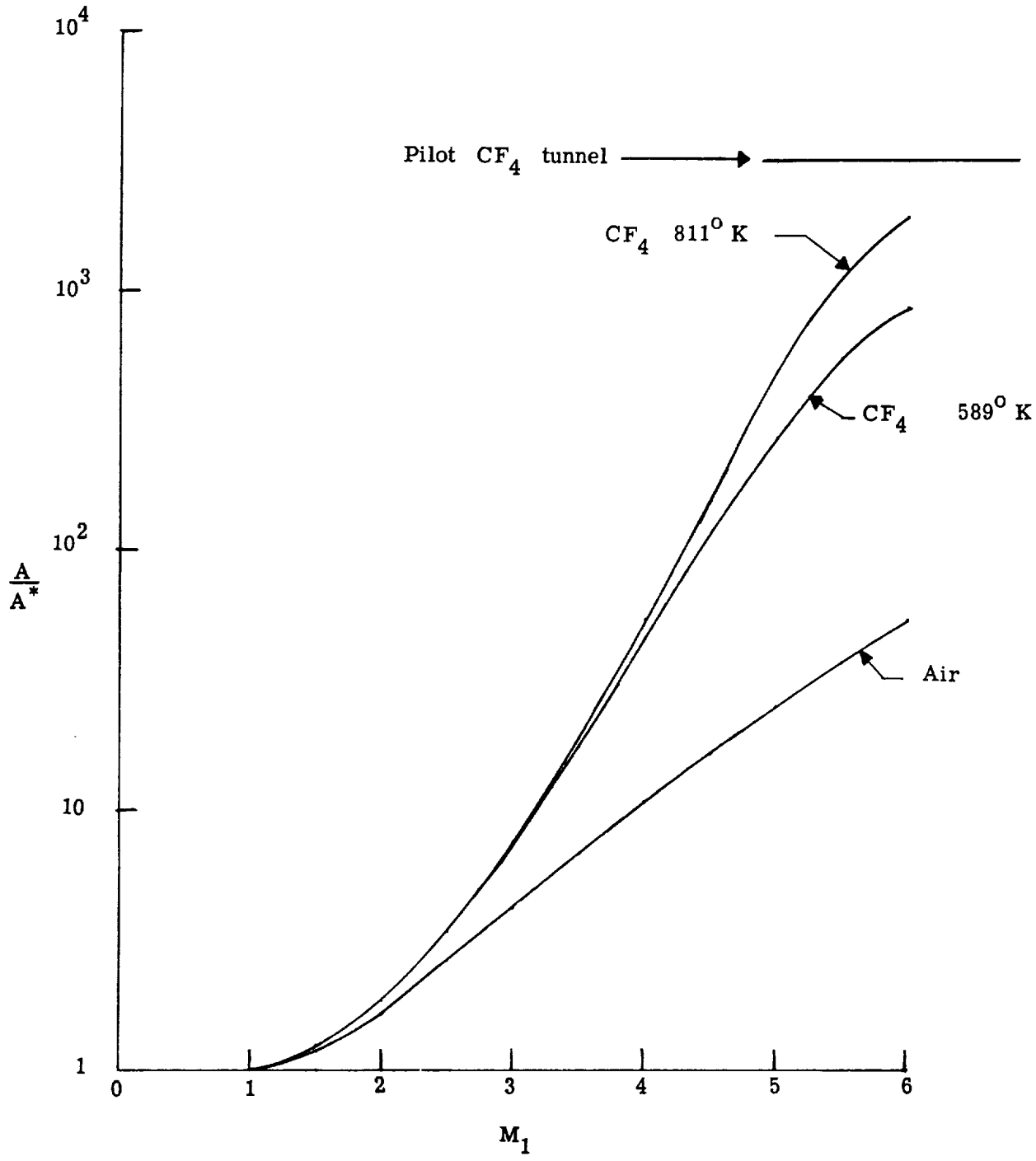

Figure 28.- Variation of area ratio with Mach number.

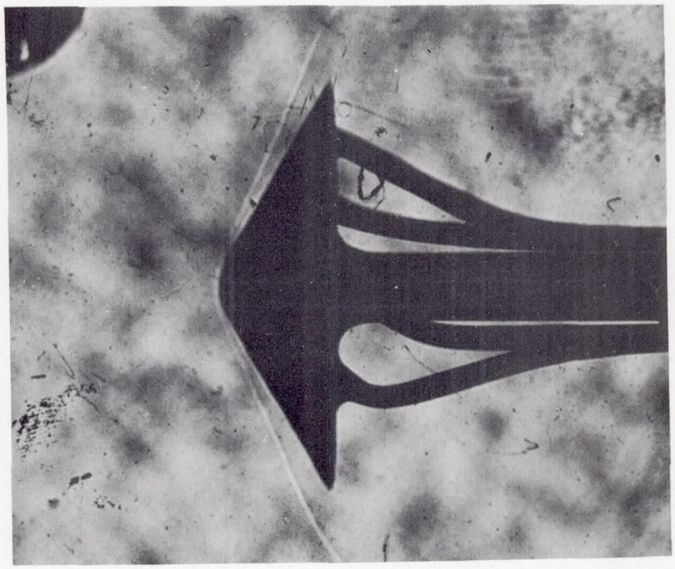

(a) Pilot CF_4 tunnel. $M_1 = 6.2$; $\rho_2/\rho_1 \approx 12.1$.

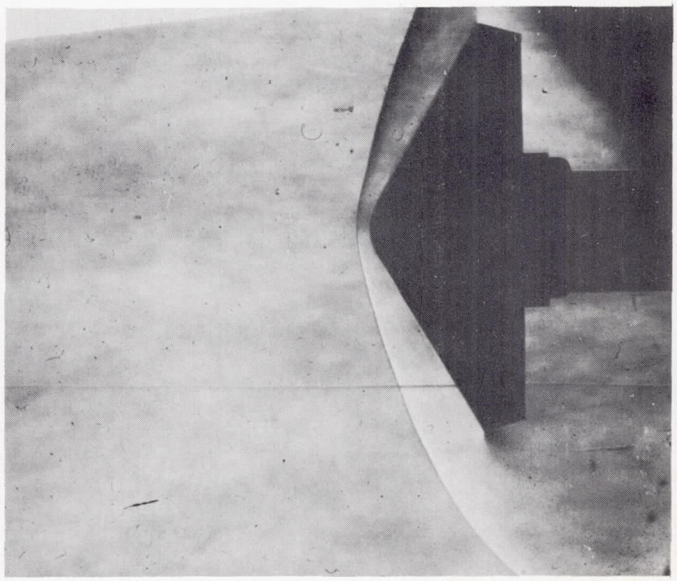

(b) Langley Mach 8 variable-density tunnel. $M_1 = 8$; $\rho_2/\rho_1 = 5.56$.

Figure 29.- Shock shape for 120^0 cone. L-69-1323

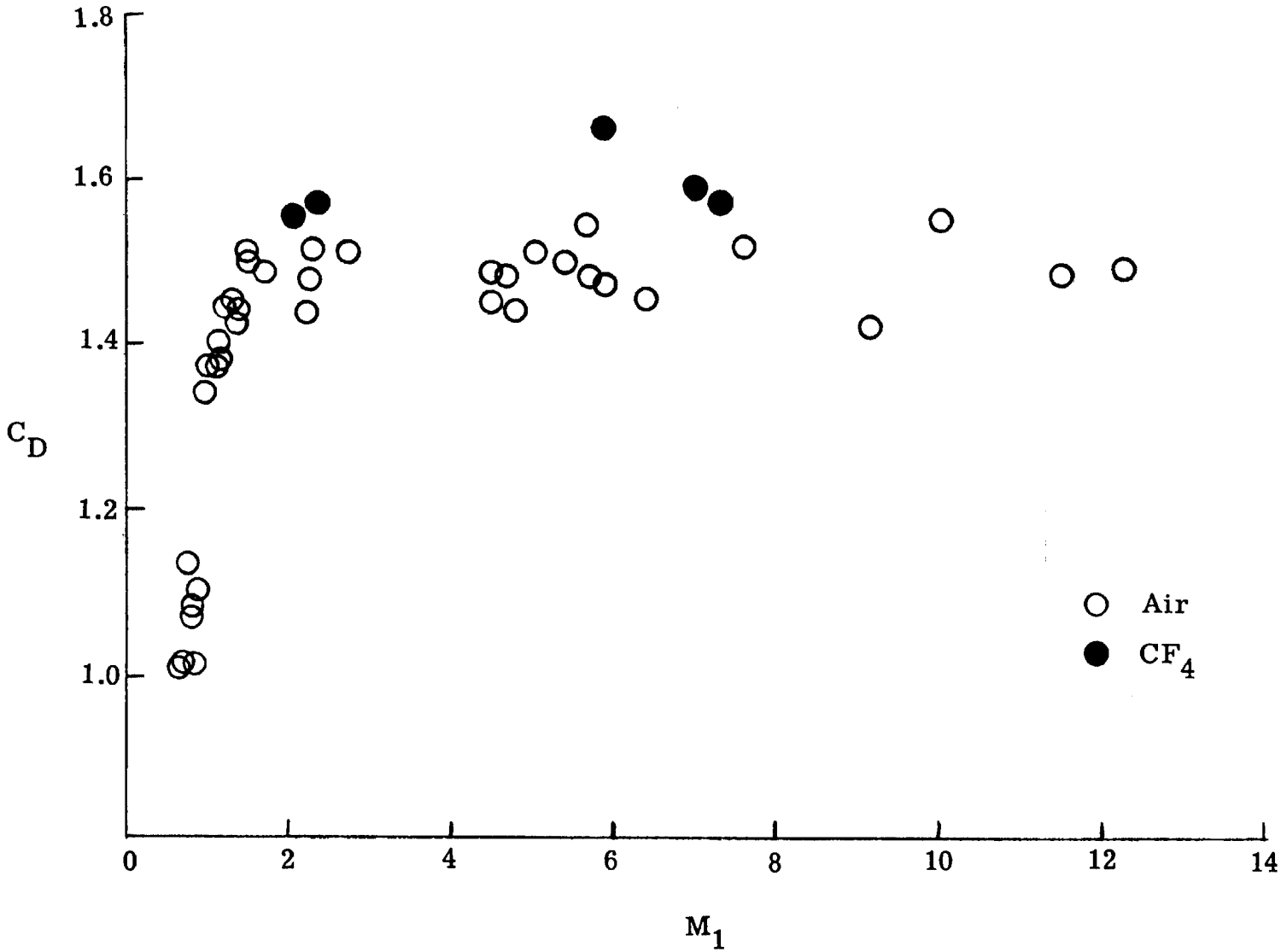

Figure 30.- Drag coefficient of 120^0 cone.

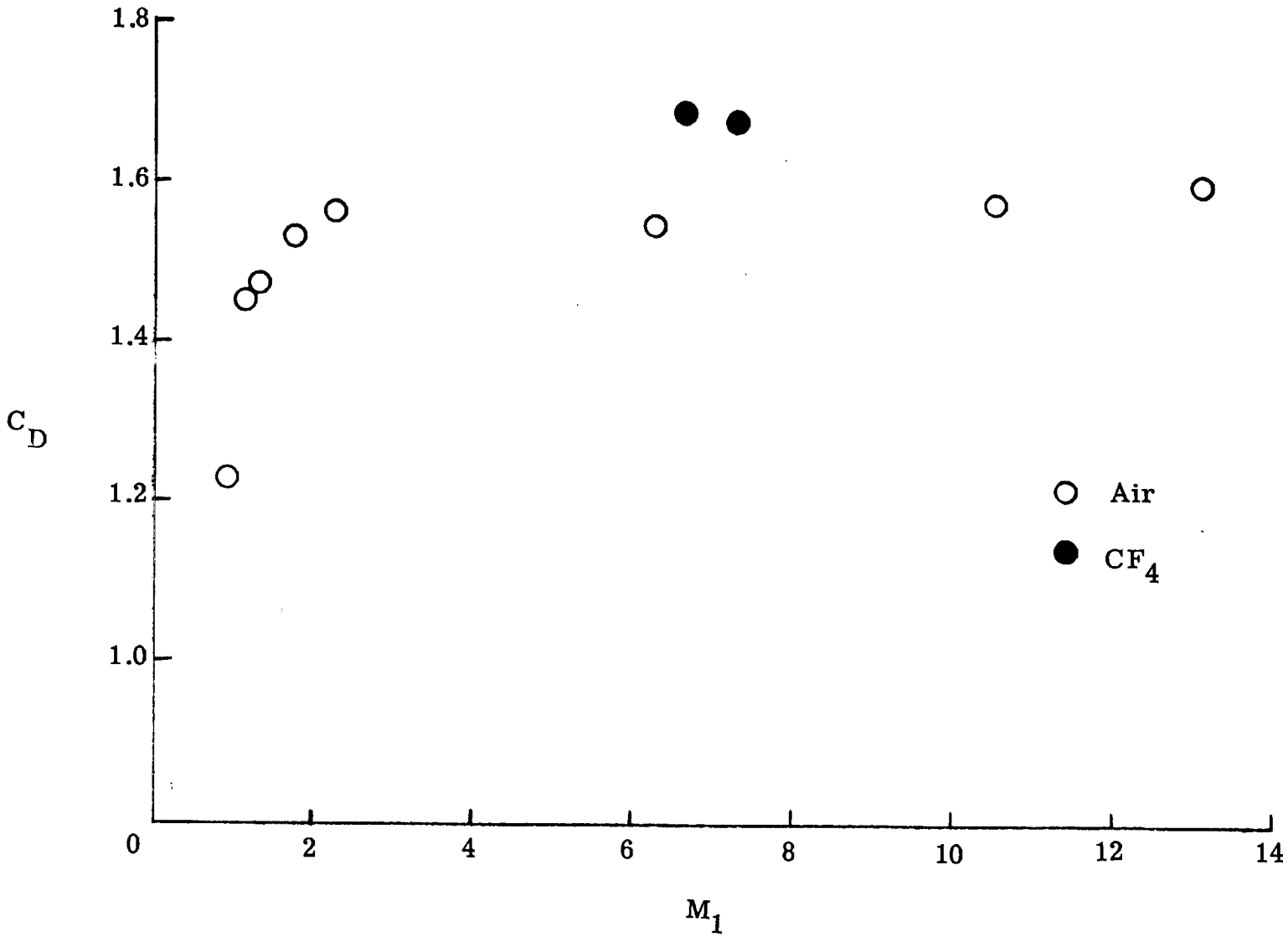

Figure 31.- Drag coefficient of spherical segment.

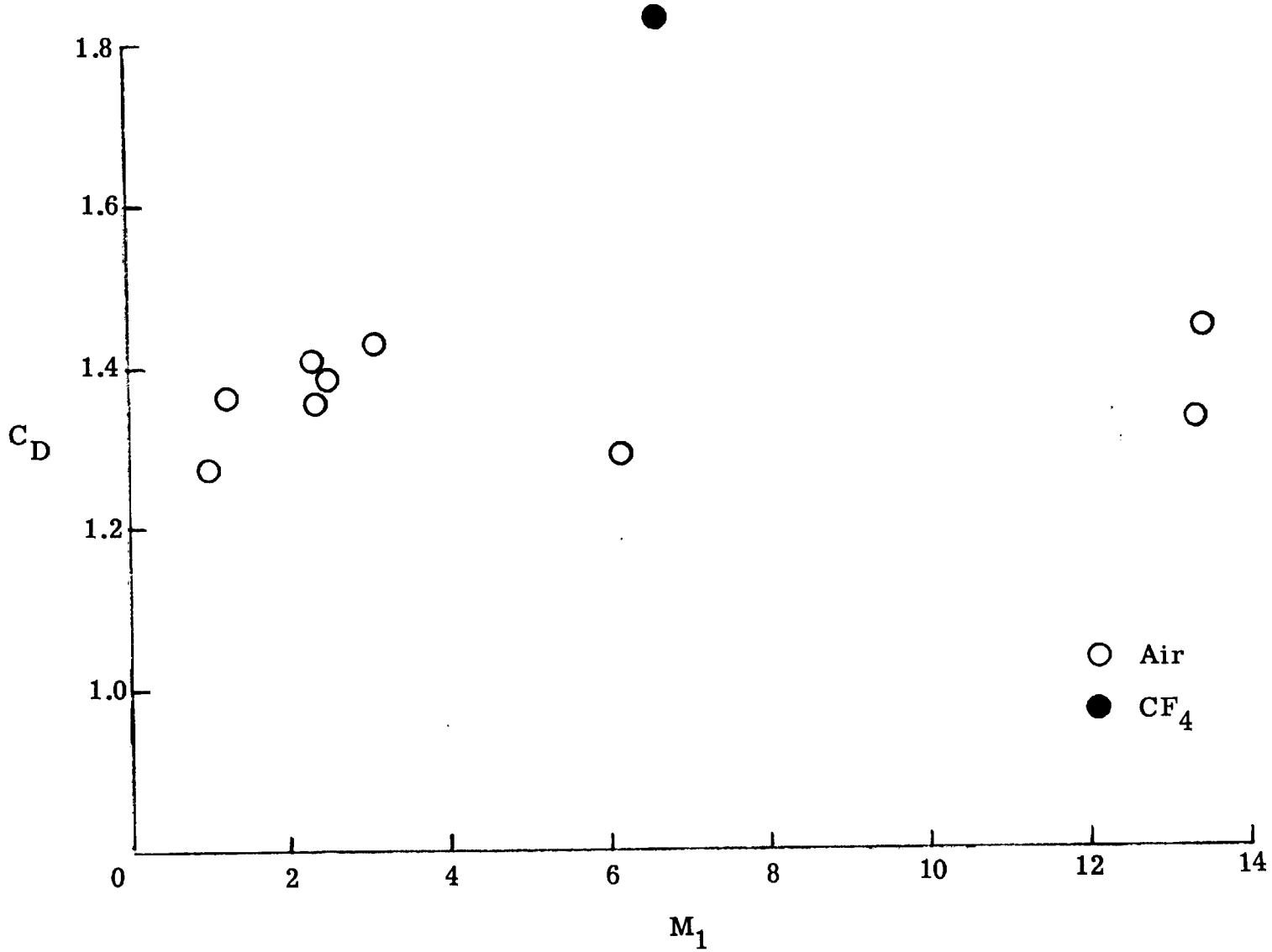

Figure 32.- Drag coefficient of tension shell.

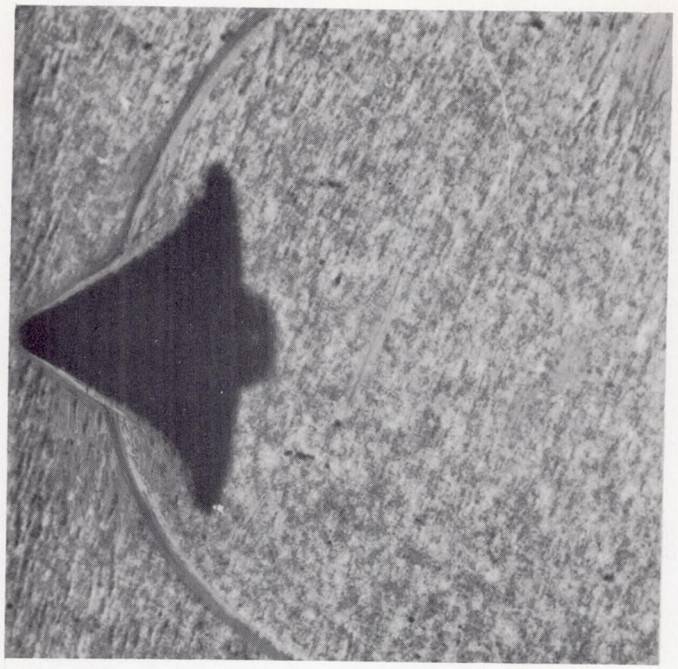

(a) M = 6.14 in air.

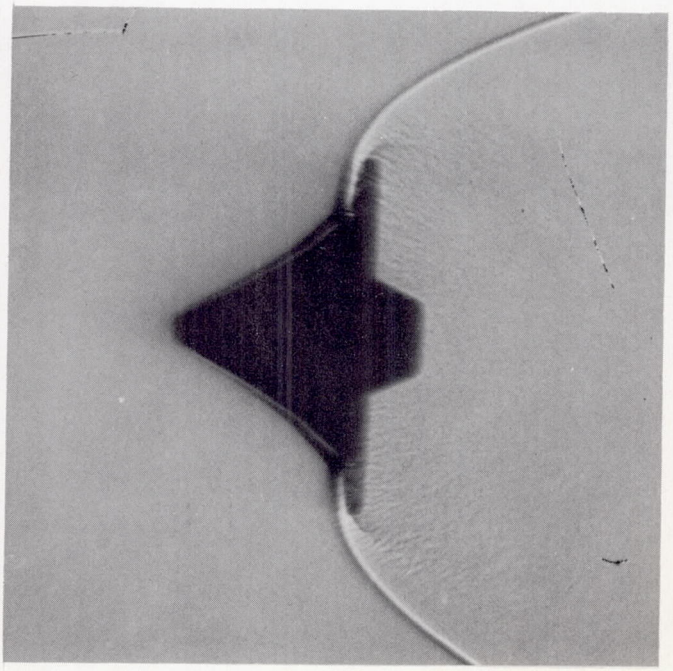

(b) M = 6.61 in CF_4.

Figure 33.- Shock shapes for tension shell. L-69-1324

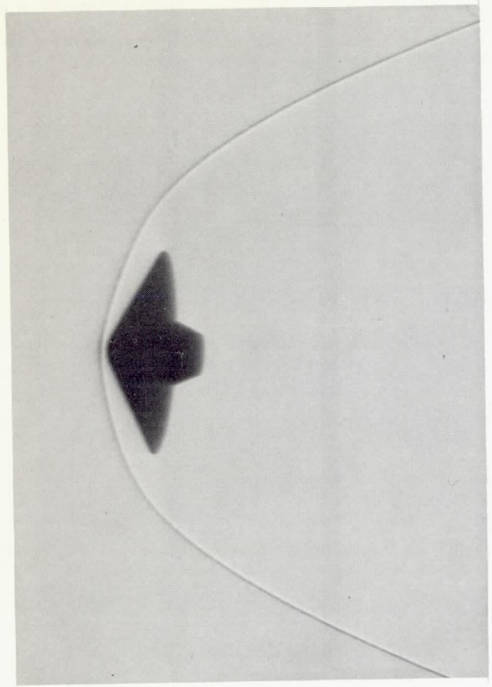

(a) Air. M = 6.

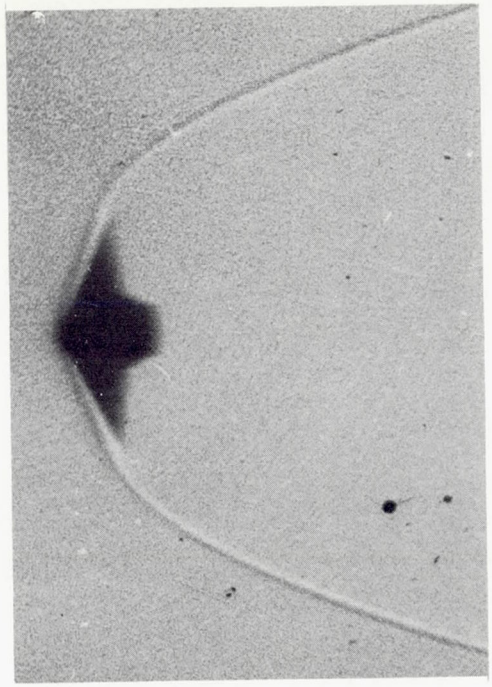

(b) Air. M = 13.

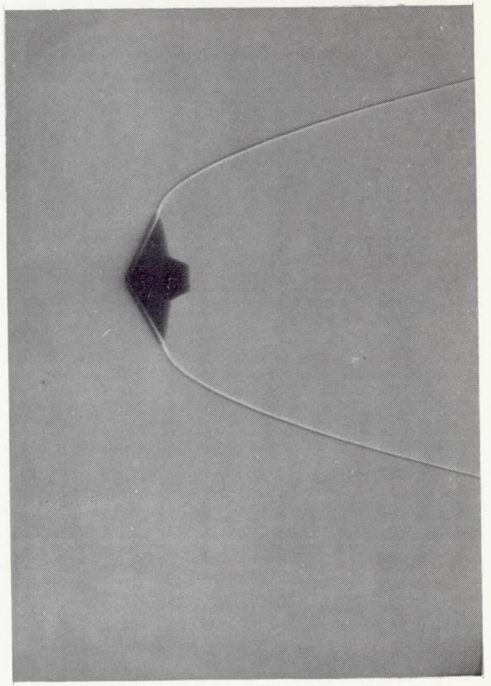

(c) CF_4. M = 7.

Figure 34.- Shadowgraphs of 120^0 cone.

L-69-1325

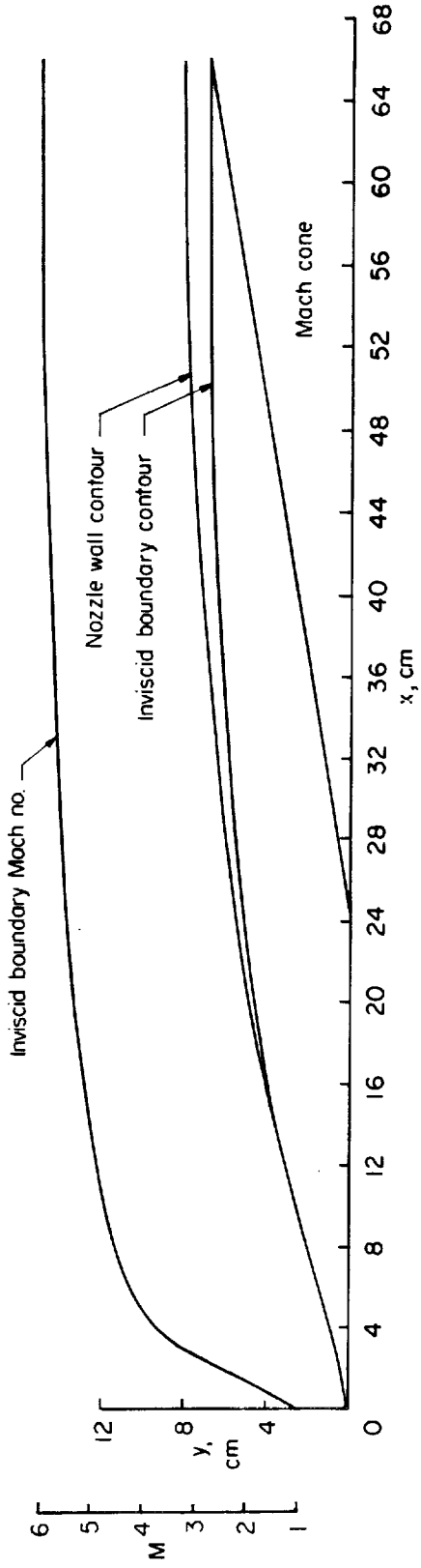

Figure 35.- Sketch of CF_4 nozzle.